USE AUTHORIZATION

In presenting this thesis in partial fulfillment of the requirements for an advanced degree at Idaho State University, I agree that the Library shall make it freely available for inspection. I further state that permission to download and/or print my thesis for scholarly purposes may be granted by the Dean of the Graduate School, Dean of my academic division, or by the University Librarian. It is understood that any copying or publication of this thesis for financial gain shall not be allowed without my written permission.

Signature .....

Date .....

Manganese-Induced Cytotoxic Mechanisms in Dorsal Root Ganglion (DRG) Neurons: Implications in Peripheral Neuropathy and Neurodegeneration

By

Anurag Kakkerla Balaraju

A thesis submitted

in partial fulfillment of the requirement for the degree of Master of Science in Biomedical and Pharmaceutical Sciences

Idaho State University

August 2014

COPY RIGHT

To the Graduate Faculty

The members of the committee appointed to examine the thesis of ANURAG KAKKERLA BALARAJU find it satisfactory and recommend that it be accepted.

.....

James C. K. Lai, Ph.D Date

Major Advisor

.....

James C. Bigelow, Ph.D. Date

Committee Member

.....

Solomon Leung, Ph.D. Date

Graduate Faculty Representative

DEDICATION

I dedicate this work to my parents for providing an opportunity to pursue education in U.S.A.

ACKNOWLEDGMENTS

I would like to express my deep gratitude to my major advisor, Dr. James C. K. Lai, for his valuable and constructive suggestions during the planning and development of this research work. His willingness to give his time so generously has been very much appreciated. I will forever be indebted to him for his guidance in developing my career path.

I am grateful to my co-advisor and committee member, Dr. James C. Bigelow, for his valuable advice and guidance throughout my studies. I am also grateful to Dr. Solomon Leung for contributing his valuable time and serving as Graduate Faculty Representative in my thesis committee. I am grateful to Dr. Pfau for her expert guidance with the operation of the flow cytometer and to the Imaging Core Facility for support and advice with confocal microscopy. I would also like extend my appreciation to the Department of Biomedical and Pharmaceutical Sciences, College of Pharmacy for research facilities and support.

I am also thankful to Idaho State University for providing an ideal atmosphere for education and research. Finally, I would like thank my parents for their constant support and encouragement throughout my education.

TABLE OF CONTENTS

LIST OF FIGURES ix

LIST OF TABLES xi

LIST OF ABBREVIATIONS xii

ABSTRACT xiv

CHAPTER 1. INTRODUCTION & LITERATURE REVIEW 1

1.1 MINERAL ELEMENT ESSENTIALITY 1

1.2 IMPORTANCE OF MANGANESE IN BIOLOGICAL SYSTEMS 3

1.3 MANGANESE ABSORPTION, TRANSPORT, METABOLISM, DISTRIBUTION AND STORAGE 4

1.4 MANGANESE DEFICIENCY AND TOXICITY 6

1.5 NEURODEGENERATION 7

1.6 MANGANISM, PARKINSON'S DISEASE (PD) AND PARKINSONISM 8

1.7 MECHANISMS INVOLVED IN NEURODEGENERATION INDUCED BY MANGANESE 10

1.8 MANGANESE AND OXIDATIVE METABOLISM 16

1.9 MITOCHONDRIA AND NEURITE FORMATION 17

1.10 RATIONALE OF THE PROJECT 20

1.11 HYPOTHESES OF THE PROPOSED RESEARCH PROJECT. 21

1.12 GOALS OF THE PROPOSED PROJECT. 21

1.13 THEMES OF THE SUBSEQUENT CHAPTERS 21

1.14 ROLES IN OTHER COLLABORATIVE RESEARCH PROJECTS 22

1.15 REFERENCES 22

CHAPTER 2. CHARACTERIZATION OF DRG NEURONS AS AN IN VITRO CELL MODEL TO STUDY MANGANESE-INDUCED NEUROTOXICITY 30

2.1 ABSTRACT 31

2.2 INTRODUCTION 32

2.3 MATERIALS AND METHODS 35

2.4 RESULTS 43

2.5 DISCUSSION AND CONCLUSIONS 46

2.6 ACKNOWLEDGEMENTS 49

2.7 REFERENCES 50

2.8 FIGURES 54

CHAPTER 3. MODULATION OF SURVIVAL OF DORSAL ROOT GANGLION (DRG) NEURONS IN MANGANESE-INDUCED NEUROTOXICITY 74
3.1 ABSTRACT 75
3.2 INTRODUCTION 76
3.3 MATERIALS AND METHODS 78
3.4 RESULTS 83
3.5 DISCUSSION AND CONCLUSION 86
3.6 ACKNOWLEDGEMENTS 88
3.7 REFERENCES 89
3.8 FIGURES 91
CHAPTER 4. GENERAL DISCUSSION, CONCLUSIONS, AND PROSPECTS FOR FUTURE STUDIES 106
4.1 GENERAL DISCUSSION AND CONCLUSIONS 106
4.2 PROSPECTS FOR FUTURE STUDIES 110
4.3 REFERENCES 110

LIST OF FIGURES

Figure 1.1 Theoretical dose-response curve for minerals 3

Figure 1.2 Manganese transport mechanisms. 5

Figure 1.3 Flow chart depicting the cell death mechanism in various neurodegenerative diseases. 8

Figure 1.4 Role of mitochondria in apoptosis 13

Figure 1.5 Neuritogenesis. Cartoons and micrographs depicting various stages observed in differentiation of a neuron 18

Figure 2.1 Effect of $MnCl_2$ on survival of DRG Neurons when treated for 48 hours. 54

Figure 2.2 Effect of $MnCl_2$ on Survival of Schwann cells when treated for 48 hours. 55

Figure 2.3 Effect of treatment with 0 (A), 10 (B), 50 (C), 100 (D), 500 (E) and 1000 (F) μM of $MnCl_2$ for 48 hours on the morphology of DRG neurons. 57

Figure 2.4 Comparison of control and UV-treated DRG neurons stained with annexin V as analyzed using a flow cytometer. 58

Figure 2.5 Effect of $MnCl_2$ on inducing apoptosis in DRG neurons. 60

Figure 2.6 Effect of $MnCl_2$ on the release of LDH into medium by DRG neurons. 62

Figure 2.7 Effect of $MnCl_2$ on necrosis in DRG neurons. 65

Figure 2.8 Effect of $MnCl_2$ on lactate dehydrogenase (LDH) activities in DRG neurons. 67

Figure 2.9 Effect of $MnCl_2$ on malate dehydrogenase (MDH) activities in DRG neurons. 68

Figure 2.10 Effect of $MnCl_2$ on p-AMPK to AMPK ratios in DRG neurons..... 69

Figure 2.11 Effect of $MnCl_2$ on the morphology of mitochondria in DRG neuron. 73

Figure 3.1 Effect of conditioned media containing $MnCl_2$ on DRG neurons. 92

Figure 3.2 Effect of conditioned media containing $MnCl_2$ from monotypic cultures on DRG neurons. 94

Figure 3.3 Effect of MOC or COC on the survival of DRG neurons. 95

Figure 3.4 Effect of MOC or COC on ROS levels in DRG neurons. 95

Figure 3.5 Effect of MOC or COC on GSH levels in DRG neurons. 96

Figure 3.6 Effect of MOC or COC on the level of caspase-3 in DRG neurons..... 96

Figure 3.7 Effect of $MnCl_2$ on the survival of DRG neurons which were pre-treated with forskolin. 97

Figure 3.8 Effect of different concentrations of forskolin on DRG neurons. 101

Figure 3.9 Changes in the morphology of DRG neurons treated with forskolin at different time points. 103

Figure 3.10 Effect of $MnCl_2$ on AMPK and p-AMPK ratio in DRG neurons pretreated with forskolin. 104

LIST OF TABLES

Table 1.1 List of essential macro- and micro-elements 2

Table 1.2 Distinguishing features of apoptosis and necrosis 14

LIST OF ABBREVIATIONS

ABAD	Aβ-binding alcohol dehydrogenase
AD	Alzheimer's disease
ALS	Amyotrophic lateral sclerosis
AMPK	AMP-activated protein kinase
ANOVA	Analysis of variance
ATCC	American type culture collection
BCA	Bicinchoninic acid
COC	Conditioned medium derived from co-cultures of dorsal root ganglion neurons and Schwann cells
DMEM	Dulbecco's minimal essential medium
DMSO	Dimethyl sulfoxide
DRG	Dorsal root ganglion
DTNB	5, 5'-dithiobis-(2-nitrobenzoic acid)
FBS	Fetal bovine serum
FK	Forskolin
GSH	Glutathione
H_2O_2	Hydrogen peroxide
HD	Huntington's disease

HK	Hexokinase
HPLC	High pressure liquid chromatography
LDH	Lactate dehydrogenase
MDH	Malate dehydrogenase
Mn	Manganese
$MnCl_2$	Manganese Chloride
MOC	Conditioned medium obtained from monotypic cultures of DRG neurons
MTT	3-(4, 5-dimethylthiazol-2-yl)-2,5-diphenyltetrazolium bromide
NAD	Nicotinamide adenine dinucleotide (oxidized form)
NADH	Nicotinamide adenine dinucleotide (reduced form)
NDD	Neurodegenerative disease
PBS	Phosphate buffer saline
PD	Parkinson's disease
p-AMPK	Phosphorylated AMP-activated protein kinase
S16	Schwann cells of rat origin obtained from ATCC

ABSTRACT

Manganese (Mn) is a micronutrient required for normal physiological functions. Mn regulates many important processes (e.g., glucose metabolism, anti-oxidant defense and bone metabolism). However, chronic exposure to toxic Mn levels results in manganism, a neurodegenerative disease. Mn-induced neurotoxic mechanisms have been mainly studied employing neurotumors cells. To address their limitations as a neural cell model, we have developed an in vitro cell model employing rat dorsal root ganglion (DRG) neurons and have determined their suitability for studying Mn neurotoxicity. Our results demonstrated the Mn-induced death of DRG neurons could be attributed, at least in part, to the Mn-induced changes in their cellular energetics and mitochondria structure and function. Our findings strongly suggest DRG neurons constitute an excellent cell model in vitro for investigating cellular and molecular mechanisms underlying Mn-induced neurotoxicity in particular and toxicant-induced neurotoxicity in general. Moreover, our results may have pathophysiological implications in peripheral neuropathy and neurodegeneration.

CHAPTER 1. INTRODUCTION & LITERATURE REVIEW

This chapter provides a concise review of the literature relevant to the research theme of my thesis, highlights the aims and hypotheses of my thesis research, and outlines the topics to be covered in the subsequent three chapters of this thesis.

1.1 MINERAL ELEMENT ESSENTIALITY

The elements that are not normally vaporized when their organic matrix is burnt to eliminate the carbonaceous material are termed mineral elements. However, the description of essentiality is more subtle, but in a general sense, a nutritionally essential element is required in the diet of animals and humans in order to support adequate growth, reproduction and health throughout life cycle (Erikson et al., 2005).

Mineral elements are clearly classified into macro-elements and micro-elements based on their daily requirement and convenience of analysis (O'Dell et al., 1997). The requirement for macro-elements is in the range of grams per kilogram of diet, while that for a micro-element is milligrams or micrograms per kilogram of diet. Microelements are also referred to as trace elements due to the inability of the early analytical methods to accurately quantify microelements (O'Dell et al., 1997). Table 1. lists macro- and micro-elements essential for mammals.

Macro-elements	calcium, phosphorus, sodium, chloride, potassium, and magnesium [[arrange in alphabetical order]]
Micro-elements	cobalt, copper, chromium, fluoride, iodine iron, manganese, molybdenum, selenium, and zinc

Table 1.1 List of essential macro- and micro-elements
(adapted from O'Dell et al., 1997)

Mineral elements have three general physiological roles in biological systems — structural, regulatory roles and roles in signal transductions (McCollum, 1957). Macronutrients largely perform structural functions; however, a few of them extensively contribute to autocrine, paracrine and intracrine signal transduction (McCay, 1973). For example, macro-elements such as calcium and phosphorus not only play a key role in the structure and function of skeletal muscle and bone but also required for activation of intracellular proteins.

By contrast with macro-elements, micro-elements primarily serve catalytic functions in biological systems. For example, manganese (Mn) is a component of several groups of enzymes such as manganese-superoxide dismutase (Mn-SOD), pyruvate carboxylase and arginase (O'Dell et al., 1997). Obviously, under or over consumption of such essential elements, respectively, results in deficiency or toxic conditions impairing the biological function(s) of the organism so afflicted (WHO).

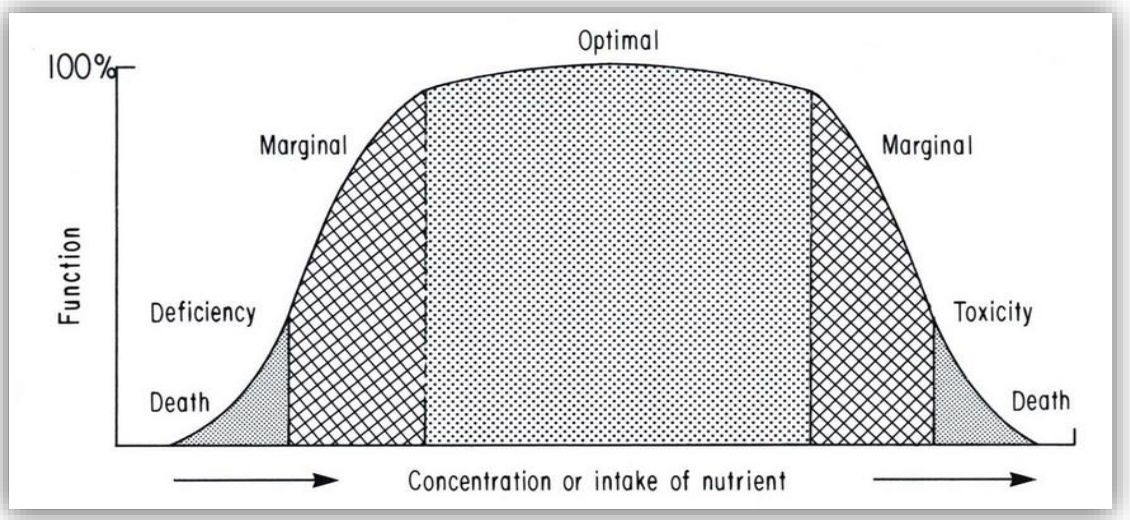

Figure 1.1 Theoretical dose-response curve for minerals

(From http://www.dartmouth.edu/~rpsmith/Heavy_Metals.html)

The dependency of physiology on the concentrations of essential minerals in the diet is depicted in the theoretical dose-response curve (Figure 1). Elucidation of the physiological responses of essential elements at a fundamental level is essential in defining cellular and molecular mechanisms underlying both metal deficiency and toxicity (O'Dell et al., 1997).

1.2 IMPORTANCE OF MANGANESE IN BIOLOGICAL SYSTEMS

Manganese (Mn) is a transition metal which lies beside iron in the periodic table. It has eleven oxidation states ranging from +7 to -3. Of these, +2 oxidation state is stable at neutral pH and allows Mn to behave as a simple divalent metal cation (Stephen et al., 2006). Manganese plays an important role in several biochemical processes such as carbohydrate metabolism, lipid metabolism, bone formation, reproduction and neurotransmitter synthesis and metabolism (O'Dell et al., 1997). Also, Mn shares

similarity with metals such magnesium (Mg), calcium (Ca) and iron (Fe) and influence their utilization by biological systems (O'Dell et al., 1997). Hence, understanding the role of Mn in regulating physiology is crucial.

1.3 MANGANESE ABSORPTION, TRANSPORT, METABOLISM, DISTRIBUTION AND STORAGE

Manganese is primarily absorbed into system circulation via gastrointestinal tract (Thomson et al., 1972). As mentioned earlier, Mn competes with Fe transport mechanism for absorption and transport into the systemic circulation (Lai et al., 1985b; Lai et al., 2000; Lai and Leung, 2013). Mn in +3 oxidative state binds to transferrin in the plasma and gets shuttled to tissues (Lai et al., 2000; Zheng and Zhao, 2001). Other plasma proteins such albumin and transmanganin may also serve as carriers of Mn. It gets further transported into the cytoplasm of a cell via divalent metal transporter (DMT), Ca channels, ZIP8 and ZIP14 symporters, the SLC39 family of zinc (Zn) transporters, magnesium (mg) transporters hip18, and the transient receptor potential melastatin 7 (TRPM7) channels (Bowmen et al., 2011).

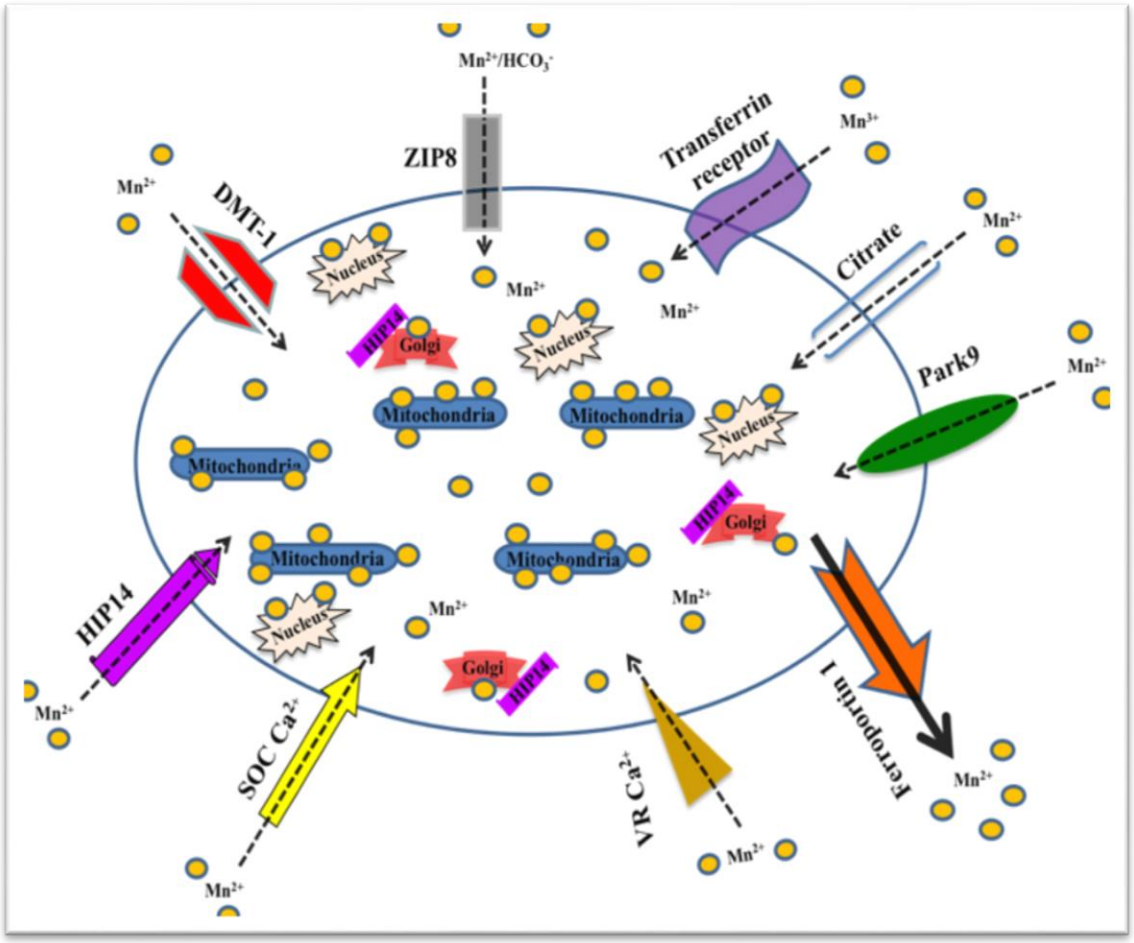

Figure 1.2 Manganese transport mechanisms.

(From Bowmen et al., 2011)

Although Mn competes with many divalent transport mechanisms, its systemic absorption and plasma levels are strictly regulated. Once absorbed, Mn is complexed with albumin and transported to liver, the key organ in Mn metabolism. Mn, in liver, can be found in two pools: a rapid and a slowly exchanging pools (Bowmen et al., 2011). The rapid exchanging pool represents a major route for manganese excretion from the body (Bowmen et al., 2011).

Distribution of Mn in the peripheral organs is uneven with significantly high levels in liver, followed by kidney. The relative rank order for Mn distribution in

peripheral organs is, liver >> kidney >> spleen ≈ heart > lung (Lai et al., 2000; Lai and Leung, 2013). This unequal distribution of the metal in different organs is indicative of the organs' storage capacity and the amount of metal-protein affinity in the various organs. Bone is another storage site for Mn but the recall mechanism to release Mn, other than release during normal bone turnover, has not been identified yet. Furthermore, Mn shows highest region-specific distribution in brain, with respect to other heavy metal ions in the order: Mn > Hg > Cu > Se (Lai et al., 2000; Lai and Leung, 2013).

1.4 MANGANESE DEFICIENCY AND TOXICITY

Manganese is an essential trace element required for energy metabolism, activity of various enzymes, function of reproductive hormones, skeletal development, development of brain, anti-oxidant ability of cells and lipid metabolism (Lai et al., 1985a,b,c; Wedler, 1993; Lai et al., 2000). Mn serves as a structural component of metalloenzymes such as manganese-superoxide dismutase (Mn-SOD), pyruvate carboxylase, and arginase (Wedler, 1993). Also, Mn activates enzymes such as phosphoenol pyruvate carboxykinase, glycosyl transferases, glutamine synthetase, farnesyl pyrophosphate synthetase and Mn-dependent peroxidases (Wedler, 1993; Eide et al., 2013). The requirement of Mn in proper of functioning of various enzymes is an indicative of its essentiality in homeostasis in humans and animals (Lai et al., 1985a,b; Wedler, 1993; Lai et al., 2000; Lai and Leung, 2013). The frequency of observing deficiency symptoms are more during pre-natal and early post-natal periods in animals (Lai et al., 1985a,b,c; Wedler, 1993; Lai et al., 2000). Mn deficiency symptoms are rarely observed in humans due to its daily requirement, distribution and storage in the body and

tight homeostatic control over absorption and excretion (Lai et al., 1985a, b,c; Wedler, 1993; Lai et al., 2000).

Conditions such as respiratory distress, cytotoxic effects, cardiovascular toxicity, hepatotoxicity, reproductive toxicity and neurotoxicity are observed during chronic exposure to high levels of Mn. (Lai et al., 1984; Lai et al., 1985a,b; Saric and Piasek, 2000; Lai et al., 2000). Though high levels of Mn affects various organs, effects seen in central nervous system are critical. Toxic levels of Mn leads to its accumulation in basal ganglia (Lai et al., 1984; Lai et al., 1985a,b; Lai et al., 2000; Dorman et al., 2006; Lai and Leung, 2013) and results in a condition called as manganism characterized by Parkinsonian-like symptoms such as tremors, bradykinesia, rigidity, dystonia, gait disturbances and psychosis (Lai et al., 1984; Lai et al., 1985a,b; Lai et al., 2000; Dorman et al., 2006; Lai and Leung, 2013).

1.5 NEURODEGENERATION

Neurodegeneration is an umbrella term for a range of conditions which includes progressive loss of structure and function of neurons (Federico et al., 2012) (Figure 3). Many diseases such as Alzheimer's disease (AD), Parkinson's disease (PS) and Huntington's disease are classic examples of neurodegenerative diseases (Federico et al., 2012). Substantial evidence has accumulated implicating metals in pathophysiology and pathogenesis of neurodegeneration (Lai et al., 1985a,b,c; Wedler, 1993; Lai et al., 2000; Lai and Leung, 2013). Interaction of free radicals, generated by metal ions, with proteins can lead to dysfunctional proteins. Consequently, a cascade of events lead to oxidative stress, neurodegeneration and cell death (Federico et al., 2012) (Figure 1.3).

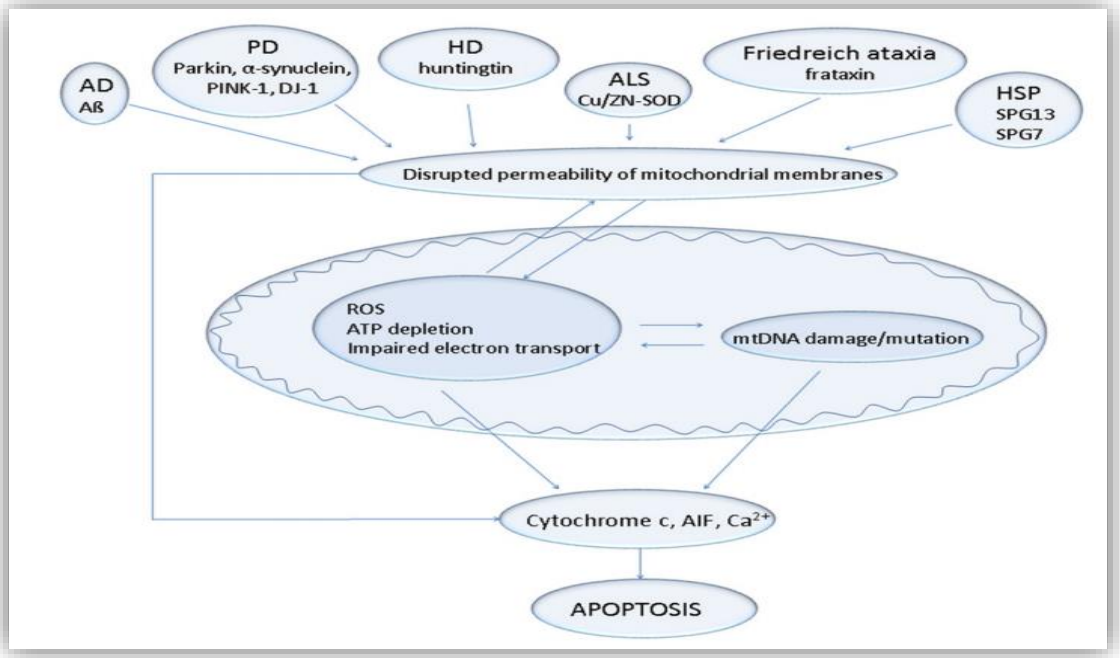

Figure 1.3 Flow chart depicting the cell death mechanism in various neurodegenerative diseases.

(From Federico et al., 2012)

Because neurodegenerative diseases such as AD and PD share many pathophysiological characteristics common to neurodegenerative diseases in general and neurodegeneration in particular, further understanding of their pathophysiological mechanisms will not only enhance our understanding of such diseases but also allow us to seek new avenues to ameliorate neurodegeneration.

1.6 MANGANISM, PARKINSON'S DISEASE (PD) AND PARKINSONISM

Parkinson's disease (PD) and Parkinsonism constitute complex syndromes of chronic and progressive motor system disorders which result from the degeneration of dopaminergic neurons in the central nervous system (CNS). The primary symptoms observed in PD are tremor, rigidity, bradykinesia and postural instability (NINDS, 2014).

Other symptoms of PD and Parkinsonism include depression, emotional disturbances and sleep disruptions (NINDS, 2014).

Interestingly, manganism, a neurological syndrome due to excessive accumulation of manganese in the CNS, results in Parkinsonian like symptoms (Lai et al., 1985a, b; Wedler, 1993; Lai et al., 2000; Bowman et al., 2011; Lai and Leung, 2013). It was reportedly first observed in individuals working in an ore-crushing facility by Couper in 1837. Individuals suffering from manganism were observed with early psychological symptoms characterized by hallucinations, psychoses and myriad of behavioral disturbances (Lai et al., 1985a,b; Wedler, 1993; Lai et al., 2000; Bowman et al., 2011; Lai and Leung, 2013). In the later stages of the disease, individuals afflicted with the disease exhibited gait disturbances, bradykinesia and speech disturbances (Bowman et al., 2011). Unlike resting tremor which is a characteristic of PD, manganism features less frequent kinetic tremor or none (Bowman et al., 2011).

Several neurodegenerative diseases, including AD, amyotropic lateral scherosis (ALS), Huntington's disease, PD and manganism, share mechanistic similarities at the subcellular level (Lai et al., 1985a,b; Wedler, 1993; Lai et al., 2000; Bowman et al., 2011; Lai and Leung, 2013). For example, presence of α-synuclein aggregates and mitochondrial dysfunction in PD and manganism is a classic example of such characteristics commonly found in such neurodegenerative diseases (Bowman et al., 2011). In the etiology of PD and manganism, mitochondria have been postulated to play a pivotal role: a damage to substantia nigra due to generation of reactive oxygen species (ROS) and reactive nitrogen species (RNS) was observed in postmortem studies of PD brain (Bowman et al., 2011). Production of ROS and RNS in cells will lead to

mitochondrial damage and dysfunction: this is especially the case with neurons because of their high metabolic demand (Bowman et al., 2011; Federico et al., 2012). Thus, neurons are vulnerable to mitochondrial damage initiated by ROS and RNS (Bowman et al., 2011; Federico et al., 2012). On the other hand, Mn is primarily accumulated in mitochondria via Ca uniport mechanism (Lai et al., 2000; Lai and Leung, 2013). Consequently, excessive accumulation of Mn in mitochondria can lead to uncoupling of oxidative phosphorylation (Lai et al., 2000; Lai and Leung, 2013) thereby enhancing the generation of ROS and RNS, a direct consequence of which is damage to mitochondria.

Because both PD and manganism show very similar molecular pathophysiological mechanisms at the level of mitochondria: consequently, elucidation of such mechanisms will greatly improve our understanding of the root causes of neurodegenerative diseases.

1.7 MECHANISMS INVOLVED IN NEURODEGENERATION INDUCED BY MANGANESE

Mitochondria dysfunction

Mitochondria, the power house of cell, are dynamic and "plastic" organelles found in the cytoplasm of eukaryotic cells. Mitochondria have two distinct membranes which are unique in appearance and physico-chemical properties. The inner and outer membrane are characterized by different phospholipid compositions and protein-to-lipid ratio, thus determining the unique biochemical functions of each membrane (Krauss et al., 2001). The structure and morphology of inner mitochondrial membrane reflect the responses of mitochondria to the energy demands of the cells they are in (Krauss et al., 2001). Their inner membrane encloses and convolutes into mitochondrial matrix, forming

cristae which carry the enzymatic machinery of electron transport and oxidative phosphorylation (OXPHOS) (Krauss et al., 2001). The mitochondrial matrix and inner mitochondrial membrane contain a range of enzymes which play major roles in cellular energetics (Krauss et al., 2001).

Unlike the outer mitochondrial membrane, the inner mitochondrial membrane is less permeable to ions and large molecules (Krauss et al., 2001). Sophisticated transport proteins are located in the inner mitochondrial membrane to facilitate the transport of specific molecules into the mitochondrial matrix from the cytoplasm and vice versa (Krauss et al., 2001). Mitochondrial calcium uniporter (MCU) is an example of transport protein in the inner mitochondrial membrane which is involved in the uptake of calcium into the mitochondrial matrix (Krauss et al., 2001). This uptake mechanism regulates one of the most versatile and fundamental cellular processes, namely, intracellular Ca+2 signaling, which is associated with a multitude of events ranging from oxidative stress to changes in action potentials (Federico et al., 2012).

Manganese can affect cellular energetics via interactions with several proteins and subsequently induce ROS, RNS and protein aggregates. Mn accumulates in mitochondria via Ca uniport mechanism (Lai et al., 2000; Krauss et al., 2001; Lai and Leung, 2013): however, there is no particular mitochondrial Mn export mechanism. Furthermore, the rate of influx of Mn into mitochondrial influx is significantly higher than the Mn efflux from mitochondria. This results in rapid accumulation of Mn in mitochondrial matrix and subsequent inhibition of Na^{+}-dependent and -independent Ca^{2+} efflux mechanisms. A rise in Ca^{2+} levels in the matrix of mitochondria leads to an increase in ROS by electron transport chain where it disturbs ATP synthesis by targeting proteins such as F1/F0 ATP

synthetase, NADH dehydrogenase, succinate dehydrogenase and glutamate/aspartate exchanger (Maciel et al., 2004).

Manganese and Oxidative stress

A disturbance in the balance between the production of ROS and anti-oxidant defenses is defined as oxidative stress. In order to maintain the vital cellular and biochemical functions, the biological system must confront and control the balance between pro-oxidants and anti-oxidants continuously. A reduction in the intracellular ATP levels contributes to an increase in oxidative stress and subsequent damage to intracellular structures (Chen & Liao, 2002). A drop in the reductive capacity of anti-oxidant proteins was also observed upon exposure to toxic levels of Mn. Such a drop in reductive capacity in addition to rise in oxidative status results in neurotoxicity and neurodegeneration.

Apoptosis and Necrosis

During pre- and post-natal developmental stages and throughout the adult life, many cells in the nervous system die. This phenomenon is normal with respect to their impact on nervous system and is called as 'Programmed cell death' (PCD). Of the different types of PCD, the one that has been extensively studies is apoptosis which is characterized by similar morphological and biochemical changes in different cell types. Morphological changes include cell shrinkage, blebbing of plasma membrane and nuclear chromatin condensation with preservation of the structure of mitochondria and endoplasmic reticulum. Release of pro-apoptotic proteins such as Bax and Par-4, formation of mitochondrial permeability transition pore and release of cytochrome c, activation of caspases and exposure of phosphatidyl serine on the plasma membrane are few biochemical changes which occur in a cell during apoptosis.

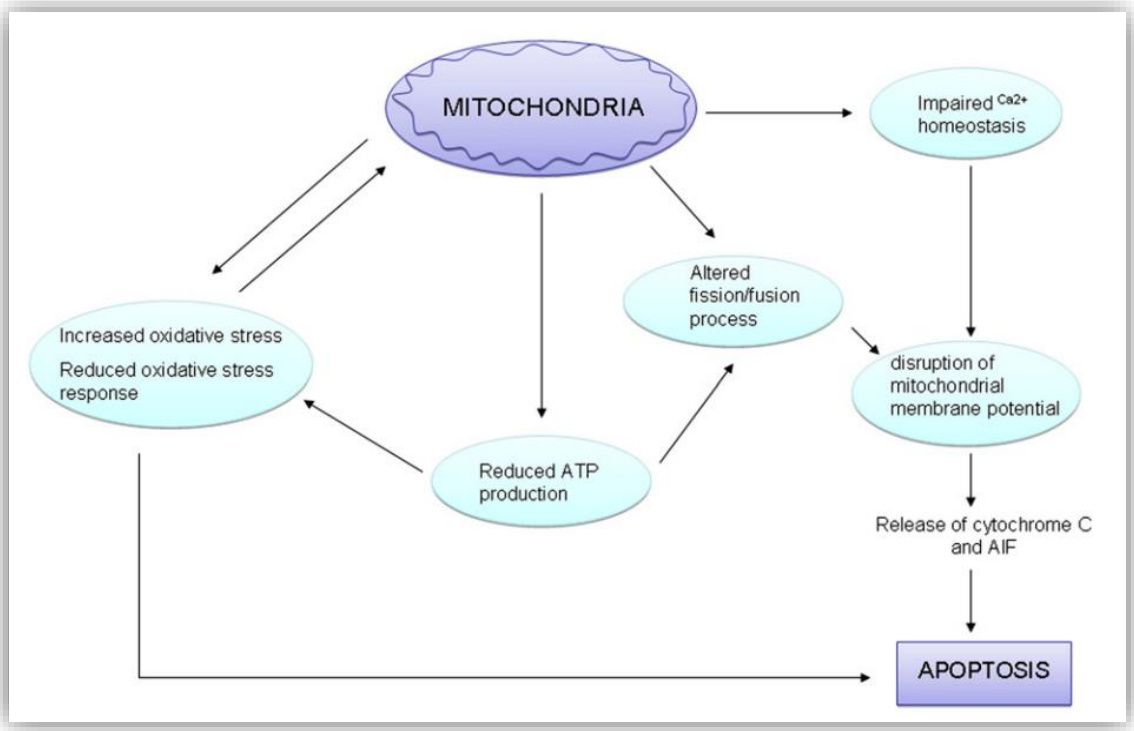

Figure 1.4 Role of mitochondria in apoptosis

(From Federico et al 2012).

However, the morphological and biochemical changes that occur during necrosis differ from the same in apoptosis. Unlike apoptosis, mitochondria and endoplasmic reticulum lose their structural integrity in necrosis and become dysfunctional. The other characteristic features of necrosis include cell swelling, depletion of ATP, loss of ion homeostasis, membrane rupture and nuclear lysis.

Apoptosis	Necrosis
Cell shrinkage	Cell swelling
Organellar integrity is maintained	Organelles swell and rupture
ATP levels are maintained	ATP levels are depleted
Membrane surface blebb	Membrane ruptures
Death effector proteins are required	Protein synthesis halts
Nuclear chromatin condensation/fragmentation is observed	Nuclear lysis is observed
Does not adversely affect neighboring cells	Promotes death in neighboring cells

Table 1.2 Distinguishing features of apoptosis and necrosis

(Table excerpted from 'Basic Neurochemistry').

The underlying conditions and signaling pathways that trigger different cell death mechanisms are different. For example, neuronal cells that are not included in the neuronal circuits during developmental stages are eliminated from the healthy neighbors via apoptosis. On the other hand, necrosis occurs as a result of physical or chemical injury such as stroke. Mn, in several cell types including N27 and PC12, has shown to activate PKC-δ via release of cytochrome-c and activation of caspase-3 and induce apoptosis at lower concentrations (Kitazawa et al., 2005). However, at higher concentrations, Mn was hypothesized to induce necrosis (Malthnkar et al., 2004).

Dopamine neurotoxicity

In neurological condition of idiopathic Parkinson's disease, dopamine has been implicated. Upon treatment with manganese, reduced dopamine levels have been

recorded both in vivo and in vitro causing dopaminergic cell death (Higashi et al., 2004). Oxidative DNA damage due to the generation of free radical via dopamine oxidation in dopaminergic neurons has been proposed as possible mechanism of cell death.

Neuroinflammation

Inflammation of nervous system may be initiated by a variety of cues such as injury, autoimmune response and toxic moieties. Studies performed by Fernsebner et al. (2014) in Sprague-Drawley rats showed that the prostaglandins levels were elevated in Mn treated samples triggering ROS production and lipid peroxidation. This pronounced increase in the inflammatory response and an increase in the levels of prostaglandins suggest the role of Mn in induction of neuroinflammation and neurodegeneration. However, the presence of a cause and effect relation between pro-inflammatory cytokines and neural damage is not clear.

Neurotransmitter signaling pathways

Metal ions are intricately associated with every aspect of synaptic transmission and neurotransmitter functions. Lai et al. (1985) have shown that Mn inhibits uptake of choline (Ch), noradrenaline (NE), dopamine (DA), serotonin (5HT), GABA and glutamate in the central nervous system. Fitsanakis et al have observed excessive release of glutamate into the extracellular space, possibly causing neurodegenerative process. However, few other studies such as Lipe et al. (1999) and Levy et al. (2003) suggested a drop in the release of glutamate and GABA upon exposure to toxic levels of Mn.

All the deleterious effects induced by exposure to toxic levels of Mn discussed above, can lead to structural and functional derangement of protein and phospholipids and initiate cell death mechanism, namely, apoptosis or necrosis.

1.8 MANGANESE AND OXIDATIVE METABOLISM

The adult mammalian brain is virtually entirely dependent on glucose oxidative metabolism for energy production and syntheses of tricarboxylic acid (TCA) cycle-related neurotransmitter synthesis (e.g., synthesis of acetylcholine, glutamate, GABA, and aspartate) (Lai and Clark, 1989; Clark and Lai, 1989).Thus, if Mn toxicity induces alterations in brain oxidative metabolism, then it will also compromise the syntheses of acetylcholine, glutamate, GABA, and aspartate. Indeed, findings of a previous study from our laboratory are relevant to this assertion. Malthankar et al. (2004) noted treatment of human neuroblastoma SK-N-SH (neurons-like) and human astrocytoma U87 (astrocytes-like) cells with 0.01 to 4.0 mM $MnCl_2$ for 48 hours also induced dose-related decreases in their activities of hexokinase, pyruvate kinase, lactate dehydrogenase, citrate synthase, and malate dehydrogenase. Hexokinase in SK-N-SH cells was the most affected by Mn treatments, even at the lower range of concentrations. Mn treatment of SK-N-SH cells affected pyruvate kinase and citrate synthase to a lesser extent as compared to its effect on other enzymes investigated. However, citrate synthase and pyruvate kinase in U87 cells were more vulnerable than other enzymes investigated to the effects of Mn. In parallel, they showed that these Mn treatments also induced cell death in these two neural cell types (Malthankar et al., 2004).

Other key enzymes affected by Mn in mitochondria are α-ketoglutarate dehydrogenase complex (Du et al., 1997) and aconitase (Zheng and Zhao, 2001).

Consequently, the studies discussed above (Du et al., 1997; Zheng and Zhao, 2001; Malthankar et al., 2004) have prompted us to propose the hypothesis that energy failure is one neurotoxic mechanism induced by Mn.

1.9 MITOCHONDRIA AND NEURITE FORMATION

A neuron is a highly polarized cell type, meaning that they develop distinct subcellular domains which serve different functions. Morphologically, three major subcellular domains can be identified in a neuron: 1. cell body or soma or perikaryon, 2. Axon, and 3. Dendrite (Lai and Clark, 1989). Nucleus and other major cytoplasmic organelles reside in the cell body of neurons whereas the organelles such as mitochondria are transported from the neuronal cell body to axon and dendrites and back to the cell body (Lai and Clark, 1989).

The axons and dendrites in a neuron differ significantly in structural and functional aspects such as length, diameter, number, branches and electrical impulse conduction velocity (Tahirovic et al., 2009). Dendrites and cell body are functionally characterized as domains of neurons which are specialized in reception of impulses from neighboring neurons via synapses (Tahirovic et al., 2009). On the other hand, axons specialize in transmitting impulses via synapses to dendrites and cell body of consequent neurons (Tahirovic et al., 2009).

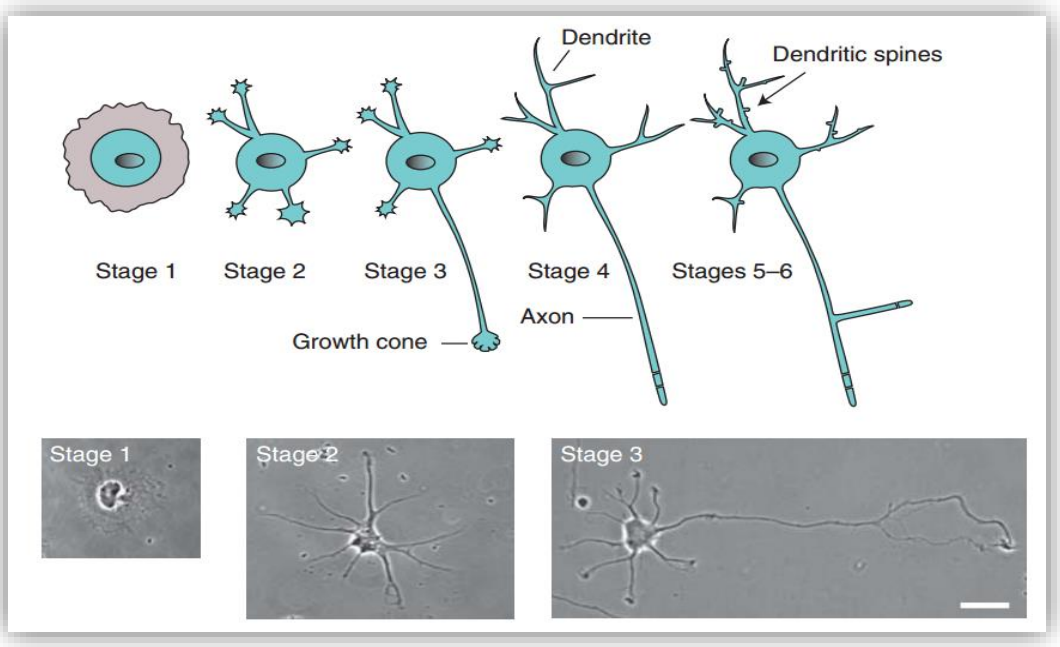

Figure 1.5 Neuritogenesis. Cartoons and micrographs depicting various stages observed in differentiation of a neuron

(From Tahirovic et al., 2009).

Owing to the post-mitotic stage and structurally and functionally differentiated nature of neurons, any cellular damage beyond the point of recovery leads to cell death and neuronal loss (Figure 5). Hence the study of repair mechanisms in a neurons after injury is essential and helps us design therapeutic interventions to promote repair process in neurodegenerative diseases. For example, study of neurite outgrowth upon damage to axonal domain in a variety of pathophysiological conditions such as diabetes and manganism helps us to progress our understanding of neuronal repair mechanisms.

Neuritogenesis and mitochondria

Neuritogenesis is a dynamic process involving the extension of long, thin protrusions called neurites that will subsequently differentiate into long axons or an elaborate dendritic arbor (Pertz el at., 2008). Neurons start growing out by projecting many broad, sheet-like extensions, called lamellipodia, which subsequently condense into a number of small, undifferentiated neurites of approximately equal length (Dotti et al., 1988).

In due course, one of the neurites grows faster than the other and develops into axons while the remaining neurites develop into dendrites (Dotti et al., 1988). The neurite which later on develops into an axon, extends in length in a direction dependent on the extracellular cues and innervate the target region (Dotti et al., 1988; Pertz el at., 2008). Similarly, when an axon is dissected, the proximal piece of axon attached to cell body sprouts out neurites one of which develops into axon (Dotti et al., 1988; Pertz el at., 2008). Exploration of this process is important as it is necessary for proper wiring of brain and nerve regeneration and has also been linked to many neurodegenerative diseases.

After injury or disease, neurons fail to regenerate due to reduced intrinsic and extrinsic factors. Usually, these factors contribute to regeneration by altering mitochondrial dynamics and function suggesting the role of mitochondria in modulating signaling mechanism controlling neurite outgrowth and hence regeneration process (Steketee et al., 2012).

1.10 RATIONALE OF THE PROJECT

Mitochondria constitute the primary intracellular storage site for manganese (Lai et al., 1985a; Lai et al., 2000; Lai and Leung, 2013). Mn competes with Ca transport mechanism and gets accumulated in mitochondria (Lai et al., 1985a; Lai et al., 2000; Lai and Leung, 2013). However, the influx of Mn into mitochondria is significantly higher than its efflux resulting in toxic levels of Mn in mitochondria. This accelerated accumulation of Mn by mitochondria leads to mitochondrial dysfunction and inhibition of ATP synthesis (Malthankar et al., 2004). Consequently, generation of reactive oxygen species (ROS) as a result of inhibition of ATP synthesis is one of the mechanism of neurotoxicity induced by Mn. In addition, Steketee et al. (2012) have shown that, in retinal ganglion cells (RGC) isolated from embryonic rats, mitochondria play a key role in modulating signaling pathways in growing neurites and affect regeneration ability of axons. Since Mn induces neurotoxicity primarily by targeting mitochondria, we propose Mn plays a role in altering ability of axons to regenerate. The importance of mitochondrial dynamics in elongating neurite has also suggested as a key role of Mn in regeneration of axon.

Much of the work pertaining to Mn neurotoxicity was performed with cortical neurons and glial cells in primary culture or with neuroblastoma (neurons-like) and astrocytoma (astrocytes-like) cell lines. However, Mn toxicity in peripheral nervous system (PNS) has not been elucidated. In fact, little is known of Mn toxicity in PNS. Consequently, we have developed neural cell models *in vitro*, consisting of dorsal root ganglion (DRG) neurons and Schwann cells derived from rat PNS (Jaiswal et al., 2010; Jaiswal et al., 2011). These cell models allow us to systematically investigate the cellular

and molecular mechanisms underlying Mn neurotoxicity in the PNS in particular, and in neurodegeneration in general.

1.11 HYPOTHESES OF THE PROPOSED RESEARCH PROJECT.

The studies outlined in this thesis address two key hypotheses:

1. Mn alters mitochondrial functions in DRG neurons and their neurite formation.
2. Schwann cells modulate manganese-induced oxidative stress in DRG neurons and imparts cyto-protection to DRG neurons.

1.12 GOALS OF THE PROPOSED PROJECT.

The goals of this project are:

1. To characterize the morphological and biochemical changes in DRG neurons upon treating them with various concentrations of Mn;
2. To study the changes in mitochondrial energetics and dynamics in DRG neurons upon treating them with various concentrations of Mn; and
3. To determine the role of Schwann cells in regulating the oxidative status in DRG neurons upon exposure to Mn.

1.13 THEMES OF THE SUBSEQUENT CHAPTERS

Chapter 2 will focus on characterizing the morphological and biochemical changes in DRG neurons as they are exposed to different concentrations of Mn. Chapter 3 will focus on elucidating the role of Schwann cells in modulating manganese induced cytotoxicity in DRG neurons. Finally, Chapter 4 will summarize the conclusions and

provide a brief discussion of my key findings as well as a brief outline of prospects for future studies

1.14 ROLES IN OTHER COLLABORATIVE RESEARCH PROJECTS

Apart from my thesis research project, I have also participated in three other studies in our laboratory: (i) depletion of mitochondrial DNA disrupts the communication between nuclear and mitochondrial genome (Neti, 2014). I have also participated in two other collaborative projects ((ii) one on nanotoxicology of metallic oxide nanoparticles; (iii) the other on the effects of glycolytic enzyme inhibitors on cell death mechanisms in human neuroblastoma and astrocytoma cells) of Dr. Lai's laboratory as part of my further training in research in areas other than my major interest in neuroscience. Some of the findings of these participated have been published in a proceedings paper presented in Nanotech 2014 (Lai et al., 2014a) and in an abstract of a paper presented at the Annual Meeting of the American Association for Cancer Research (Bhushan et al., 2014). However, discussion of these collaborative projects (see Bhushan et al., 2014 for details) that I have participated in is beyond the scope of this thesis.

1.15 REFERENCES

Bhushan, A., Chatterji, T., Wong, Y. Y. W., Rizvi, N., Balaraju, A. K, Neti, A., Lai, J. C. K. Iodoacetate and 3-Bromopyruvate exert differential effects on human neurotumor SK-N-SH and U-87 cells. Annual Meeting of American Association for Cancer Research, April 5-9, 2014, San Diego, CA (in Abstracts Volume).

Bowman, A. B., Kwakye, G. F., Hernandez, E. H., Aschner, M. Role of manganese in neurodegenerative diseases. J Trace Elem Med Biol. 2011; 25 (4): 191-203.

Couper, J. "On the effects of black oxide of manganese when inhaled into the lungs". Br. Ann. Med. Pharm. 1837; 1: 41–42.

Clark, J. B., Lai, J. C. K. Glycolytic, Tricarboxylic Acid Cycle, and Related Enzymes in Brain. In NeuroMethods (Boulton AA, Baker GB & Butterworth RF, eds.). Humana, Clifton, NJ. 1989; 11: 233-281.

Dorman, D. C., Struve, M. F., Clewell, H. J. Application of pharmacokinetic data to the risk assessment of inhaled manganese. Eurotoxicology. 2006; 27(5): 752-764.

Dotti, C. G., Sullivan, C. A., Banker, G. A. The establishment of polarity by hippocampal neurons in culture. J Neurosci. 1988; 8: 1454–1468.

Dukhande, V. V., Malthankar, G. H., Hugus, J. J., Daniels, C. K. Manganese induced neurotoxicity is differentially enhanced by glutathione depletion in astrocytoma and neuroblastoma cells. Neurochem. Res. 2006; 31(11): 1349-1357

Dukhande, V. V., Kawikova, I., Bothwell, A. L. M., Lai, J. C. K. Neuroprotection against neuroblastoma cell death induced by depletion of mitochondrial glutathione. Apoptosis. 2013; 18(6): 702-712.

Du, P., Buerstatte, C. R., Chan, A. W. K., Minski, M. J., Bennett, L., Lai, J. C. K. Accumulation of manganese in liver can result in decreases in energy metabolism in mitochondria. Conference Proceedings of 1997 Conference on Hazardous Wastes & Materials, 1997; 1-14.

Eid, T., Tu, N., Lee, T. S. W., Lai, J. C. K. Regulation of Astrocyte Glutamine Synthetase in Epilepsy. Neurochem Int. 2013; 63(7): 670-681.

Erikson, K. M., Syversen, T., Aschner, J., Aschner, M. Ineractions between excessive manganese-exposure and dietary iron-deficiency in neurodegeneration. Environ Toxicol Pharmacol. 2005; 19: 415-421.

Federico, A., Cardaioli, E., Da Pozzo, P., Formichi, P., Gallus, G. N., Radi, E. Mitochondria, oxidative stress and neurodegeneration. J Neurol Sci. 2012; 322(1-2): 254-262.

Fernsebner, K., Zorn, J., Kanawati, B., Walker, A., Michalke, B. Manganese leads to an increase in markers of oxidative stress as well as to a shift in the ratio of Fe(II)/(III) in rat brain tissue. Metallomics. 2014; 6(4): 921-931.

Fitsanakis, V. A, Aschner, M. The importance of glutamate, glycine, and gamma-aminobutyric acid transport and regulation in manganese, mercury and lead neurotoxicity. Toxicol Appl Pharmacol. 2005; 204(3): 343–354.

Higashi, Y., Asanuma, M., Miyazaki, I. Parkin attenuates manganese induced dopaminergic cell death. J Neurochem 2004; 89(6): 1490-1497.

Parkinson's disease: Hope through research. http://www.ninds.nih.gov/disorders/parkinsons_disease/parkinsons_disease.htm. Accessed on May 2014.

Heavy metals. http://www.dartmouth.edu/~rpsmith/Heavy_Metals.html. Accessed on May 2014.

Jaiswal, A. R., Wong, Y. Y. W., Bhushan, A., Daniels, C. K., Lai, J. C. K. A noncontact co-culture model of peripheral neural cells for nanotoxicity, tissue engineering and

pathophysiological studies. In chapter 8: Environment, Health and Safety, in Technical Proceedings of the 2010 NSTI Nanotechnology Conference and Expo-Nanotech 2010. 2010; 3: 527–531.

Jaiswal, A. R., Lu, S. Y., Pfau, J., Wong, Y. Y. W., Bhushan, A., Leung, S. W., Daniels, C. K., Lai, J. C. K. Effects of silicon dioxide nanoparticles on peripheral nervous system neural cell models. In chapter 7: Environment, Health and Safety, Technical Proceedings of the 2011 NSTI Nanotechnology Conference and Expo-Nanotech 2011. 2011; 3: 541–544.

Kitazawa, M., Anantharam, V., Yang, Y., Hirata, Y., Kanthasamy, A., Kanthasamy, A. G. Activation of protein kinase C delta by proteolytic cleavage contributes to manganese-induced apoptosis in dopaminergic cells: protective role of Bcl-2. Biochem Pharmacol. 2005; 69(1): 133-146.

Lai, J. C. K., Clark, J. B. Isolation and characterization of synaptic and non-synaptic mitochondria from mammalian brain. In NeuroMethods, Vol. 11 (Boulton AA, Baker GB & Butterworth RF, eds.). 1989; pp. 43-98, Humana, Clifton, NJ.

Lai, J. C. K., Leung, T. K. C., Lim, L. Differences in the neurotoxic effects of manganese during development and aging: Some observations on brain regional neurotransmitter and non-neurotransmitter metabolism in a developmental rat model of chronic manganese encephalopathy. Neurotoxicol. 1984; 5: 37-48.

Lai, J. C. K., Leung, T. K. C., Lim, L. Effects of metal ions on neurotransmitter function and metabolism. In metal ions in neurology and psychiatry (Neurology and

Neurobiology, Vol. 15) (Gabay S, Harris J & Ho BT, eds.). 1985a; 15: 177-197, Alan Liss, New York.

Lai, J. C. K., Chan, A. W. K., Minski, M. J., Leung, T. K. C., Lim, L., Davison, A. N. Application of instrumental neutron activation analysis to the study of trace metals in brain and metal toxicity. Metal ions in neurology and psychiatry (Neurology and Neurobiology, Vol. 15) (Gabay S, Harris J & Ho BT, eds.). 1985b; 15: 323-343, Alan Liss, New York.

Lai, J. C. K., Chan, A. W. K., Minski, M. J., Lim, L. Roles of metal ions in brain development and aging. Metal ions in neurology and psychiatry (neurology and neurobiology, vol. 15) (Gabay S, Harris J & Ho BT, eds.). 1985c; 15: 49-67, Alan Liss, New York.

Lai, J. C. K., Minski M. J., Chan, A. W. K., Lim, L. Interrelations between manganese and other metal ions in health and disease. Metal ions in biological systems (Sigel A & Sigel H, eds.). 2000; 37: 123-156, Marcel Dekker, New York, NY.

Lai, J. C. K., Leung, S. W. Manganese and its interrelation with other metal ions in health and disease. Encyclopedia of Metalloproteins (Kretsinger RH, Uversky VN & Permyakov EA, eds.). 2013; pp. 1308-1314, Springer, New York, NY.

Lai, J. C. K., Balaraju, A. K., Neti, A., Lai, M. B., Tadinada, S. M., Idikuda, V. K., Singh, M. R. M., Mukka, K., Pfau, J., Bhushan, A., Leung, S. W. Zinc oxide nanoparticles induced apoptosis and necrosis in human neuroblastoma and astrocytoma cells. Technical proceedings of the 2014 NSTI nanotechnology conference & expo,

nanotech 2014 Vol. 3, section 2. sustainable nanotechnolog: environmental apps. & EHS implications. 2014a; pp. 138-141.

Levy, B.S., Nassetta, W.J. Neurologic effects of manganese in humans: a review. Int J Occup Environ. Health. 2003; 9: 153–163.

Liao, S. L., Chen, C. J. Manganese stimulates stellation of cultured rat cortical astrocytes. Neuroreport. 2001; 12(18): 3877–3881.

Lipe, G. W., Du hart, H., Newport, G. D. Effect of manganese on the concentration of amino acids in different regions of the rat brain. J Environ Sci Health Part B, Pesticides, Food Contaminants, and Agricultural Wastes. 1999; 34(1): 119-132.

Lloyd, R. V. Mechanism of the manganese-catalyzed autooxidation of dopamine. Chem Res Toxicol. 1995; 8(1): 111-116.

Maciel, E. N., Kowaltowski, A. J., Schwalm, F. D., Rodrigues, J. M., Souza, D. O., Vercesi, A. E., Wajner, M., Castilho, R. F. Mitochondrial permeability transition in neuronal damage promoted by Ca^{2+} and respiratory chain complex II inhibition. J Neurochem. 2004; 90(5): 1025-1035.

Malthankar, G. V., White, B. K., Bhushan, A., Daniels, C. K, Rodnick, K. J., Lai J. C. K. Differential lowering by manganese treatment of activities of glycolytic and tricarboxylic acid (TCA) cycle enzymes investigated in neuroblastoma and astrocytoma cells is associated with manganese-induced cell death. Neurochem Res. 2004; 29(4): 709-717.

McCollum, E. V. A History of nutrition. Boston: Houghton Mifflin Company. 1957; pp. 203-212.

McCay, C. M. Notes on the History of nutrition research, (Verzar F,ed) Berne: Hans Huber, 1973.

O'Dell, B. L., Sunde, R. A. Hand book of essential mineral elements. Marcel Decker Inc. 1997; ISBN 0-8247-9312-9.

Pertz, O. C., Wang. Y., Yang, F., Wang, W., Gay, L. J., Gristenko, M. A., Clauss, T. R., Anderson, D. J., Liu, T., Auberry, K. J., Camp II, D. G., Smith, R. D., Klemke, R. L. Spatial mapping of the neurite and soma proteomes reveals a functional Cdc42/Rac regulatory network. PNAS. 2008; 105 (6): 1931-1936

Parkinson's disease. http://www.ninds.nih.gov/disorders/parkinsons_disease/parkinsons_disease.htm. Accessed on July 2014.

Tahirovic, S., Bradke, F. Neuronal Polarity. Cold Spring Harb Perspect Biol 2009; 1(3): a001644.

Saric, M., Piasek, M. Environmental exposure to manganese and combined exposure to gaseous upper respiratory irritants: Mechanism of action and adverse health effects. Reviews on Environmental Health. 2000; 15(4), 413-419.

Stefan, K. Mitochondria: Structure and Role in Respiration. eLS. John Wiley & Sons Ltd, Chichester. 2001.

Steketee, M. B., Moysidis, S. N., Weinstein, J. E., Kreymerman, A., Silva, J. P., Iqbal, S., Goldberg, G. L. Mitochondrial dynamics regulate growth cone motility, guidance, and

neurite growth rate in perinatal retinal ganglion cells in vitro. Invest Ophthalmol Vis Sci. 2012; 53(11): 7402-7411.

Stephen, H. R., Graham, B., Donald, R. S. Brain accumulation and toxicity of Mn(ii) and Mn(iii) exposures. Toxicol Sci. 2006; 93(1): 114-124.

Thomson, A. B. R, Volberg, L. S. Intestinal uptake of iron, cobalt, and manganese in the iron deficient rat. Am J Physiol. 1972; 223: 1327-1329.

Wedler, F. C. Biological significance of manganese in mammalian systems. Prog Med Chem. 1993; 30: 89-133.

http://www.who.int/water_sanitation_health/dwq/chemicals/manganese/en/. Accessed on July 2014.

Zheng, W., Zhao, Q. Tron overload following manganese exposure in cultured neuronal, but not neuroglial cells. Brain Res. 2001; 897 (1-2): 175-179.

CHAPTER 2. CHARACTERIZATION OF DRG NEURONS AS AN IN VITRO CELL MODEL TO STUDY MANGANESE-INDUCED NEUROTOXICITY

Anurag K. Balaraju[1], Solomon W. Leung[2], Alok Bhushan[3], and James C.K. Lai[1]

[1]Department of Biomedical & Pharmaceutical Sciences, College of Pharmacy, Division of Health Sciences and Biomedical Research Institute, Idaho State University, Pocatello, ID 83209;

[2]Department of Civil & Environmental Engineering,, College of Science & Engineering, Idaho State University, Pocatello, ID 83209; and

[3]Department of Pharmaceutical Sciences, Jefferson School of Pharmacy, Thomas Jefferson University, Philadelphia, PA 19107.

2.1 ABSTRACT

Manganism is a neurodegenerative disease resulting from the chronic exposure of neurons to toxic levels of manganese. In manganism, manganese accumulates in mitochondria and causes mitochondrial dysfunction and a rise in oxidative stress which is followed by neuronal cell death. Mitochondrial dysfunction is a feature not only found in manganism but also in many other neurodegenerative diseases. The study of manganese-induced neurotoxic mechanisms in neurons will allow us to gain insights into pathogenentic mechanisms. To date, manganese-induced neurotoxic mechanisms have been studied in neurotumors cells which have limitations as they are tumor cells. To bypass the limitations of employing neurotumor cells as a model, we have developed an in vitro cell model employing rat dorsal root ganglion (DRG) neurons derived from the peripheral nervous system and have determined their suitability as a neuronal model for studying manganese neurotoxicity by investigating the manganese-induced effects on cellular energetics and mitochondrial dynamics in DRG neurons. Our results demonstrated that the manganese-induced death of DRG neurons could be attributed, at least in part, to the manganese-induced changes in their cellular energetics and mitochondria structure and function. Our findings strongly suggest DRG neurons constitute an excellent cell model in vitro for investigating the cellular and molecular mechanisms underlying manganese-induced neurotoxicity in particular and toxicant-induced neurotoxicity in general. Moreover, our results may have pathophysiological implications in peripheral neuropathy and neurodegeneration.

Key Words: manganism, neurodegenerative diseases, dorsal root ganglion (DRG) neurons, oxidative stress, mitochondrial dynamics, apoptosis, necrosis, lactate

dehydrogenase, malate dehydrogenase, mitochondrial fission, mitochondrial fusion, flow cytometer, confocal imaging, AMPK and p-AMPK.

2.2 INTRODUCTION

Neurodegenerative diseases (NDD) comprise a wide range of diseases such as Alzheimer's disease (AD), Parkinson's disease (PD), Huntington's disease (HD) and Manganism: they share a characteristic feature of progressive loss of neurons. Although many neurodegenerative diseases affect specific neuronal populations, there are many similarities which include atypical protein assemblies and oligomerization, along with cell death. These similarities among various neurodegenerative diseases suggest a common underlying mechanism of neurodegeneration (Winner et al., 2011). Mitochondria, which play a critical role in regulating and/or mediating cell death, are often associated with atypical protein assemblies (Winner et al., 2011).

Mitochondria are known to play an essential role in many cellular functions such as cellular energetics, calcium buffering and apoptosis. Mitochondrial dysfunction is a common theme in many neurodegenerative diseases. For example, a chronic exposure of PC-12 cells to sub-lethal doses of Aβ peptide inhibited transport of nuclear encoded proteins to mitochondria and impaired mitochondrial function (Sirk et al., 2007). Also, Aβ peptides binds to a mitochondrial protein called Aβ-binding alcohol dehydrogenase (ABAD) and blocking the interaction of Aβ and ABAD can suppress Aβ-induced apoptosis and free-radical generation in neurons (Lustbader et al., 2004). Similarly, in other neurodegenerative diseases such as PD, HD and amyotrophic lateral sclerosis (ALS) morphological and functional changes in mitochondria have been observed (Lezi

et al., 2012). Thus, elucidation of the role(s) of mitochondria in neurodegenerative conditions will not only better define the underlying molecular mechanisms but also reveal some of the pathophysiological features common to most, if not all, neurodegenerative diseases.

Manganism, another neurodegenerative condition similar to PD in many respects, is induced by chronic exposure to toxic levels of manganese (Mn) (Lai and Leung, 2013). Upon entering cells, Mn primarily targets mitochondria and accumulates in the mitochondrial matrix (Lai et al., 1985; Lai et al., 1999). Excessive Mn accumulation in mitochondria impairs calcium homeostasis (Lai et al., 1985; Lai et al., 1999) and ultimately disrupts the mitochondrial membrane potential, leading to altered mitochondrial function and enhanced oxidative stress (Gavin et al., 1999). It is this enhanced oxidative stress resulting from an imbalance between the pro- and anti-oxidants, that exposes the intracellular structures to higher than normal levels of free radicals, the dire consequence of which is the death of the cell(s) so afflicted (Dukhande et al., 2006; Dukhande et al., 2013).

Accumulation of Mn in mitochondria in neural cells also impairs electron transport chain and uncouples oxidative phosphorylation, leading to mitochondrial dysfunction, followed by neurodegeneration (Lai et al., 1985; Lai et al., 1999; Gavin et al., 1999). Therefore, these observations reinforce the utility of investigating Mn-induced neurotoxicity as a means of better understanding the role of mitochondria in NDD.

Employing human neuroblastoma SK-N-SH (neurons-like) and astrocytoma U87 (astrocytes-like) cells as neural cell models in vitro, we previously demonstrated Mn toxicity exerted differential cytotoxicity on SK-N-SH (neurons-like) and U87 (astrocytes-

like) cells, SK-N-SH cells being more susceptible than U87 cells to manganese toxicity (Malthankar et al., 2004; Dukhande et al., 2006; Dukhande et al., 2013). The Mn-induced differential cytotoxicity on SK-N-SH and U87 cells led to both apoptosis and necrosis, depending on the concentration of Mn (Malthankar et al., 2004; Dukhande et al., 2006; Dukhande et al., 2013): associated with the two cell death modes induced by Mn were the Mn-induced differential lowering of energy-metabolizing enzymes in the two neural cell types (Malthankar et al., 2004). Moreover, one clear cytotoxic effect of Mn was to induce oxidative stress in these two neural cell types and SK-N-SH cells were also more susceptible than U87 cells to this Mn-induced oxidative stress, in part because their gluthathione (GSH) levels were significantly lower than those in U87 cells (Dukhande et al., 2006; Dukhande et al., 2013). Additionally, depletion of their mitochondrial GSH rendered the already vulnerable SK-N-SN (neurons-like) cells even more vulnerable to the cytotoxicity of Mn (Dukhande et al., 2013). Thus, these two neural cell types (namely SK-N-SH and U87 cells) have allowed the elucidation of some of the mechanisms underlying the Mn-induced neurodegeneration.

We have previously shown that SK-N-SH and U87 cells are respectively good models in vitro of neurons and astrocytes, especially in view of the fact they closely resemble neurons and astrocytes in brain in that, similar to neurons and astrocytes (Raps et al., 1989), SK-N-SH (neurons-like) and U87 (astrocytes-like) cells contain very low and much higher endogenous levels of GSH, respectively (Dukhande et al., 2006; Dukhande et al., 2013). Nevertheless, because both SK-N-SH and U87 cells are tumor cells, we recognize they have their limitations. Indeed, the recent availability of dorsal root ganglion (DRG) neurons not derived from tumor cells (Chen et al., 2007) have

allowed us to employ them to develop neural cell models in vitro for investigating cellular and molecular mechanisms of peripheral neuropathy and those underlying toxin-induced neurodegeneration (Jaiswal et al., 2010; Lai et al., 2011; Jaiswal et al., 2011).

The major goal of this study is to further develop DRG neurons (Chen et al., 2007) as a neuronal cell model in vitro for systematic investigation of cellular and molecular mechanisms underlying Mn toxicity. In particular, we have investigated our hypothesis that Mn induces apoptosis at lower concentrations but necrosis at higher concentrations through disrupting cellular bioenergetics and mitochondrial dynamics.

2.3 MATERIALS AND METHODS

Materials

Dorsal root ganglion (DRG) neurons (Chen et al., 2007) were a gift from Dr. Höke of Johns Hopkins University School of Medicine and Schwann cells (S16) were obtained and ATCC (Manassas, VA). MTT (3-(4,5-dimethylthiazol-2-yl)-2,5-diphenyltetrazolium bromide), DTNB (5,5'-dithiobis-(2-nitrobenzoic acid), Dulbecco's minimal essential medium (DMEM), dimethyl sulfoxide (DMSO) and fetal bovine serum (FBS) were obtained from Sigma - Aldrich (St. Louis, MO). The fluorescent dye (Chloro methyl derivative of 2',7'-dichlorodihydrofluorescein diacetate or CM-H2DCFDA) and BCA protein assay kit were obtained from Molecular probes (Eugene, OR) and Thermo-Pierce (Rockford, IL), respectively.

Cell Culture

DRG neurons and S16 Schwann cells were cultured in DMEM medium supplemented with glucose (25.19 mM), sodium pyruvate (1 mM), sodium bicarbonate (17.8 mM), L-glutamine (2 mM) and 10 % (v/v) FBS. Cells were maintained at 37 °C and 5 % (v/v) CO_2 until they were 70 % confluent when they were usually then used for experiments (Lai et al., 2008).

Equal number of DRG neurons or S16 Schwann cells (i.e., the monotypic cultures) or both cell types together (i.e., the co-cultures) were seeded into T-75 flasks and the cells were allowed to reach 70 % confluency. The cultures were then treated with various concentrations (0, 100, 200, 300, 400 or 500 µM) of manganese chloride for 24 hours. The medium from the treated cells (i.e., conditioned medium) was collected, centrifuged at 1000 x g for 5 minutes to remove any cells in suspension and stored at -80 °C until they were employed for experiments.

Conditioned media from the co-cultures and monotypic cultures were used separately to culture DRG neurons in T-75 flasks, 96-well plates or 24-well plates until they were 70 % confluent. They were then used for various experiments and to prepare lysates for Western blot analysis.

MTT assay

Viability and survival of DRG neurons and Schwann cells were determined by MTT assay as described by Lai et al. (2008). Cells were seeded at a density of 4000 cells per well in a 96-well plate. Cells were allowed to settle and then treated with manganese chloride (0 µM, 100 µM or 200 µM) for 48 hours at 37 °C. 20µL of MTT dye (0.5 %

(w/v) in phosphate-buffered saline) was added to each well and the plate was incubated for another 4 hours at 37 °C. Immediately thereafter, the medium in the wells was aspirated carefully without unsettling the formazan crystals formed on the bottom of the wells. Subsequently, the formazan crystals were dissolved using 100 µL of HPLC grade dimethyl sulfoxide (DMSO) per well. The absorbance of the solution in each well was measured at 567 nm using a multi-detection microplate reader (Bio-Tek Synergy HT, Winooski, VT).

Cellular morphology

The putative changes in the morphology of DRG neurons treated with specified concentrations of manganese chloride for 48 hours at 37 °C as described above were compared to the morphology of untreated (i.e., control) DRG neurons by light microscopy. Bright field images of the Mn-treated and control DRG neurons were acquired using a Leica light microscope (Leica DM IRB, Bannockburn, IL), equipped with a digital camera (Leica DFC 300FX) as described previously (Lai et al., 2008).

LDH release assay

Necrotic damage to the DRG neurons was determined by measuring the release of lactate dehydrogenase (LDH) from the cells into the culture medium. LDH release into the extracellular fluid serves as a marker of necrotic cell damage and cell death (Lai et al., 2008; Bhardwaj et al., 2010; Tadinada et al., 2013). DRG neurons were cultured in DMEM in 75 cm^2 flasks until they were 70 % confluent and then treated with 0, 10, 50, 100, 500 or 1000 µM of manganese chloride for 48 hours at 37 °C. Then the culture medium from each flask was removed and kept at −70 °C until they were used for

assaying LDH activity therein. LDH activity released by DRG neurons into the culture medium was measured by the procedure of Clark and Lai (1989).

Treatment of DRG neurons to be used for lactate dehydrogenase and malate dehydrogenase assays

DRG neurons were plated in T-75 flasks and incubated at 37 °C and 5 % (v/v) CO_2 until they were 70 % confluent. They were then treated with 100 or 200 µM $MnCl_2$ in DMEM medium for 24 hours at 37°C and 5 % (v/v) CO_2.

Preparation of cell homogenates for enzyme assays

The medium from flasks containing Mn-treated or untreated (i.e., the control) DRG neurons was aspirated and flasks placed on ice to slow down cell metabolism. Traces of medium remaining were completely removed by washing the cells gently with ice-cold and particulate-free sterile phosphate-buffered saline (PBS). Trypsin was employed to detach cells from the surface of flask. Ice-cold and particulate-free sterile PBS was later added to the detached cells to minimize the adverse effects of trypsin. Immediately, cells were collected by centrifuging the suspension at 1000 x g for 5 minutes at 4 °C and washing steps were performed with sterile PBS. The cells were then suspended in sterile ice-cold isolation medium (0.32 M Sucrose-5 mM HEPES-Tris, pH 7.4), transferred to a Dounce homogenizer, and homogenized at 4 °C. The cell homogenate so prepared was immediately employed for assaying activities of lactate dehydrogenase and malate dehydrogenase therein. The protein contents of the cell homogenates were determined using the Bicinchoninic protein assay.

Protein determination using the Bicinchoninic protein assay

Protein contents of cell homogenates or lysates had to be determined because protein levels are generally used as a reference quantity when different biochemical parameters (e.g., enzyme activities, sample loading in Western blots, etc.) were to be compared. Bicinchoninic protein assay was therefore employed to determine protein contents of cell homogenates or lysates (Lai et al., 2008). Various concentrations of bovine serum albumin were used to construct the protein standard curve.

Lactate dehydrogenase assay

Lactate dehydrogenase assay was performed as described by Lai and Blass (1984). Pyruvate was converted to lactate by LDH with the simultaneous oxidation of NADH. The reaction mixture contained 0.1 M potassium phosphate buffer (pH 7.4), 0.25 mM NADH, 0.5 % (v/v) Triton X-100, 1.65 mM pyruvate, pre-determined volume of cell homogenate in a final volume of 1 ml. The rate of NADH oxidation was monitored at 340 nm by measuring the rate of decrease in absorbance.

NAD-linked malate dehydrogenase assay

Malate dehydrogenase assay was performed as described by Lai and Clark (1976, 1978). The principle of the enzyme-catalyzed reaction involves conversion of oxaloacetate to malate with simultaneous oxidation of NADH. The reaction mixture contained 0.1 M potassium phosphate buffer (pH 7.4), 0.16 mM NADH, 0.16 % (v/v) Triton X-100, 0.133 mM oxaloacetate, and pre-determined volume of cell homogenate in a final volume of 1 ml. The rate of NADH oxidation was monitored at 340 nm by measuring the rate of decrease in absorbance.

Immunocytochemical analysis

The PBS-washed Mn-treated or control DRG neurons in T-25 flasks (see procedures depicted above) were placed on ice to slow down metabolism in cells. To detach cells from the surface of the flasks, cells were exposed to trypsin for a few minutes. Ice-cold, particulate-free and sterile PBS was then added to the flasks to minimize the adverse effect of the trypsin. Subsequently, the cell suspension was centrifuged at 1000 x g for 5 minutes and washed with additional PBS to remove the traces of trypsin remaining. The washed cells were re-suspended in 200 µL of ice-cold, particulate-free and sterile PBS and 200 µL of 4 % (w/v) paraformaldehyde was added. The suspension was incubated in the dark at 4 °C for 2 hours. The paraformaldehyde-fixed cells were collected by centrifugation at 1000 x g for 5 minutes, then washed twice, and later centrifuged at 1000 x g for 5 minutes and washed with ice-cold, particulate-free and sterile PBS. The washed fixed cells were re-suspended in 500 µL of permeabilization buffer (0.1 % (v/v) Triton X-100 in PBS) for 30 min at 4 °C. Immediately thereafter, the suspension was centrifuged at 1000 x g for 5 minutes and the cell pellet was suspended in the primary staining buffer (primary antibody at 1:1000 dilution in PBS supplemented with 5 % FBS) and incubated in the dark for 30 minutes. The above step was repeated with the secondary staining buffer (conjugated secondary antibody at 1:1000 dilution in 1X PBS supplemented with 5 % FBS). The stained cells were washed thrice with ice-cold, particulate-free and sterile PBS and finally re-suspended in 500 µL of the same PBS.

Apoptosis and necrosis assays

DRG neurons plated in T-25 flasks were treated with various specified concentrations (0, 100, 200, 300, 400 or 500 µM) of Mn as described above for 24 or 48 hours and untreated DRG neurons served as the control. A flask containing untreated DRG neurons was exposed to ultraviolet radiation (UV light) for 45 minutes. (UV light induces apoptosis in cells: hence, the flask exposed to UV light served as a positive control for apoptosis (Torsten et al., 2001).) The various aliquots of Mn-treated or control DRG neurons were then collected after treatment with trypsin and washed with BPS as described above. For each type of prepared aliquot of DRG neurons, the following staining procedure was carried out: (i) cell aliquot was unstained (i.e., the control); (ii) cell aliquot was stained with annexin V only; (iii) cell aliquot was stained with propidium iodide only; (iv) cell aliquot was stained with both annexin V and propidium iodide. Cell staining occurred at room temperature in the dark for 30 minutes. The stained cell aliquots were then washed thrive with ice-cold, particulate-free and sterile PBS to remove the dyes. The washed, stained cell aliquots were finally analyzed in a flow cytometer (Becton Dickinson Biosciences FACS Calibur 2-laser/4-color flow cytometer, analyzed using CellQuest software, BD Biosciences, San Jose CA).

Confocal microscopy

DRG neurons were plated on a coverslip in each well of 6-well flat-bottom cell culture plates. The cell seeding density (20000 cells per well) was kept low to make sure that the cells were far apart for easy observation and analysis. DRG neurons were treated with 0, 100, 200 or 300 µM of manganese chloride in medium for 48 hours. At the end of the treatment, the medium in the 6-well plates was replaced with warm serum-free

DMEM medium containing Mitotracker Red dye (40 nM) and the cells were incubated for 20 minutes at 37 °C and 5 % (v/v) CO_2. Then the dye-containing medium was replaced with serum-free DMEM medium and the cells were gently washed. The cell-washing step was repeated thrice and the medium in the final washing step was replaced with 4 % (w/v) paraformaldehyde in 1X sterile PBS and incubated at 37 °C and 5 % (v/v) CO_2 for 20 minutes. After the fixation step, the cells were washed thrice in sterile PBS. Subsequently, the PBS was aspirated and each coverslip containing cells was mounted on a glass slide using hard mount medium in such a way that the cells on the cover slip faced the surface of the glass slide. The slides were stored at 4 °C or immediately analyzed using confocal microscopy. All images of the stained cells were captured using the Olympus FV 1000 inverted laser scanning confocal microscope with 4-channel simultaneous acquisition employing the 100 X oil objective.

Statistical analysis of data

Results are presented as mean ± standard error of mean (SEM) of at least 3 replicates in each experiment. Analysis of data was performed employing one-way analysis of variance (ANOVA) followed by the post-hoc Tukey test for multiple comparisons using KaleidaGraph version 4 (Synergy Software, Reading, PA). Significance level was set at $p < 0.05$.

2.4 RESULTS

Manganese induced cell death in DRG neurons and Schwann cells as evaluated by cell survival/death assays and photomicrographs.

Treatment of dorsal root ganglion (DRG) neurons with manganese chloride for 48 hours at concentrations higher than 1 μM induced concentration-related decreases in their survival with an apparent IC_{50} (i.e., concentration of manganese that gave rise to 50% decrease in survival) of ~ 200 μM (Figure 2.1). At the highest manganese treatment of 1 mM, only some 10% of DRG neurons survived (Figure 2.1). By contrast with the effect of manganese on DRG neurons, treatment of Schwann cells with manganese chloride for 48 hours at concentrations higher than 100 μM induced concentration-related decreases in their survival with an apparent IC_{50} of ~300 μM (Figure 2.2). Nevertheless, at the highest manganese treatment of 1 mM, only some 10% of Schwann cells survived (Figure 2.2). Thus, these findings (Figures 2.1 and 2.2) strongly suggested DRG neurons were more susceptible than Schwann cells to the cytotoxic effects of manganese.

Morphological examination of DRG neurons treated with increasing concentrations of manganese chloride (Figure 2.3) under light microscopy also revealed that manganese treatment induced a concentration-related changes in the morphology of DRG neurons: at the highest manganese treatment concentrations of 500 and 1000 μM, DRG neurons appeared more swollen (a sign of necrotic damage) and few intact neurons were seen (Figure 2.3, E and F). Thus, these morphological findings were compatible with the findings employing cell survival assays (Figure 2.1).

Effect of manganese on cell death mechanisms

To determine the cell death mechanisms occurring in DRG neurons resulting from the treatment with various concentrations of manganese, we employed flow cytometry and assay of LDH release from DRG neurons into their medium. In cell death assay performed using flow cytometry, we observed an uptake of annexin V dye (an indicator of apoptosis) by DRG neurons treated with manganese (Figs. 2.4-2.5). The results of this cell death assay using flow cytometry suggested apoptosis as one possible cell death mechanism in DRG neurons treated with manganese (Figs. 2.4-2.5). Indeed, while treatment with 100 µM $MnCl_2$ (Fig. 2.5, panel 1) did not significantly increase the % of apoptotic DRG neurons (from 3.45% to 3.77%), treatment with $MnCl_2$ from 200 to 500 µM induced concentration-related increases in the % of apoptotic DRG neurons (from 25.48% to 72.51%) (Figs. 2.4-2.5).

Treatment with increasing Mn concentrations induced both apoptosis and necrosis in DRG neurons (Figs. 2.4-2.7). Results from flow cytometric analysis employing propidium iodide to label necrotic DRG neurons (Fig. 2.7) indicated that treatment with $MnCl_2$ from 100-300 µM induced some Mn-related increases in necrosis in these neurons (Fig. 2.7). However, at $MnCl_2$ higher than 300 µM, the Mn-treated DRG neurons showed some decreases in necrosis (Fig. 2.7). We also detected the presence of lactate dehydrogenase (LDH), an indicator of necrotic cell death, in the medium after treating DRG neurons with various concentrations of $MnCl_2$ (Fig. 2.6). The release of LDH by DRG neurons treated with $MnCl_2$ was dose-related but biphasic, showing dose-related increases between 10-300 µM $MnCl_2$ but decreases beyond 300 µM $MnCl_2$ (Fig. 2.6). Thus, the results of the Mn-induced LDH release from DRG neurons (Fig. 6) closely

paralleled the results obtained employing propidium iodide staining of DRG neurons analyzed with flow cytometry (Fig. 2.7).

Effect of manganese on LDH and MDH activities in DRG neurons

Based on the findings of the cytotoxic effects of $MnCl_2$ discussed thus far, we examined the effects of treatment with 100 µM and 200 µM $MnCl_2$ on the activities of lactate dehydrogenase (LDH) (Fig. 2.8) and malate dehydrogenase (MDH) (Fig. 2.9) in DRG neurons. We found both 100 µM and 200 µM $MnCl_2$ induced significant lowering of LDH (Fig. 2.8) and MDH (Fig. 2.9) activities in DRG neurons indicating the Mn-induced decreases in energy metabolism in these neurons.

Effect of manganese on AMP-activated protein kinase (AMPK) and phospho-AMPK levels

AMP activated protein kinase (AMPK) is an enzyme which plays a crucial and central role in energy homeostasis. We performed immunocytochemical analysis employing anti-AMPK and anti-phospho-AMPK antibodies using flow cytometry and then calculated the ratios of phopho-AMPK (p-AMPK) to AMPK ratios in DRG neurons treated with various concentrations of $MnCl_2$ (Fig. 2.10). We found the p-AMPK to AMPK ratios showed a trend of increase in DRG neurons treated with 400 µM $MnCl_2$ but this ratio was decreased in DRG neurons treated with 500 µM $MnCl_2$ (Fig. 2.10) suggesting that Mn induced disturbances in energy homeostasis in DRG neurons

Effect of manganese on mitochondrial dynamics

Results of our confocal studies suggested a change in the morphology of mitochondria in DRG neurons treated with manganese compared to those in control DRG

neurons (Fig. 2.11). In general, mitochondria in control DRG neurons appeared to form clusters and chains in series both immediately surrounding their nuclei suggesting both fusion and fission were occurring (Fig. 2.11A). On the other hand, as DRG neurons were treated with increasing $MnCl_2$ concentrations from 100 to 300 μM (Fig. 2.11B to D), their mitochondria appeared to form smaller clusters and fewer chains in series compared to those in control DRG neurons (compare Fig. 2.11B to D with Fig. 2.11A). Moreover, the mitochondria in Mn-treated DRG neurons appeared to be more clustered around the nuclei rather than more evenly distributed in various parts of the cytoplasm as in control DRG neurons (Fig. 2.11). Thus, these findings suggested that Mn treatment induced a shift in the dynamic balance between fusion and fission in favor of fission.

2.5 DISCUSSION AND CONCLUSIONS

This is the first study that demonstrated manganese (Mn) treatment induces (i) differential cytotoxic effects on DRG neurons and Schwann cells, (ii) both apoptosis and necrosis in DRG neurons depending on its concentration, (iii) alterations in energy metabolism in DRG neurons; and (iv) changes in mitochondrial dynamics favoring a shift from fusion to fission.

Similar to the study of Lai et al. (1985) who showed that cerebrocortical neurons in primary culture are more susceptible than glial cells to neurotoxic effects of manganese, this study also demonstrated that DRG neurons are more sensitive to Mn toxicity compared to Schwann cells (Figs. 2.1 and 2.2). For example, the IC_{50} values for $MnCl_2$ in lowering the survival of DRG neurons (Fig. 2.1) and Schwann cells (Fig. 2.2) are, respectively, ~200 and ~300 μM. (Interestingly, Hernandez et al. (2011) also reported very similar values for $MnCl_2$ in lowering the survival of cerebrocortical

neurons in primary culture.) We have previously shown that human neuroblastoma SK-N-SH (neurons-like) cells are also more susceptible than human astrocytoma U87 (astrocytes-like) cells to the neurotoxicity of Mn (Malthankar et al., 2004); however, the IC_{50} values for $MnCl_2$ in lowering the survival of SK-N-SH and U87 cells (>500 µM; Malthankar et al., 2004) are much higher than the corresponding values in DRG neurons and Schwann cells.

To further determine the mechanism(s) underlying the Mn-induced cell death in DRG neurons, we employed annexin V to stain apoptotic (Figs. 2.4 and 2.5) and propidium iodide to stain necrotic (Fig. 2.7) DRG neurons and analyzed the stained neurons using flow cytometry. We also employed LDH release by DRG neurons into the medium as an indicator to monitor the Mn-induced necrosis in these neurons (Fig. 2.6). We found that treatment with increasing Mn levels induced both apoptosis and necrosis in DRG neurons (Figs. 2.4-2.7). This finding is compatible with our previous observation that Mn also induces both apoptosis and necrosis in human neuroblastoma SK-N-SH (neurons-like) cells (Dukhande et al., 2006). Treatment with $MnCl_2$ from 200 to 500 µM induced dose-related increases in % of apoptotic DRG neurons (Figs. 2.4-2.5). Results from propidium iodide staining of DRG neurons indicated treatment with $MnCl_2$ from 100-300 µM induced some Mn-related increases in necrosis in these neurons (Fig. 2.7). However, at $MnCl_2$ higher than 300 µM, the Mn-treated DRG neurons showed some decreases in necrosis (Fig. 2.7). The LDH release assay findings (Fig. 2.6) confirmed this dose-related but biphasic effect of Mn in inducing necrosis in DRG neurons.

In many neurodegenerative diseases, the underlying cell death mechanisms have not been fully elucidated; however, morphological, biochemical and genetic studies have

suggested a potential role of mitochondria (Martin, 2010). In studies related to neurodegenerative conditions induced by manganese exposure, mitochondrial dysfunction was commonly observed (Martin, 2010). Manganese primarily targets mitochondria and disturbs calcium homeostasis, thereby, causes mitochondrial dysfunction (Lai et al., 1985; Lai and Leung, 2013). Consequently, many physiological processes such as oxidative metabolism and cellular respiration located in mitochondria are expected to be disturbed in neurodegeneration. In this study, we found treatment with 100 µM and 200 µM $MnCl_2$ induced substantial decreases in activities of LDH (Fig. 2.8) and MDH (Fig. 2.9) in DRG neurons, suggesting that Mn treatment induced energy failure. These findings and conclusion are consistent with our previous observation that Mn treatment induced dose-related decreases in many glycolytic, tricarboxylic acid cycle and related enzymes in human neuroblastoma SK-N-SH (neurons-like) cells (Malthankar et al., 2004).

AMPK is an important sensor of energy status of a cell and controls cell metabolism. We found the p-AMPK to AMPK ratios showed a trend of increase in DRG neurons treated with 400 µM $MnCl_2$ but this ratio was decreased in DRG neurons treated with 500 µM $MnCl_2$ (Fig. 2.10) suggesting that Mn induced disturbances in energy homeostasis in DRG neurons. These findings are compatible with our observation that Mn induced decreases in LDH and MDH in DRG neurons (Figs. 2.8 and 2.9).

Employing light microscopy, we found that Mn treatment induces dose-related in morphology in DRG neurons (Fig. 2.3). Using Mitotracker red to stain mitochondria and confocal microscopy to reveal the fine structure and localization of mitochondria within DRG neurons (Fig. 2.11), we noted as DRG neurons were treated with increasing $MnCl_2$

concentrations from 100 to 300 μM (Fig. 2.11B to D), their mitochondria appeared to form smaller clusters and fewer chains in series compared to those in control DRG neurons (compare Fig. 2.11B to D with Fig. 2.11A). Moreover, the mitochondria in Mn-treated DRG neurons appeared to be more clustered around the nuclei rather than more evenly distributed in various parts of the cytoplasm as in control DRG neurons (Fig. 2.11). These findings (Fig. 2.11) suggested Mn treatment induced a shift in the dynamic balance between fusion and fission in favor of fission. Thus, ours is the first report of a Mn-induced shift in mitochondrial dynamics in DRG neurons in favor of fission. This conclusion is important and pathophysiological relevant because a balance between mitochondrial fusion and fission is critical in maintaining normal functioning of mitochondria (Galloway et al., 2012).

All in all, the results of this study allow us to make two conclusions. (i) DRG neurons constitute an excellent neural cell model in vitro for elucidating the cellular and molecular mechanisms underlying manganese neurotoxicity and Mn-induced peripheral neuropathy. (ii) Our results may assume pathophysiological importance in Mn-induced neurodegeneration in particular and neurodegeneration in general.

2.6 ACKNOWLEDGEMENTS

We thank Dr. Ahmet Höke of Johns Hopkins University School of Medicine for his gift of the DRG neurons. Our studies were supported, in part, by a DoD USAMRMC Project Grant (Contract #W81XWH-07-2-0078) and a small project grant from MSTMRI.

2.7 REFERENCES

Bhardwaj, V., Rizvi, N., Lai, M. B., Lai, J. C. K., Bhushan, A. Glycolytic enzyme inhibitors affect pancreatic cancer survival by modulating its signaling and energetics. Anticancer Res. 2010; 30 (3): 743-749.

Chen, W., Ruifa, M., Haughey, N., Oz, M., Höke, A. Immortalization and characterization of a nociceptive dorsal root ganglion sensory neuronal line. J Peripher Nerv Syst. 2007; 12(2): 121–130.

Dukhande, V.V., Malthankar-Phatak, G. H., Hugus, J. J., Daniels, C. K., Lai, J. C. K. Manganese-induced neurotoxicity is differentially enhanced by glutathione depletion in astrocytoma and neuroblastoma cells. Neurochem. 2006; 31(11): 1349-1357.

Dukhande, V.V., Kavikova, I., Bothwell, A. L., Lai, J. C. K. Neuroprotection against neuroblastoma cell death induced by depletion of mitochondrial glutathione. Apoptosis. 2013; 18(6):702-712.

Galloway, C. A., Yoon, Y. Perspectives on: SGP symposium on mitochondrial physiology and medicine. What comes first, misshape or dysfunction? The view from metabolic excess. J. Gen. Physiol. 2012; 139(6): 455–463.

Gavin, C.E., Gunter, K.K., Gunter, T.E. Manganese and calcium transport in mitochondria: implications for manganese toxicity. Neurotoxicol. 1999; 20(2-3): 445-453.

Hernandez, R. B., Farina, M., Esposito, B. P., Souza-Pinto, N. C., Barbosa, Jr, F., Sunol, C. Mechanisms of manganese-induced neurotoxicity in primary neuronal cultures: The role of manganese speciation and cell type. Toxicol Sci. 2011; 124(2): 414–423.

Jaiswal, A. R., Wong, Y. Y. W., Bhushan, A., Daniels, C. K., Lai, J. C. K. A noncontact co-culture model of peripheral neural cells for nanotoxicity, tissue engineering and pathophysiological studies. In chapter 8: Environment, Health and Safety, in Technical Proceedings of the 2010 NSTI Nanotechnology Conference and Expo-Nanotech 2010. 2010; 3: 527–531.

Jaiswal, A. R., Lu, S. Y., Pfau, J., Wong, Y. Y. W., Bhushan, A., Leung, S. W., Daniels, C. K., Lai, J. C. K. Effects of silicon dioxide nanoparticles on peripheral nervous system neural cell models. In chapter 7: Environment, Health and Safety, Technical Proceedings of the 2011 NSTI Nanotechnology Conference and Expo-Nanotech 2011. 2011; 3: 541–544.

Lai, J. C. K., Blass, J. P., Inhibition of brain glycolysis by aluminium. J. Neurochem. 1984a; 42: 438-446.

Lai, J. C. K., Clark, J. B. Isolation and characterization of synaptic and non-synaptic mitochondria from mammalian brain. Neuromethods. 1989; 11: 43-98.

Lai, J. C. K., Clark, J. B. Preparation and properties of mitochondria derived from synaptosomes. Biochem J. 1976; 154: 423-432.

Lai, J. C. K., Clark, J. B. Isocitric dehydrogenase and malate dehydrogenase in synaptic and non-synaptic rat brain mitochondria: a comparison of their kinetic constants. Biochem Soc Trans. 1978; 6:993-995.

Lai, J. C. K., Leung, T. K. C., Lim, L. Effects of metal ions on neurotransmitter function and metabolism. In metal ions in neurology and psychiatry (Neurology and Neurobiology, Vol. 15) (Gabay S, Harris J & Ho BT, eds.). 1985; 15: 177-197, Alan Liss, New York.

Lai, J. C. K., Lai, M. B., Jandhyam, S., Dukhande, V. V., Bhushan. A., Daniels, C. K., Leung, S. W. Exposure to titanium dioxide and other metallic oxide nanoparticles induces cytotoxicity on human neural cells and fibroblasts. Int J Nanomedicine. 2008; 3(4): 533–545.

Lai, J. C. K., Leung, S. W. Manganese, interrelation with other metal ions in health and disease. Encyclopedia of Metalloproteins. 2013; pp. 1308-1314.

Lezi, E., Swerdlow, R. H. Mitochondria in neurodegeneration. Adv Exp Med Biol. 2012; 942: 269–286.

Lustbader, J. W., Cirilli, M., Lin, C., Xu, H. W., Takuma, K., Wang, N., Caspersen, C., Chen, X., Pollak, S., Chaney, M., Trinchese, F., Liu, S., Gunn-Moore, F., Lue, L. F.,

Malthankar, G. V., White, B. K., Bhushan, A., Daniels, C. K, Rodnick, K. J. Lai J. C. K. Differential lowering by manganese treatment of activities of glycolytic and tricarboxylic acid (TCA) cycle enzymes investigated in neuroblastoma and astrocytoma cells is associated with manganese-induced cell death. Neurochem Res. 2004; 29(4): 709-717.

Martin, L. J. Mitochondrial and cell death mechanisms in neurodegenerative diseases. Pharmaceuticals. 2010; 3: 839-915.

Sirk, D., Zhu, Z., Wadia, J. S., Shulyakova, N., Phan, N., Fong, J., Mills, L. R. Chronic exposure to sub-lethal beta-amyloid (Abeta) inhibits the import of nuclear-encoded proteins to mitochondria in differentiated PC12 cells. J Neurochem. 2007; 103: 1989–2003.

Tadinada, S. M., Lai, M. B., Idikuda, V. K., Mukka, K., Singh, R. M., Pfau, J., Bhushan, A., Leung, S., Lai, J. C. K. Zinc oxide nanparticles induce apoptosis and necrosis in hepatocellular carcinoma hepg2 cells. FASEB J. 2013; 27:1106.5.

Torsten, R. D., Gerhard, F., Bernd, K. Ultraviolet light-induced DNA damage triggers apoptosis in nucleotide excision repair-deficient cells via Bcl-2 decline and caspase-3/-8 activation. Oncogene. 2001; 20: 6026-6038.

Walker, D. G., Kuppusamy, P., Zewier, Z. L., Arancio, O., Stern, D., Yan, S. S., Wu, H. ABAD directly links Abeta to mitochondrial toxicity in Alzheimer's disease. Science. 2004; 304(5669): 448-452.

Winner, B., Kohl, Z., Gage, F. H. Neurodegenerative disease and adult neurogenesis. Eur J Neurosci. 2011; 33: 1139–1151.

2.8 FIGURES

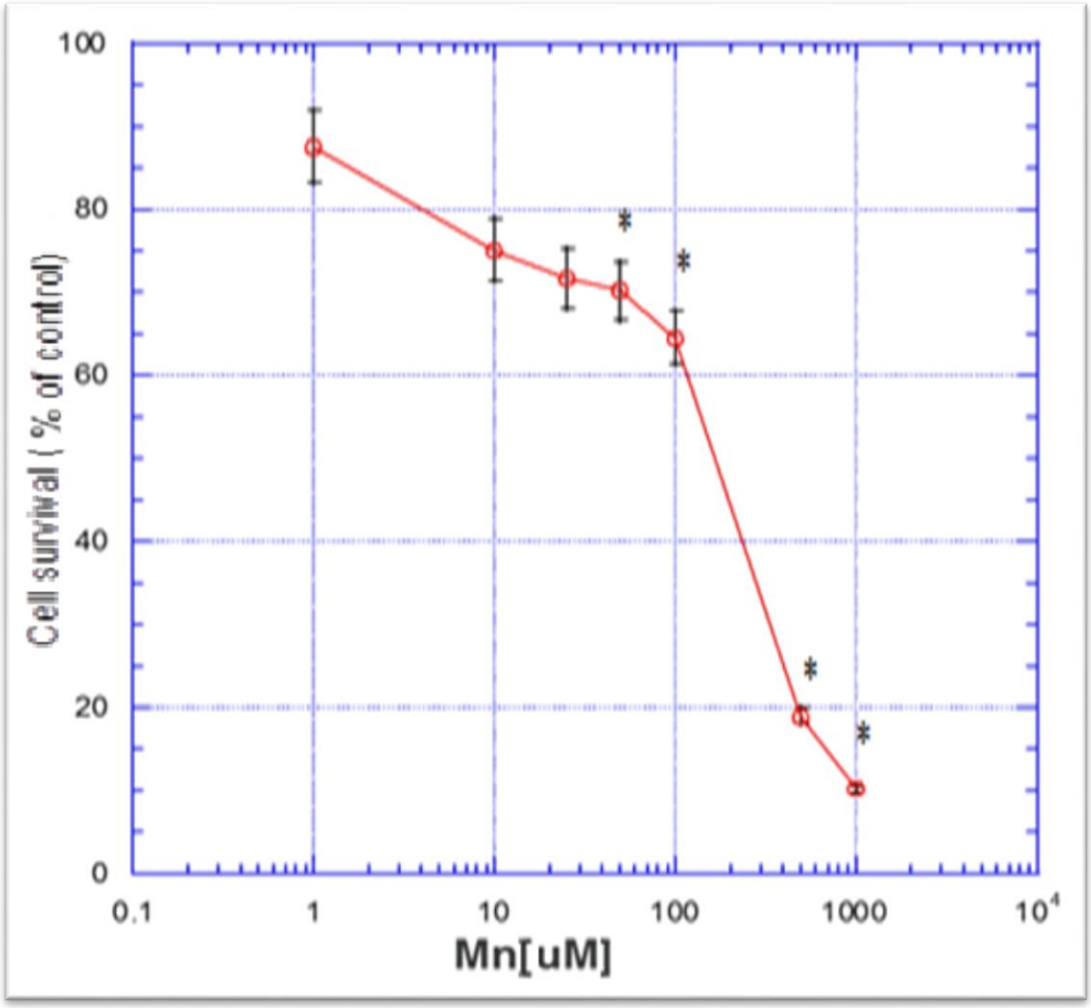

Figure 2.1 Effect of $MnCl_2$ on survival of DRG Neurons when treated for 48 hours.

The neurons were treated with increasing concentrations of manganese chloride for 48 hours and after which their survival was determined employing MTT assay. Values are mean ± SEM of 6 replicates; *p < 0.05 vs. control. Two additional experiments showed results with the same trend as that depicted here.

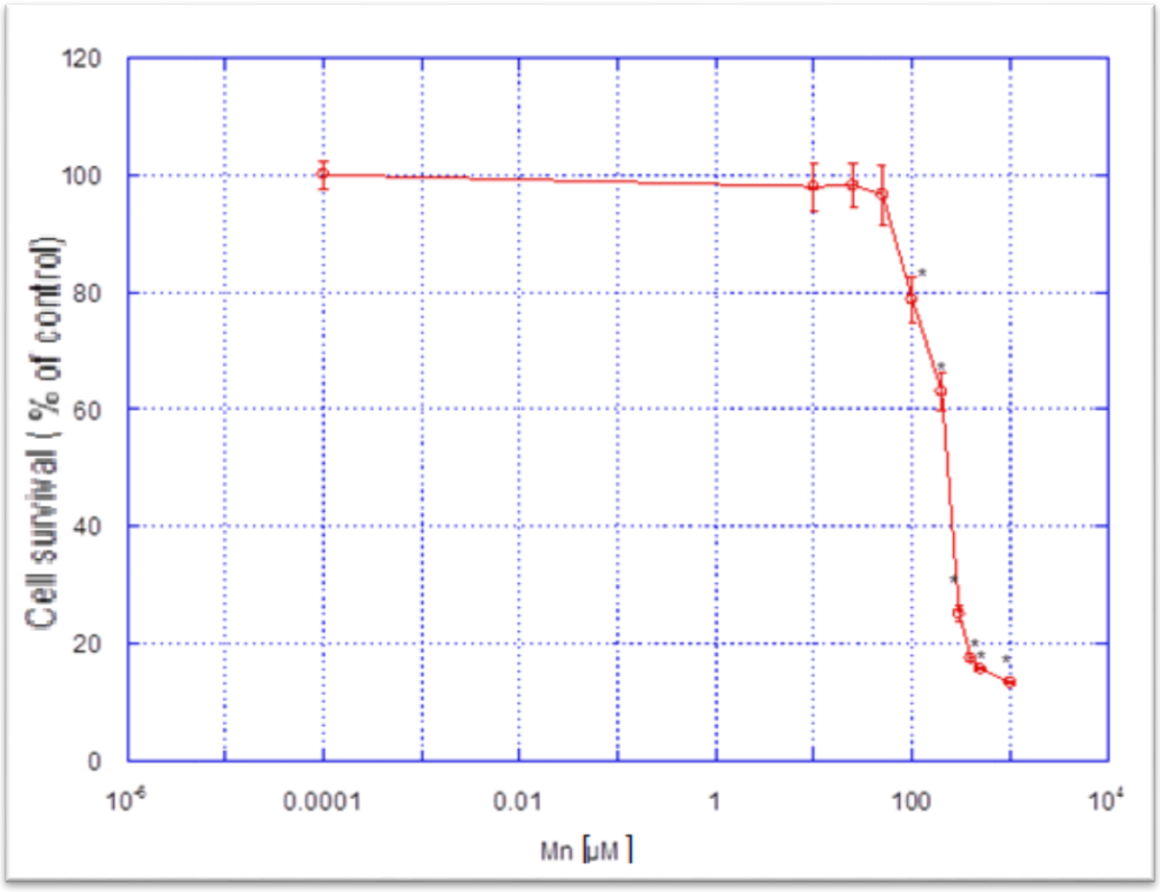

Figure 2.2 Effect of $MnCl_2$ on Survival of Schwann cells when treated for 48 hours.

Schwann cells were treated with increasing concentrations of manganese chloride for 48 hours and after which their survival was determined employing MTT assay. Values are mean ± SEM of 6 replicates; *p < 0.05 vs. control. Two additional experiments showed results with the same trend as that depicted here.

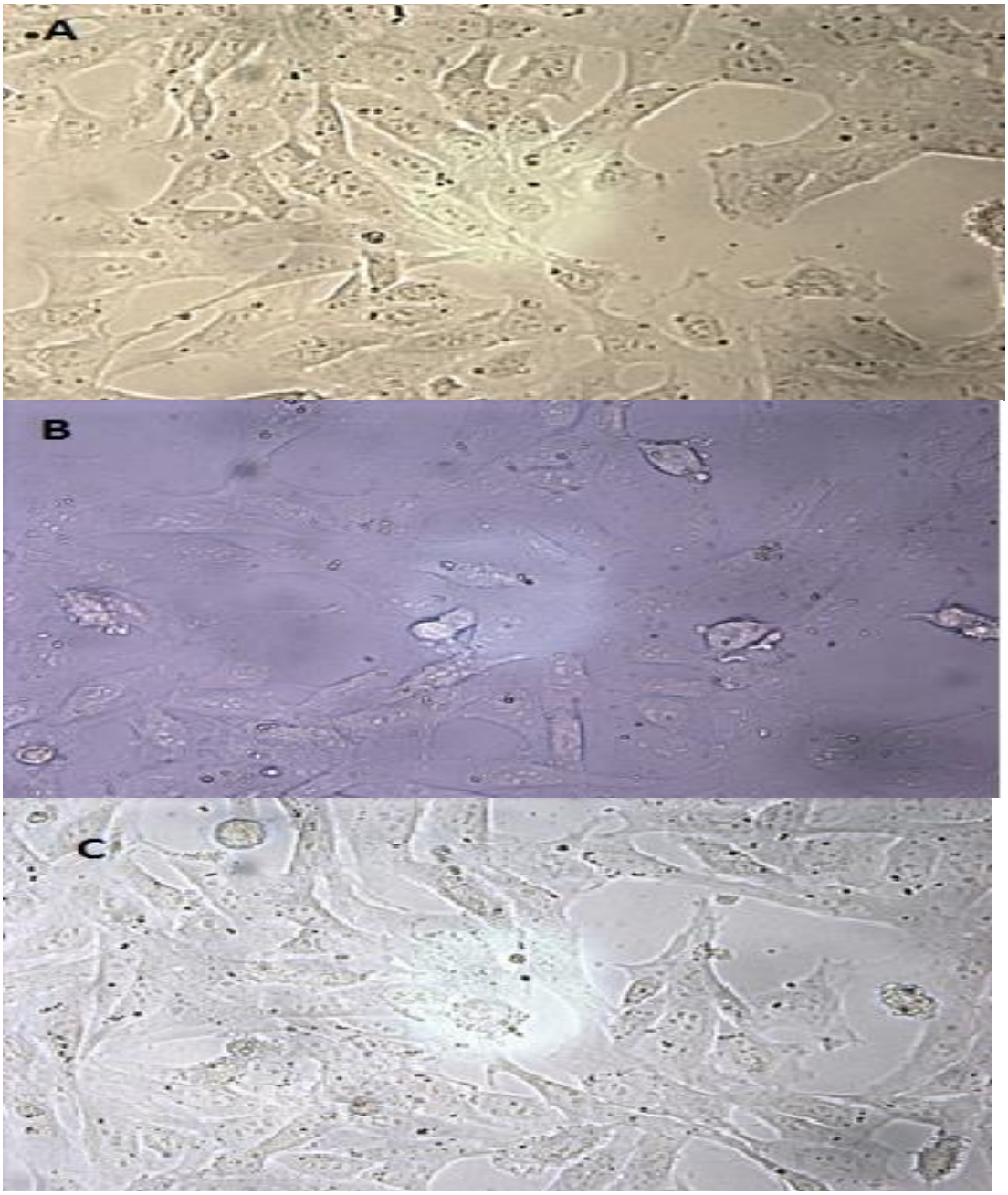
A
B
C

Figure 2.3 Effect of treatment with 0 (A), 10 (B), 50 (C), 100 (D), 500 (E) and 1000 (F) µM of $MnCl_2$ for 48 hours on the morphology of DRG neurons.

The neurons were treated as described and then examined under light microscopy at a magnification of 400 x.

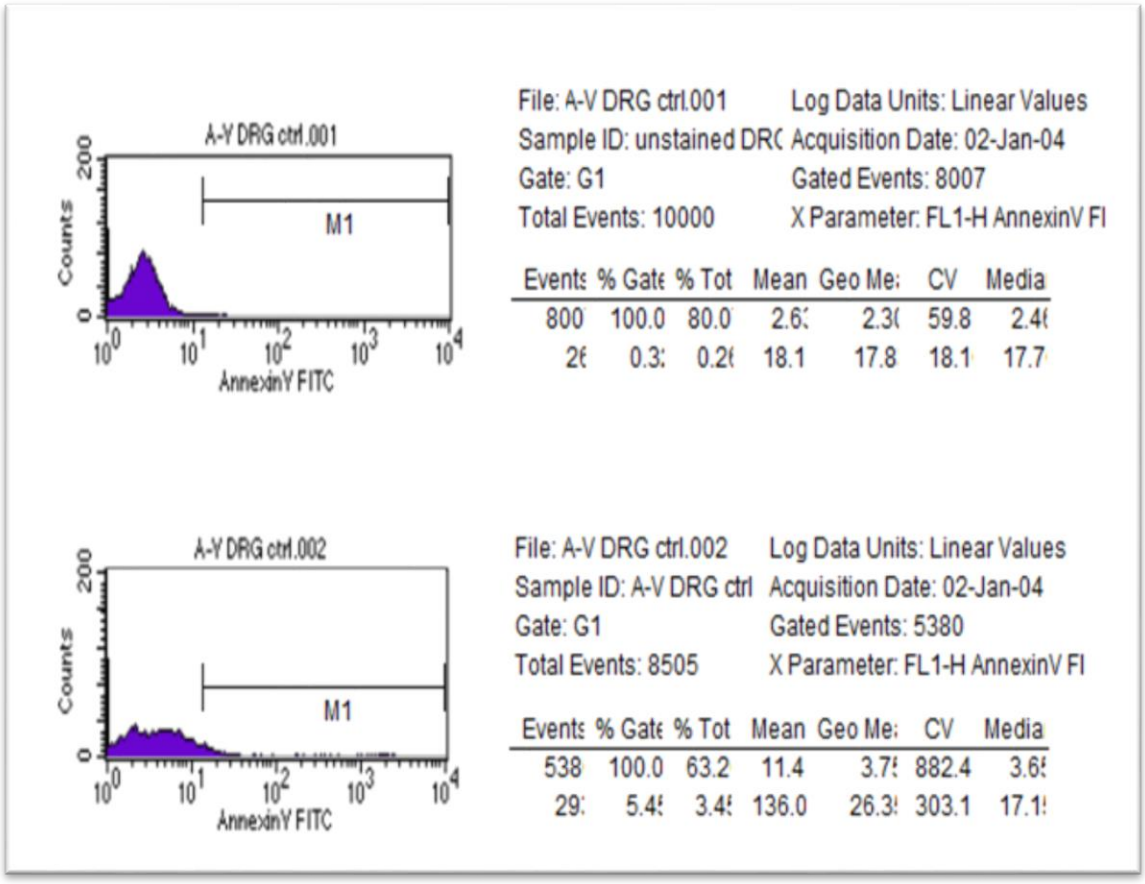

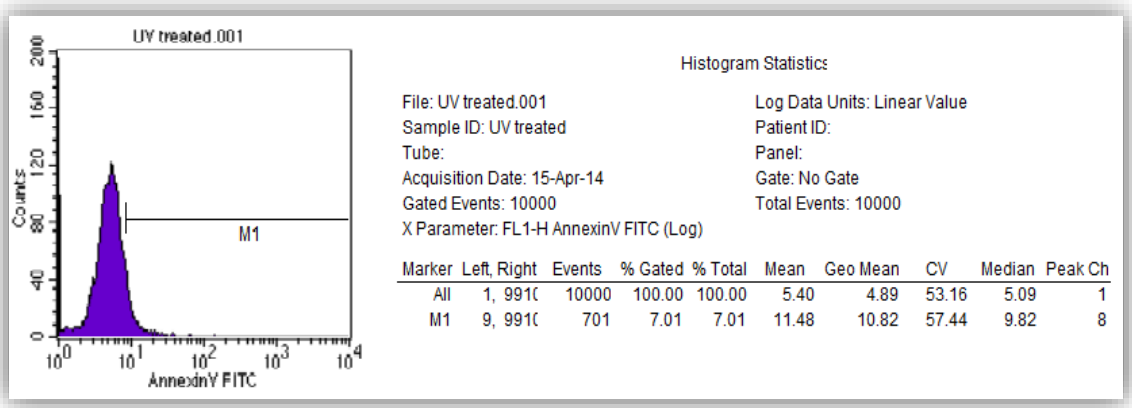

Figure 2.4 Comparison of control and UV-treated DRG neurons stained with annexin V as analyzed using a flow cytometer.

The panels sequentially from the top of this figure represent: panel 1, control (i.e., untreated) DRG neurons, unstained; panel 2, control DRG neurons stained with annexin V; and the bottom panel, DRG neurons treated with ultra-violet light for 30 minutes and subsequently stained with annexin V. The X-axis denotes fluorescence intensity in arbitrary units and the Y-axis denotes cell counts; the M1 window demarcates fluorescence intensities of apoptotic (annexin V-stained) cells whose data are summarized in bottom row of the summary table on the right side of each panel. Panel 1 shows the auto-fluorescence of untreated DRG neurons and less than 0.3% of the cells analyzed were within the M1 window and after staining (panel 2) some 3.45% of the cells analyzed were within the M1 window indicating the low number of DRG neurons that were apoptotic in that control DRG neuron populations. When control DRG neurons were treated with UV light for 30 minutes and then stained with annexin V (panel 3), some 7% of the cells in the DRG neurons were annexin V positive, indicating UV treatment (a positive control for apoptosis) enhanced apoptosis in DRG neurons. Results of two other experiments showed the essentially same trends.

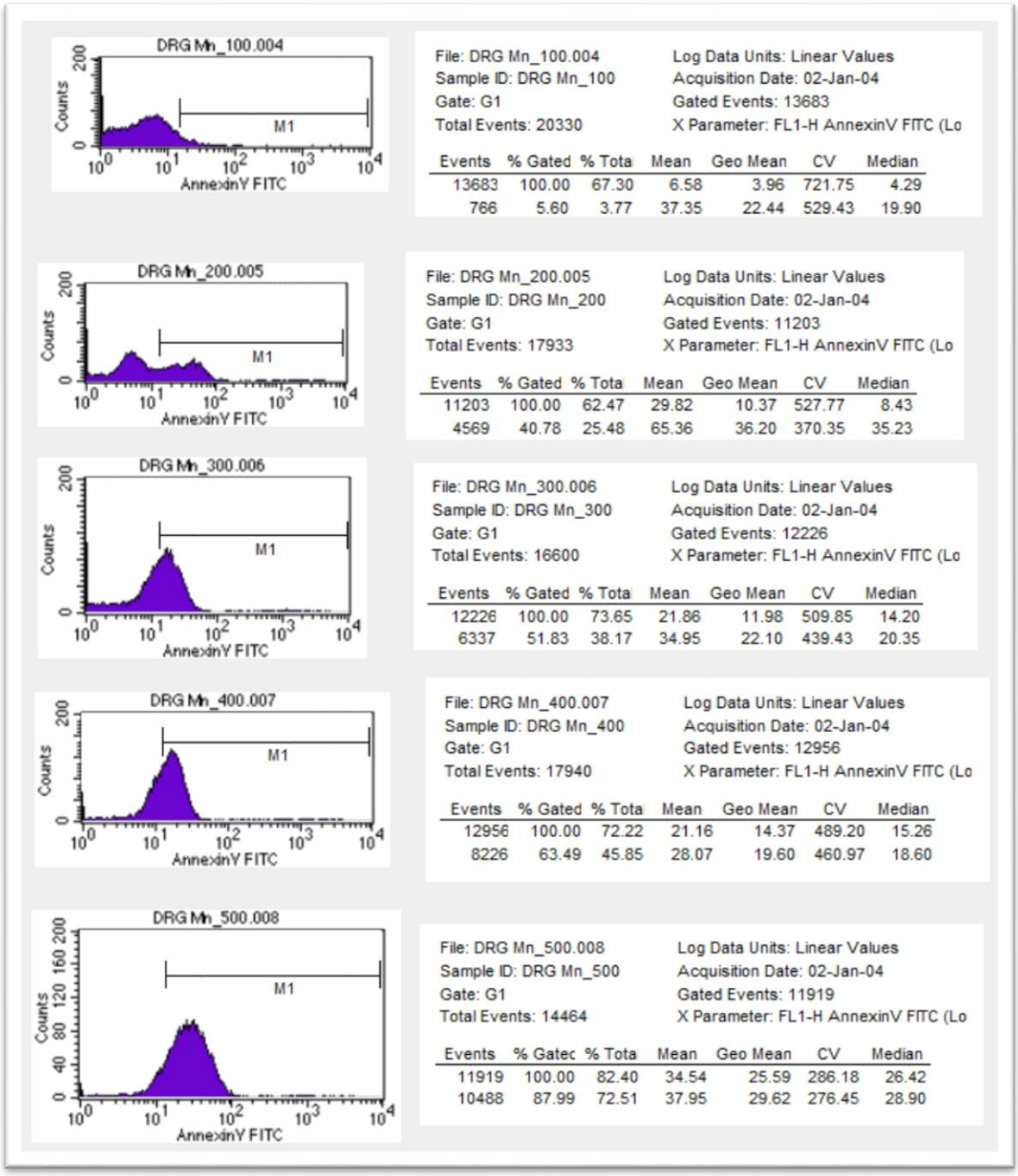

Figure 2.5 Effect of $MnCl_2$ on inducing apoptosis in DRG neurons.

DRG neurons were treated with increasing concentrations (100, 200, 300, 400 or 500 μM) of $MnCl_2$ for 48 hours, followed by staining with annexin V and then analyzed by flow cytometry. The panels sequentially from the top of this figure represent: panel 1,

DRG neurons treated with 100 μM $MnCl_2$ then stained with annexin V; panel 2, DRG neurons treated with 200 μM $MnCl_2$ then stained with annexin V; panel 3, DRG neurons treated with 300 μM $MnCl_2$ then stained with annexin V; panel 4, DRG neurons treated with 400 μM $MnCl_2$ then stained with annexin V; and the bottom panel (panel 5), DRG neurons treated with 500 μM $MnCl_2$ then stained with annexin V. The X-axis denotes fluorescence intensity in arbitrary units and the Y-axis denotes cell counts; the M1 window demarcates fluorescence intensities of apoptotic (annexin V-stained) cells whose data are summarized in bottom row of the summary table on the right side of each panel. Compared with control (i.e., untreated) DRG neurons (see Fig. 2.4), treatment with 100 μM $MnCl_2$ (panel 1) did not significantly increase the % of apoptotic DRG neurons (from 3.45% to 3.77%). However, treatment with $MnCl_2$ from 200 to 500 μM induced concentration-related increases in the % of apoptotic DRG neurons (from 25.48% to 72.51%). Two additional studies also showed trends of Mn-induced effects essentially the same as that depicted here.

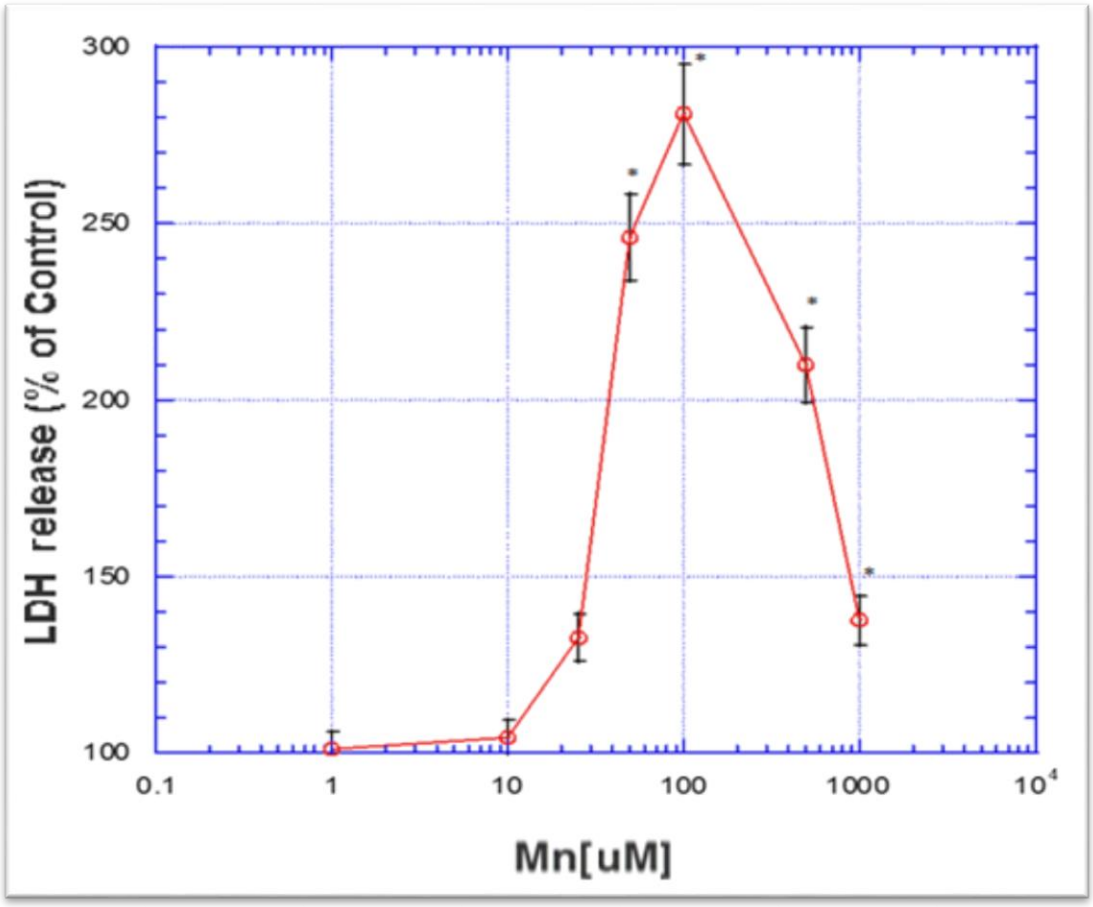

Figure 2.6 Effect of $MnCl_2$ on the release of LDH into medium by DRG neurons.

DRG neurons were treated with 1, 10, 50, 100, 500 or 1000 µM of $MnCl_2$ for 48 hours. Subsequently, the LDH activities in the media were determined and expressed as % of control means. The values are mean ± SEM of 3 replicates; *$p < 0.05$ vs. control. Results of two other studies showed essentially the same trend.

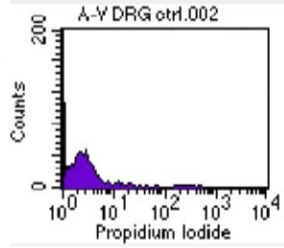

File: A-V DRG ctrl.002
Sample ID: A-V DRG ctrl
Gate: G1
X Parameter: FL2-H Propidium Iodide (Log)

Log Data Units: Linear
Acquisition Date: 02-Ja
Total Events: 8505

Marker	Left, Right	Events	% Total	CV	Median	Peak Ch
All	1, 9910	4497	52.87	450.90	2.29	1

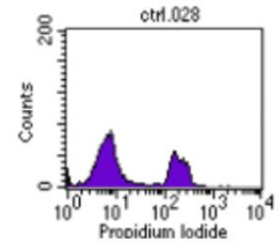

File: ctrl.028
Sample ID: UV-2 ctrl
Gate: G1
Total Events: 13763

Log Data Units: Linear Values
Acquisition Date: 29-Apr-14
Gated Events: 9280
X Parameter: FL2-H Propidium

Event:	% Gat	% Tot	Mear	Geo Me	CV	Media
928	100.(	67.4	66.6	19.4	138.4	8.3

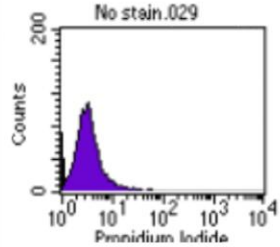

File: No stain.029
Sample ID: No stain
Gate: G1
Total Events: 11298

Log Data Units: Linear Values
Acquisition Date: 29-Apr-14
Gated Events: 9951
X Parameter: FL2-H Propidium

Event:	% Gat	% Tot	Mear	Geo Me	CV	Media
995	100.(	88.0	3.6	3.1	72.8	3.0

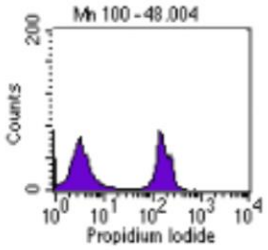

File: Mn 100 - 48.004
Sample ID: Mn 100 - 48
Gate: G1
Total Events: 13367

Log Data Units: Linear Values
Acquisition Date: 29-Apr-14
Gated Events: 9317
X Parameter: FL2-H Propidium Iodide (Log)

Events	% Gated	% Total	Mean	Geo Mean	CV	Median
9317	100.00	69.70	79.40	19.86	114.55	6.67

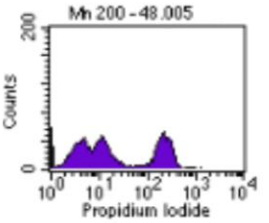

File: Mn 200 - 48.005
Sample ID: Mn 200 - 48
Gate: G1
Total Events: 14466

Log Data Units: Linear Values
Acquisition Date: 29-Apr-14
Gated Events: 9968
X Parameter: FL2-H Propidium Iodide (Log)

Events	% Gated	% Total	Mean	Geo Mean	CV	Median
9968	100.00	68.91	79.94	22.46	130.19	12.08

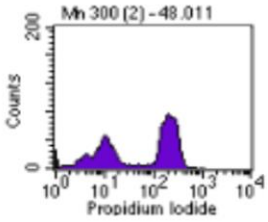

File: Mn 300 (2) - 48.011
Sample ID: Mn 300 (2) - 48
Gate: G1
Total Events: 15016

Log Data Units: Linear Values
Acquisition Date: 29-Apr-14
Gated Events: 10736
X Parameter: FL2-H Propidium Iodide (Log)

Events	% Gated	% Total	Mean	Geo Mean	CV	Median
10736	100.00	71.50	120.49	51.56	87.42	134.56

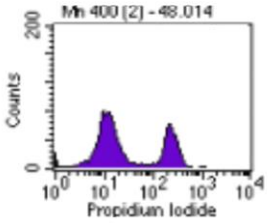

File: Mn 400 (2) - 48.014
Sample ID: Mn 400 (2) - 48
Gate: G1
Total Events: 16459

Log Data Units: Linear Values
Acquisition Date: 29-Apr-14
Gated Events: 11061
X Parameter: FL2-H Propidium Iodide (Log)

Events	% Gated	% Total	Mean	Geo Mean	CV	Median
11061	100.00	67.20	83.05	30.10	131.53	15.26

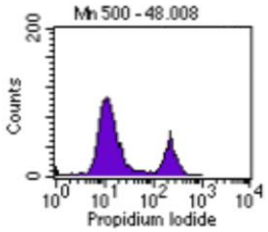

File: Mn 500 - 48.008
Sample ID: Mn 500 - 48
Gate: G1
Total Events: 20193

Log Data Units: Linear Values
Acquisition Date: 29-Apr-14
Gated Events: 12253
X Parameter: FL2-H Propidium Iodide (L

Events	% Gated	% Total	Mean	Geo Mean	CV	Median
12253	100.00	60.68	52.88	20.96	160.54	12.86

Figure 2.7 Effect of $MnCl_2$ on necrosis in DRG neurons.

DRG neurons were treated with 100, 200, 300, 400 or 500 μM of $MnCl_2$ for 48 hours and then stained with propidium iodide and subsequently analyzed by flow cytometry.

The panels sequentially from the top of this figure represent: panel 1, control (i.e., untreated) DRG neurons stained with propidium iodide; panel 2, DRG neurons treated with UV and then stained with propidium iodide; panel 3, control DRG neurons not stained with propidium iodide; panel 4, DRG neurons treated with 100 μM $MnCl_2$ for 48 hours and then stained with propidium iodide; panel 5, DRG neurons treated with 200 μM $MnCl_2$ for 48 hours and then stained with propidium iodide; panel 6, DRG neurons treated with 300 μM $MnCl_2$ for 48 hours and then stained with propidium iodide; panel 7, DRG neurons treated with 400 μM $MnCl_2$ for 48 hours and then stained with propidium iodide; and panel 8, DRG neurons treated with 500 μM $MnCl_2$ for 48 hours and then stained with propidium iodide. The X-axis denotes fluorescence intensity in arbitrary units and the Y-axis denotes cell counts. Panels 1 and 3 showed DRG neurons with one fluorescence peak at intensity less than 10 units: that both propidium iodide-stained and unstained control DRG neurons showed approximately the same single fluorescence peak at intensity less than 10 units suggested control DRG neurons contained few necrotic cells. Panel 2 showed two fluorescence intensity peaks, one at 8 intensity units and the second one at 30 intensity units: this distribution of DRG neurons treated with UV light suggested the peak at ~8 intensity units likely represented intact, non-necrotic DRG neurons whereas the second peak at ~30 intensity units likely represented necrotic DRG neurons. Panel 4, representing DRG neurons treated with 100 μM $MnCl_2$ for 48 hours and

then stained with propidium iodide, showed two fluorescence intensity peaks, suggesting that the one at ~4 intensity units represented control, non-necrotic DRG neurons and the one at ~300 intensity units represented the presence of significant number of necrotic DRG neurons. Panel 5, representing DRG neurons treated with 200 μM $MnCl_2$ for 48 hours and then stained with propidium iodide, showed three fluorescence intensity peaks, suggesting that the one at ~5 intensity units represented mainly non-necrotic DRG neurons, whereas the peaks at ~20 and ~300 intensity units respectively represented two populations of necrotic DRG neurons with increasing fluorescence intensities. Panel 6, representing DRG neurons treated with 300 μM $MnCl_2$ for 48 hours and then stained with propidium iodide, showed three fluorescence intensity peaks, suggesting that the one at ~5 intensity units represented mainly non-necrotic DRG neurons, whereas the peaks at ~20 and ~300 intensity units respectively represented two populations of necrotic DRG neurons with increasing fluorescence intensities. It is noteworthy that the area under the peak with ~300 intensity units reached a maximum in DRG neurons treated with 300 μM $MnCl_2$ because in DRG neurons treated with $MnCl_2$ at concentrations higher than 300 μM, the area under the peak with ~300 intensity units showed Mn-related decreases (compare panel 6 with panels 7 and 8). Panel 7, representing DRG neurons treated with 400 μM $MnCl_2$ for 48 hours and then stained with propidium iodide, showed mainly two fluorescence intensity peaks, suggesting the one at ~5 intensity units had disappeared implying few intact DRG neurons remained whereas the peaks at ~20 and ~300 intensity units respectively represented two populations of necrotic DRG neurons. Similarly, panel 8, representing DRG neurons treated with 500 μM $MnCl_2$ and then stained with propidium iodide, also showed mainly two fluorescence intensity peaks, suggesting the

one at ~5 intensity units had disappeared implying few intact DRG neurons remained whereas the peaks at ~20 and ~300 intensity units respectively represented two populations of necrotic DRG neurons. It is noteworthy that, compared with DRG neurons treated with 400 µM $MnCl_2$ for 48 hours as shown in panel 7, DRG neurons treated with 500 µM $MnCl_2$, as depicted in panel 8, showed a larger peak at ~20 intensity units but a small peak at ~300 intensity units. Two additional studies also showed trends of Mn-induced effects essentially the same as that depicted here.

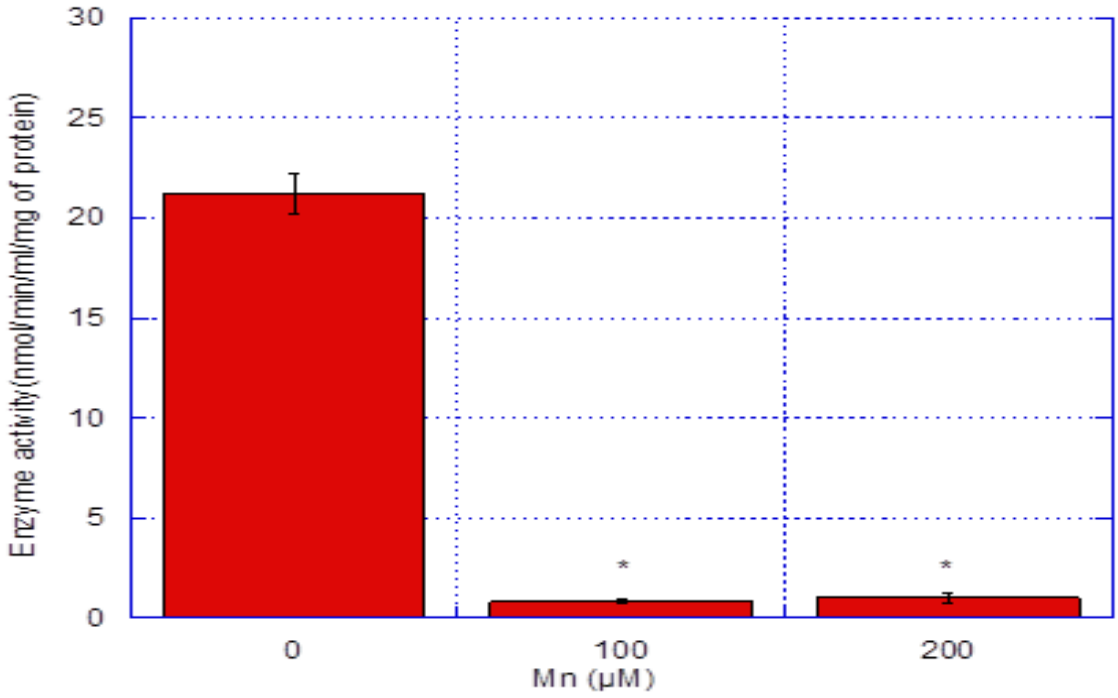

Figure 2.8 Effect of $MnCl_2$ on lactate dehydrogenase (LDH) activities in DRG neurons.

DRG neurons were treated with 100 or 200 of $MnCl_2$ for 48 hours. The treated or control neurons were harvested and the activities of LDH therein were assayed. The activities were expressed per mg of protein. The values are mean ± SEM of 3 replicates; *$p < 0.05$ vs. control.

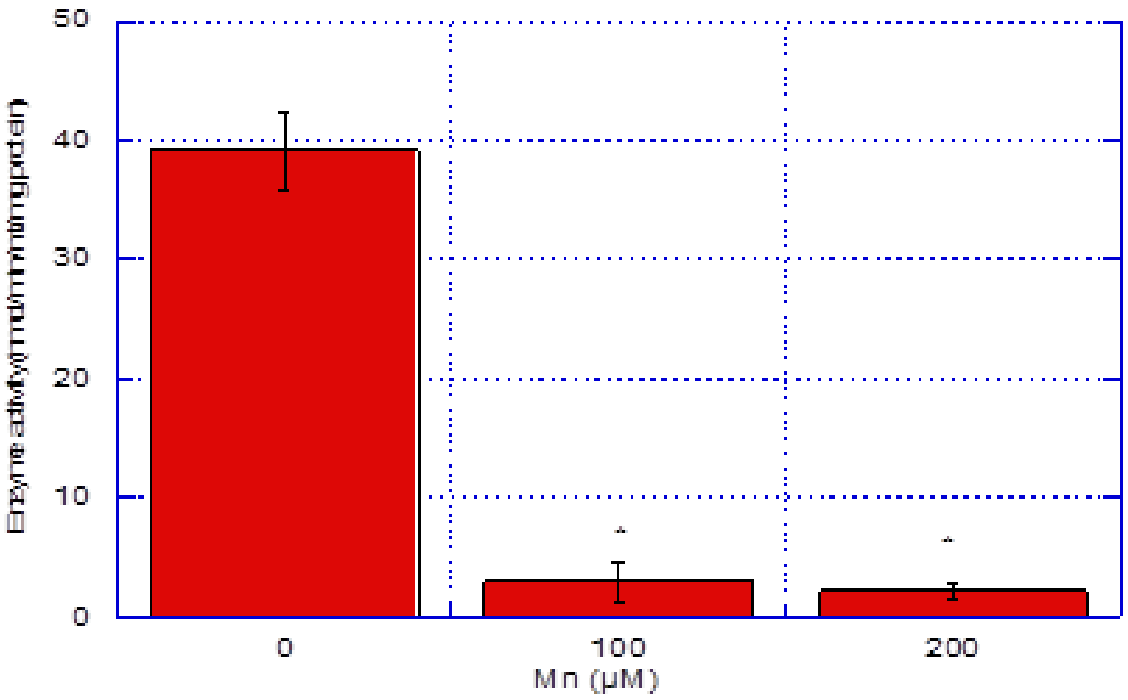

Figure 2.9 Effect of $MnCl_2$ on malate dehydrogenase (MDH) activities in DRG neurons.

DRG neurons were treated with 100 or 200 of $MnCl_2$ for 48 hours. The treated or control neurons were harvested and the activities of MDH therein were assayed. The activities were expressed per mg of protein. The values are mean ± SEM of 3 replicates; *$p < 0.05$ vs. control.

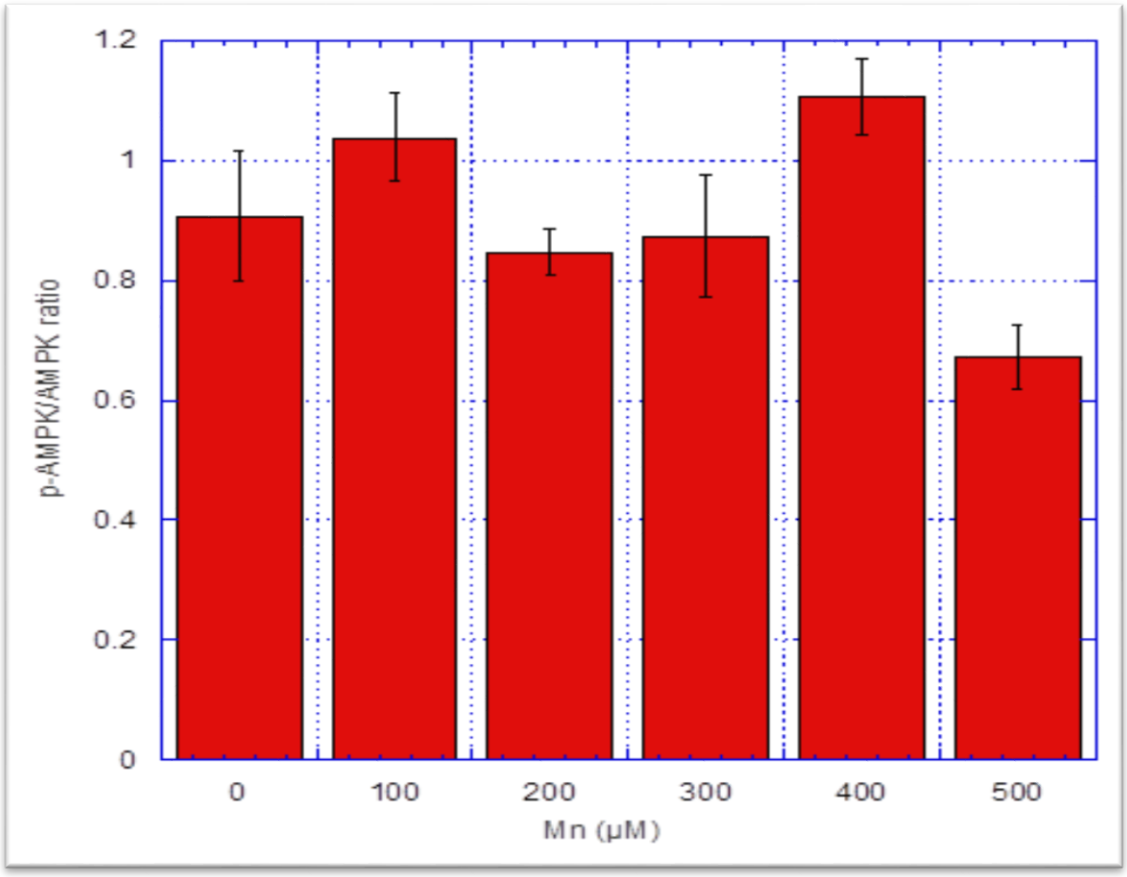

Figure 2.10 Effect of $MnCl_2$ on p-AMPK to AMPK ratios in DRG neurons.

DRG neurons were treated with 100, 200, 300, 400 or 500 μM of $MnCl_2$ for 24 hours. The treated or the control neurons were harvested and immunocytochemical analysis for AMPK and p-AMPK was performed as described earlier. The ratios of the median fluorescent intensities of p-AMPK to AMPK for different treatment conditions were calculated. Values are mean ± SEM of 3 replicates.

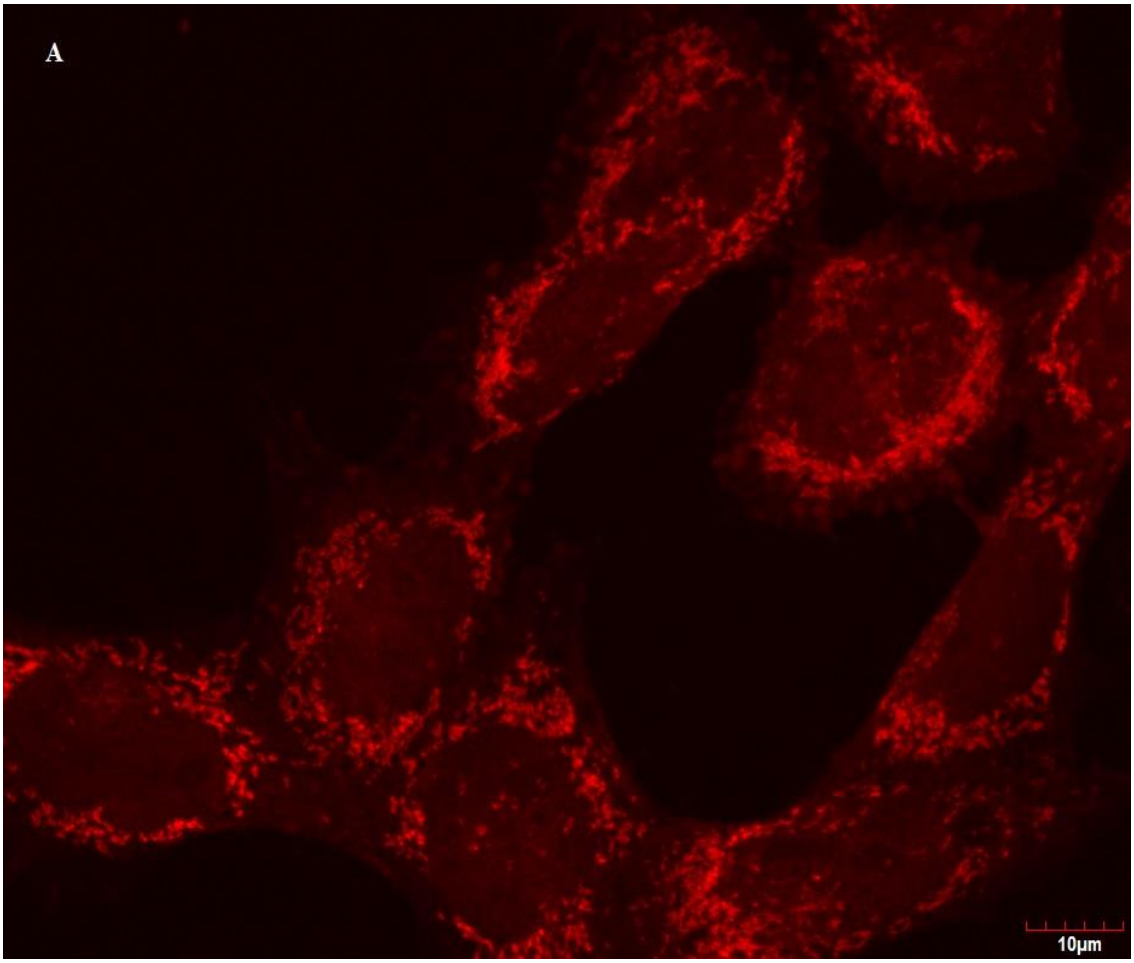
A
10µm

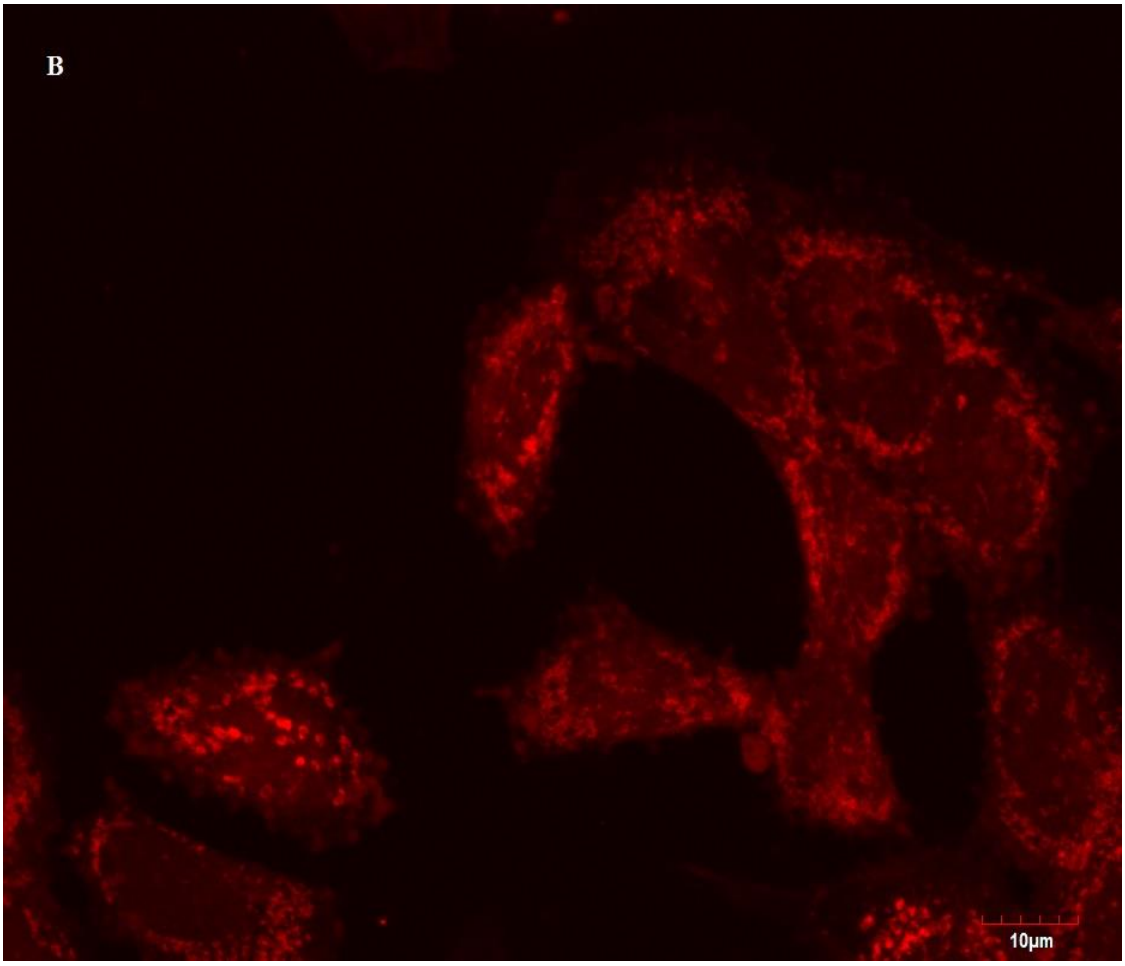
B
10µm

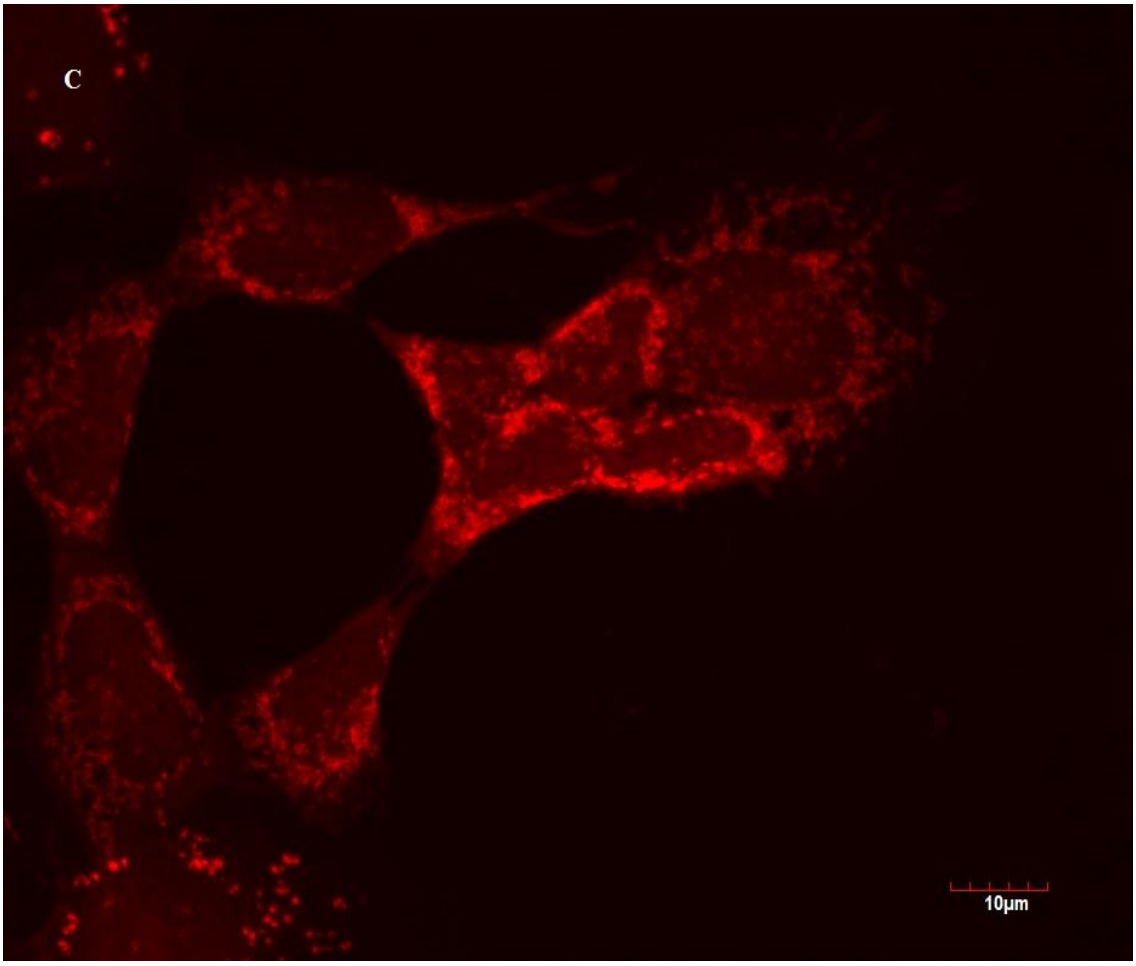
C
10µm

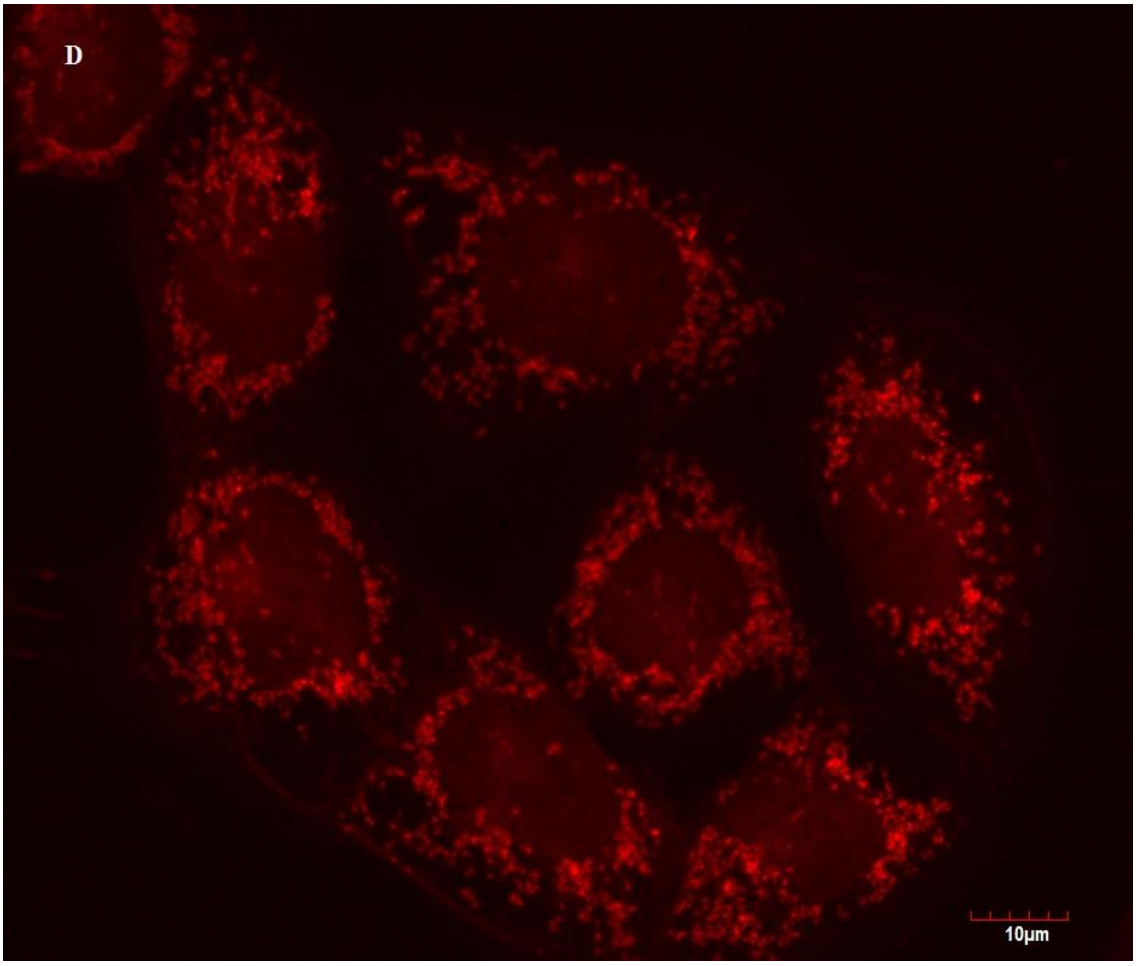

Figure 2.11 Effect of $MnCl_2$ on the morphology of mitochondria in DRG neuron.

DRG neurons were cultured on cover slips in 6-well plates and were treated with 0 (A), 100(B), 200(C) and 300(D) µM of Mn for 24 hours. The neurons were later stained with Mitotracker red as described earlier and the cover slips were mounted on microscope slide. Images were captured by using a 100x objective lens on confocal microscope at 1000 times magnification.

CHAPTER 3. MODULATION OF SURVIVAL OF DORSAL ROOT GANGLION (DRG) NEURONS IN MANGANESE-INDUCED NEUROTOXICITY

Anurag K. Balaraju[1], Aishwarya Neti[1], Vinay K. Idikuda[1], Solomon W. Leung[2], Alok Bhushan[3], and James C.K. Lai[1]

[1]Department of Biomedical & Pharmaceutical Sciences, College of Pharmacy, Division of Health Sciences and Biomedical Research Institute, Idaho State University, Pocatello, ID 83209.

[2]Department of Civil & Environmental Engineering, School of Engineering, College of Science & Engineering, Pocatello, ID 83209.

[3]Department of Pharmaceutical Sciences, Jefferson School of Pharmacy, Thomas Jefferson University, Philadelphia, PA 19107.

3.1 ABSTRACT

Many physiological important processes such as glucose metabolism, antioxidant defense and bone metabolism are regulated by manganese (Mn). Mn is an essential micronutrient but is toxic when taken in excess. Mn toxicity induces Parkinsonism-like signs and symptoms. We have demonstrated that Mn treatment induces neurodegeneration via inhibition of oxidative metabolism and induction of oxidative stress in neurotumors cells. Because Mn toxicity in non-tumor neural cells has not been fully elucidated, we have developed co-culture models of the peripheral nervous system, namely dorsal root ganglion (DRG) neurons and Schwann cells to investigate the putative role of glial cells in protecting neurons from Mn-induced neurodegeneration. Our previous and ongoing studies indicate Mn is more toxic to neurons than glial cells. Results of our studies employing monotypic and co-cultures of DRG neurons and Schwann cells suggest Schwann cells may exert protective effects on DRG neurons against Mn-induced toxicity through decreasing the Mn-induced oxidative stress. We have also observed a correlation between neuro-protection and AMPK levels in DRG neurons treated with Mn. Thus, our results may assume pathophysiological importance in peripheral nerve degeneration and manganese-induced neurodegeneration.

Key words: Manganese, Schwann cells, DRG neurons, neurodegeneration, glutathione, caspase-3, forskolin, neurite, AMP-activated protein kinase (AMPK).

3.2 INTRODUCTION

Manganese (Mn), an essential trace nutrient and a component of many proteins including several classes of enzymes, metallo-proteins and polypeptides, is required for normal development and functions of mammals (Greger et al., 1999). It is needed for several important physiological processes such as glucose and antioxidant metabolism, antioxidant activity, and bone development (Greger et al., 1999). Although manganese deficiency is uncommon as it is readily available in the normal human diet, overexposure to Mn is a major concern because Mn toxicity induces behavioral and motor disturbances (Lai et al., 1984; Lai et al., 1985; Neal et al., 2013).

Food, drinking water, and inhalation serve as important routes for manganese entry and accumulation in the body (Lai et al., 1984; Lai et al., 1985; Greger et al., 1999). Even though Mn toxicity in humans are rare because of improved work place hygiene, in chronic low level exposure, Mn accumulates in different regions of brain, including globus pallidus, basal ganglia, pars compacta and substantia nigra (Lai et al., 1985; Lai et al., 1999; Ascher et al., 2006; Lai and Leung, 2013).

Several mechanisms have been postulated to account for Mn-induced neurotoxicity. Induction of oxidative stress leading to cytotoxic and detrimental effects is one of the putative mechanisms (Dukhande et al., 2006). Mn enters a cell via facilitated diffusion and receptor-gated cation and calcium channels accumulates in the mitochondria and nucleus (Lai et al., 1985; Lai et al., 1999; Lai and Leung, 2013). Upon entering mitochondria, Mn binds to the inner mitochondrial membrane and inhibits the activity of ATPase complex and Complex 1 (Brouillet et al., 1993). It interferes with the oxidative metabolism and leads to production of reactive oxygen species (ROS) (Cohen,

1984) and can activate glutamate-gated channels (Brouillet et al., 1993). In its divalent oxidative state, Mn can exert toxicity on dopaminergic system (Archibald et al., 1987). Dopamine oxidation by Mn induces oxidative DNA damage (Oikawa et al., 2006). Mn can induce production of 6-hydroxy dopamine (Graham, 1984). Despite these diverse proposed neurotoxic mechanisms reportedly induced by Mn, there is some consensus that Mn-induced alteration in the dopaminergic system and Mn-induced disruption of normal mitochondrial functions upon Mn accumulation in mitochondria are the favored neurotoxic and cytotoxic mechanisms underlying in vivo Mn neurotoxicity (Lai et al., 1984; Lai et al., 1985; Ascher et al., 2006; Dukhande et al., 2006). The importance of GSH in cellular integrity and survival and how alterations of cellular GSH could result in apoptosis has been reviewed by Circu and Aw (2008). Indeed, our recent finding that depletion of mitochondrial GSH leads to mitochondrial dysfunction and apoptosis (Dukhande et al., 2013) provides strong support for the notion that these aspects of neurotoxicity of Mn merit further and systematic investigation.

There is a complex interrelationship between neurons and glial cells in terms of their metabolic and neurotransmitter cycling (see Patel et al. (2014) for detailed discussion). Furthermore, astrocytes may play an important role in protecting neurons against Mn-induced neurotoxicity (Lai et al., 1985; Aschner and Wegrzynowicz, 2013). Consequently, this study was initiated to investigate the hypothesis that Schwann cells exert protective effect on DRG neurons against Mn-induced cytotoxicity and neurotoxicity.

3.3 MATERIALS AND METHODS

Materials

Dorsal root ganglion (DRG) neurons are a kind gift from Dr. Höke of Johns Hopkins University School of Medicine and Schwann cells (S16) were obtained from ATCC (Manassas, VA). MTT, DTNB, dimethyl sulfoxide (DMSO), Dulbecco's minimal essential medium (DMEM) and fetal bovine serum (FBS) were obtained from Sigma-Aldrich (St. Louis, MO). The fluorescent dye (CM-H2DCFHA) and BCA protein assay kit were obtained from Molecular probes (Eugene, OR) and Thermo-Pierce (Rockford, IL), respectively. Antibodies against caspase-3 was obtained from Santa Cruz Biotechnologies (Santa Cruz, CA).

Cell Culture

DRG neurons and S16 Schwann cells were cultured in DMEM medium supplemented with glucose, sodium pyruvate, sodium bicarbonate, L-glutamine and 10 % FBS. Incubation was done at 37 °C and 5% (v/v) CO_2 until 70 % confluency was reached. Equal number of DRG neurons and S16 Schwann cells were plated in T-75 flasks and allowed to reach 70 % confluency. The cultures were then treated with various concentrations (0, 100 or 200 µM) of manganese chloride for 24 hours. The conditioned medium was collected, centrifuged at 1000 g for 5 minutes and stored at -80 °C until they were used for experiments. DRG neurons alone were separately plated in T-75 flasks and were treated with various concentrations (0, 100 or 200 µM) of manganese chloride for 24 hours. Their conditioned medium was collected, centrifuged at 1000g and 5 minutes and stored at -80 °C until they were used for experiments. Conditioned media from the co-cultures and monotypic cultures were used separately to culture DRG neurons in T-75

flasks, 96-well plates or 24-well plates until 70 % confluent. Various experiments were performed on the cultures and their lysates (see below).

Cell survival/viability assay

The survival/viability of DRG neurons was determined by the MTT assay as described previously (Dukhande et al., 2006). DRG neurons were plated in a 96-well plate and treated with conditioned media as described above. After incubation, MTT dye was added to each well and the plates were incubated for 4 hours at 37 °C. Dimethyl sulfoxide (DMSO) was employed to dissolve the formazan crystals formed and the absorbance of each well of the 96-well plate was read at 567 nm using a multi-detection microplate reader (Bio-Tek Synergy HT, Winooski, VT).

Cell survival/viability assay to measure the survival/viability of DRG neurons upon treatment with forskolin followed by manganese

The survival/viability of DRG neurons was determined by the MTT assay as described previously (Dukhande et al., 2006). DRG neurons were plated in a 96-well plate and treated with the medium containing 50 µM forskolin for 24 hours. Subsequently, the forskolin-containing medium was replaced with medium containing 10, 20, 50, 100, 200, 300, 400 or 500 µM manganese chloride and DRG neurons were incubated for another 24 hours. Then 20 µL of MTT dye (0.5 % (w/v) in phosphate-buffered saline) was added to each well and the plate was incubated for another 4 hours at 37 °C. Immediately thereafter, the medium in the wells was aspirated carefully without unsettling the formazan crystals formed on the bottom of the wells. Subsequently, the formazan crystals were dissolved using 100 µL of HPLC grade dimethyl sulfoxide

(DMSO) per well. The absorbance of the solution in each well was measured at 567 nm using a multi-detection microplate reader (Bio-Tek Synergy HT, Winooski, VT).

Determination of ROS production in treated and untreated DRG neurons

DRG neurons were plated in a 24-well plate and treated with conditioned medium as described above. After incubation for 24 hours, in the absence of light, the medium was aspirated and the cells were treated with 10 µM CM-H2DCFDA fluorescent dye (in 1X sterile PBS) and incubated for 45 minutes at 37 °C. Thereafter, the medium in each well was aspirated and 200 µL of sterile PBS was added to each well. Employing a microplate reader the fluorescence of the oxidized form of the dye in each well was measured at an excitation of 492 nm and emission of 521 nm using a 96 well plate reader.

GSH assay

Total GSH level was assessed by GSH recycling assay, based on a modified method of Griffith (1980). Treated or control DRG neurons were collected, centrifuged at 1000 g for 5 min and suspended in extraction buffer. The treated or control DRG neurons were homogenized, sonicated for 1 minute (in cycles of 10 seconds sonication followed by 10 seconds rest) at 180 watt and then centrifuged . The resultant supernatant was employed for assaying GSH content therein. Glutathione reductase was used to reduce oxidized glutathione in each sample and the total GSH levels in the supernatants were determined by reacting reduced glutathione with DTNB (Ellmann's reagent). The absorbance of the reaction product was measured at 412 nm using 96 well plate reader.

Western Blot Analysis

Protein expression of caspase 3 in treated or untreated DRG neurons was determined by Western blot analysis using rabbit monoantibodies against caspase 3 (Santa Cruz Biotechnologies, Dallas, Texas) as described previously (Dukhande et al., 2006). Briefly, the proteins in the DRG samples were separated by sodium dodecyl sulfate-polyacrylamide gel electrophoresis (SDS-PAGE) using 12% (w/v) gels. The separated proteins were then transferred onto a polyvinylidene difluoride (PVDF) membrane at 90 v and were blocked by using 5% (w/v) milk powder solution for an hour at room temperature. These blots were then washed with Tris-buffered saline (TBS) and incubated with the desired primary antibody overnight. The blots were then washed using TBS and incubated with HRP-conjugated secondary antibody for an hour and developed using chemiluminescence detection kit (Thermo Scientific, Rockford, Illinois).

Treatment of DRG neurons with forskolin

Usually, DRG neurons were cultured in DMEM medium supplemented with 10 % (v/v) FBS on an uncoated surface at 37 °C and in 5 % (v/v) CO_2. However, under these conditions, DRG neurons did not usually develop to assume the differentiated morphology (i.e., showing extended neurites (axons and dendrites) and synaptic connectivity). Therefore, forskolin, a labdane diterpinoid, was employed to stimulate DRG neurons to develop and assume a differentiated morphology with protruding neurites according to the procedures of Chen et al. (2007). To prevent precipitation, a pre-determined amount of forskolin was first solubilized in DMSO (a solvent) and then added to the DMEM drop-wise. Subsequently, DRG neurons were treated with DMEM containing forskolin under aseptic conditions at 37 °C and in 5 % (v/v) CO_2 for a predetermined length of time.

Determination of the forskolin concentration and length of treatment time

To determine the appropriate forskolin concentration and its treatment time to induce DRG neurons to develop and assume a differentiated morphology with protruding neurites according to the procedures of Chen et al. (2007), the DRG neurons were treated with several different forskolin concentrations and for different times and their morphologies monitored employing light microscopy. Light photomicrographs were acquired with a Leica microscope.

Immunocytochemical analysis

Intracellular antigen-staining in DRG neurons was performed according to the the protocol of Abcam (Cambridge, Massachusetts) with some modifications. Briefly, DRG neurons were plated in T-25 flasks and allowed to reach 70 % confluency. Then, DRG neurons were treated with DMEM medium containing 50 µM forskolin for 24 hours. Later, the medium was replaced with medium containing 100, 200, 300, 400 or 500 µM $MnCl_2$. In between the treatments, the medium was completely removed and DRG neurons were rinsed with warm, particulate-free and sterile PBS. After the treatments, the treatment medium was aspirated and the cells were gently washed with ice-cold, particulate-free and sterile PBS to remove traces of medium. Immediately thereafter, the flasks were transferred onto ice to slow down metabolism in DRG neurons. To detach DRG neurons from the surface of the flasks, trypsin was added and DRG neurons were exposed to the trypsin for a few minutes. Then, ice-cold, particulate-free and sterile PBS was added to the flasks to inactivate the effect of the trypsin. Subsequently, DRG neurons were collected by centrifugation at 1000 g for 5 minutes and then washed with ice-cold,

particulate-free and sterile PBS to remove the traces of trypsin. Finally, the washed DRG neurons were re-suspended in 200 µL of ice-cold, particulate-free and sterile PBS and 200 µL of 4 % paraformaldehyde was added and incubated in the dark at 4°C for 2 hours. The paraformaldehyde-fixed DRG neurons were then washed with ice-cold, particulate-free and sterile PBS twice. The washed DRG neurons were re-suspended in 500 µL of permeabilization buffer (PBS containing 0.25 % (v/v) Triton X-100) and allowed to incubate for 30 min at 4°C. Immediately thereafter, the permeabilized DRG neurons were centrifuged at 1000 g for 5 min and the cell pellet was suspended in primary staining buffer (1% (v/v) BSA in 1X PBST supplemented with primary antibody at a dilution of 1: 1000) and incubated in the dark for 30 minutes. After staining, the stained DRG neurons were washed twice with ice-cold, particulate-free and sterile PBS (500 µL) twice. The above steps were repeated with secondary staining buffer (1% (v/v) BSA in PBS supplemented with secondary antibody at a dilution of 1: 1000). Finally, the DRG neurons so stained were re-suspended in 500 µL of PBS and analyzed with a flow cytometer (Becton Dickinson Biosciences FACS Calibur 2-laser/4-color flow cytometer, analyzed using CellQuest software, BD Biosciences, San Jose CA).

3.4 RESULTS

Cell viability studies

Schwann cells conferred protection to DRG neurons from manganese induced toxicity as assessed by cell survival/death assay (Fig 3). Viability of DRG neurons treated with conditioned media from co-culture was more with respect to those treated with media from mono-cultures. Also, the photomicrographs of DRG neurons, as shown in

Figure 1 and 2, obtained from Leica microscope suggest the absence of characteristic necrotic features in cells treated with conditioned media from co-cultures.

Apoptosis and oxidative stress

Caspase-3 activation is an early event in an apoptotic cell death mechanism. The western blot analysis of caspase-3 (Fig 6) from the extract prepared from DRG neurons treated with conditioned media from mono and co-cultures showed a significant difference in caspase-3 levels. The caspase-3 levels in DRG neurons treated with conditioned medium from co-cultures were insignificantly low compared to those treated with conditioned medium from monocultures. The photomicrographs of DRG neurons treated with conditioned medium from co-culture and mono-cultures support the above result. The morphological features observed during apoptosis were significant in photomicrographs of DRG neurons treated with conditioned medium from monocultures than that of co-cultures.

Also, through GSH assay (Fig 5) we were able to demonstrate that manganese induced neurodegeneration via inhibition of oxidative metabolism. Further, we found that the induction of oxidative stress was less in neurons treated with conditioned media from co-cultures than those treated with conditioned media from mono-cultures. Reactive oxygen species levels, as shown in figure 4, were less in DRG neurons treated with conditioned media from Co-cultures suggesting the role of Schwann cells in regulating the oxidative status of the cells. Mean velocity of the GSH enzyme activity was found to be more in DRG neurons treated with conditioned media from co-cultures.

Morphological observations of DRG neurons treated with forskolin and Mn in succession

It was well documented by Chen et al., 2007 that forskolin (FK), a labdane diterpenoid, induces neurite induction and elongation in DRG neurons. A protrusion from the surface of the cell body of neurons was considered as a neurite only when it is at least twice the diameter of the cell body. Accordingly, we have determined the concentration of forskolin and treatment time based on morphological observation of pictures of DRG neurons treated with varying concentrations of FK at varying time points. Our observations suggest that a concentration of 50 µM of FK can induce neurite formation and elongation significantly in DRG neurons when treated for 24 hours. Thus, we have employed 50 µM of FK in our further studies. At concentrations above 50 µM of FK and at treatment period above 24 hours, we have observed morphological features of apoptosis in DRG neurons.

Morphological observations of photomicrographs of DRG neurons treated with forskolin and manganese in succession, showed differences in various treatments with respect to length of the neurites in DRG neurons. The length of neurite in DRG neurons treated with FK and Mn in succession was less compared to DRG neurons treated with FK alone.

Immunocytochemical analysis of DRG neurons treated with forskolin and Mn in succession

AMP activated protein kinase (AMPK) is an enzyme which plays a crucial and central role in energy homeostasis. In our studies, we have performed intracellular

fluorescent staining of AMPK and p-AMPK in DRG neurons treated with varying concentrations of manganese and observed the levels of the proteins employing flow cytometry. We have observed a bi-phasic response in the levels of the above proteins with increasing concentration of manganese.

3.5 DISCUSSION AND CONCLUSION

In summary, our results showed a cyto-protective role of Schwann cells. Survival of DRG neurons in stress induced by toxic levels of manganese was improved by Schwann cells. Our results show that Schwann cells reduces oxidative stress and inhibits apoptosis in DRG neurons by regulating their GSH levels and caspase-3 levels. GSH activity in DRG neurons dropped in a dose dependent fashion in DRG neurons treated with conditioned media from mono-cultures and co-cultures. However, the GSH activity in DRG neurons treated with conditioned media from co-cultures was more compared to the DRG neurons treated with conditioned media from mono-cultures. This suggest that the paracrine signaling between Schwann cells and DRG neurons reduced oxidative stress in DRG neurons and prevented the depletion of GSH levels.

The role of glial cells is critical for maintaining the structural and functional integrity of neurons (Aschner et al., 2013). Neurons are dependent on many metabolic intermediates from Schwann cells. Our study which is focused on understanding the mechanisms involved Mn Neurotoxicity and metabolic demands of DRG neurons to Schwann cells, found a significant change in structural and functional aspects in DRG neurons. Earlier work on manganese neurotoxicity in peripheral neurons inferred the role of oxidative stress in mediating manganese neurotoxicity (Dukhande et al., 2006). Oxidative stress generates high energy free radicals which tends to destroy the structural

and functional integrity of a cells. Cell counters the detrimental effects of these free radicals by employing anti-oxidants such as GSH, a chief cellular detoxifying agent. A depletion in GSH levels or a reduction in the activity of GSH suggest a rise in oxidative environment in a cell. The results of our GSH recycling assay which is a modified Griffith's GSH assay, indicate a dose dependent rise in oxidative stress (or a drop in GSH activities) in DRG neurons treated with conditioned media from mono and co-cultures. However, higher GSH activities in DRG neurons treated with conditioned media from co-cultures suggest the role of Schwann cells in regulating oxidative stress in DRG neurons. We hypothesized that Schwann cells play a key role in deciding the fate of DRG neurons under stress conditions by influencing their oxidative environment.

Our previous work on Mn neurotoxicity has shown a gradual shift in cell death mechanism from apoptosis to necrosis with increasing levels of manganese treatment. However, morphological observations of the photomicrographs suggest no characteristic features of necrosis in DRG neurons treated with conditioned media from co-cultures. So, we looked at cytoplasmic levels of Caspase-3, indicator of apoptosis, in DRG neurons treated with conditioned media from mono and co-cultures. We found a significant dose dependent rise in caspase-3 levels, however, the DRG neurons treated with conditioned media from co-cultures showed lower levels of caspase-3. Our results implicate Schwann cells in regulating the cell death and repair mechanisms in neurons.

In addition, we have also determined the fate of DRG neurons which were treated with forskolin in Mn-induced neurotoxicity. Forskolin is a labdane diterpinoid which up-regulates cAMP levels along with activating AMPK. Since Mn induces cell death by targeting mitochondria and hence cellular energetics, we hypothesized that by up-

regulating levels of AMPK and p-AMPK we could promote cell survival. Interestingly, we have found a multiphasic response in the levels of AMPK and p-AMPK in DRG neurons at varying concentrations of manganese. At concentrations of 100, 200 and 300 µM of manganese, we found a dose dependent increase in the frequency of DRG neurons with up-regulated AMPK and p-AMPK. However, at concentrations above 300 µM of manganese, there was a decrease in the frequency of DRG neurons with up-regulated AMPK and p-AMPK. Our hypothesis stands true for the DRG neurons treated with concentrations of manganese ranging from 100-300 µM. However, in our previous studies we have observed necrosis at concentrations above 300 µM. The appearance of necrosis suggest a failing cellular energetics and hence explains the drop in the frequency of DRG neurons with up-regulated AMPK and p-AMPK at concentration above 300 µM.

Thus, results of studies are consistent with the hypothesis that Schwann cells can protect DRG neurons from Mn neurotoxicity by decreasing Mn induced oxidative stress via elevating glutathione and by decreasing Mn-induced caspase-3 expression. Additionally, we also observed that activation of AMPK in DRG neurons prior to treatment with Mn provides neuro-protection. Our results may have pathophysiological implications in neurodevelopment along with neurodegeneration.

3.6 ACKNOWLEDGEMENTS

We thank Dr. Ahmet Hoke of Johns Hopkins University School of Medicine for his gift of the DRG neurons. Our studies were supported, in part, by a DoD MRMC Project Grant (Contract#W81XWH-07-2-0078) and small project grant from MSTMRI.

3.7 REFERENCES

Archibald, F.S., Tyree, C. Manganese poisoning and the attack of trivalent manganese upon catecholamines. Arch Biochem Biophys. 1987; 256(2): 638-650.

Aschner, M., Lukey, B., Tremblay, A. The manganese health research program (MHRP): Status report and future research needs and directions. Neurotoxicol. 2006; 27(5): 733-736.

Aschner, M., Wegrzynowicz, M.S. Role of astrocytes in manganese mediated neurotoxicity. BMC Pharmacol Toxicol. 2013; 14(23): 1-10.

Brouillet, E.P., Shinobu, L., McGarvey, U. Manganese injection into the rat striatum produces excitotoxic lesions by impairing energy metabolism. Exp Neurol. 1993; 120(1): 89-94.

Chen, C., Liao, S. Oxidative stress involves in astrocytic alterations induced by manganese. Exp Neurol. 2002; 175(1): 216-225.

Chen, W., Ruifa, M., Haughey, N., Oz, M., Höke, A. Immortalization and characterization of a nociceptive dorsal root ganglion sensory neuronal line. J Peripher Nerv Syst. 2007; 12(2): 121–130.

Cohen, G. Oxy-radical toxicity in catecholamine neurons. Neurotoxicol. 1984; 5(1): 77-82.

Dukhande, V.V., Malthankar-Phatak, G. H., Hugus, J. J Daniels, C. K., Lai, J. C. K. Manganese-induced neurotoxicity is differentially enhanced by glutathione depletion in astrocytoma and neuroblastoma cells. Neurochem. 2006; 31(11): 1349-1357.

Graham, D.G. Catecholamine toxicity: A proposal for the molecular pathogenesis of manganese neurotoxicity and Parkinson's disease. Neurotoxicol. 1984; 5(1): 83-95.

Greger, J.L. Nutrition versus toxicology of manganese in humans: Evaluation of potential biomarkers. Neurotoxicol. 1999; 20(2-3): 205-212.

Griffith, O. W. Anal Biochem. 1969; 106: 207-212.

Lai, J.C., Minski, M.J., Chan, A.W., Leung, T. K., Lim, L. Manganese mineral interactions in brain. Neurotoxicol. 1999; 20(2-3): 433-444.

April, P. N., Tomas, R. G.. Mechanisms of lead and manganese neurotoxicity. Toxicology Research. 2013; 1 (2): 99-114.

Oikawa, S., Hirosawa, I., Tada-Oikawa, S., Furukawa, A., Nishiura, K., Kawanishi, S. Mechanism for manganese enhancement of dopamine-induced oxidative DNA damage and neuronal cell death. Free Radical Biol Med. 2006; 41(5): 748-756.

3.8 FIGURES

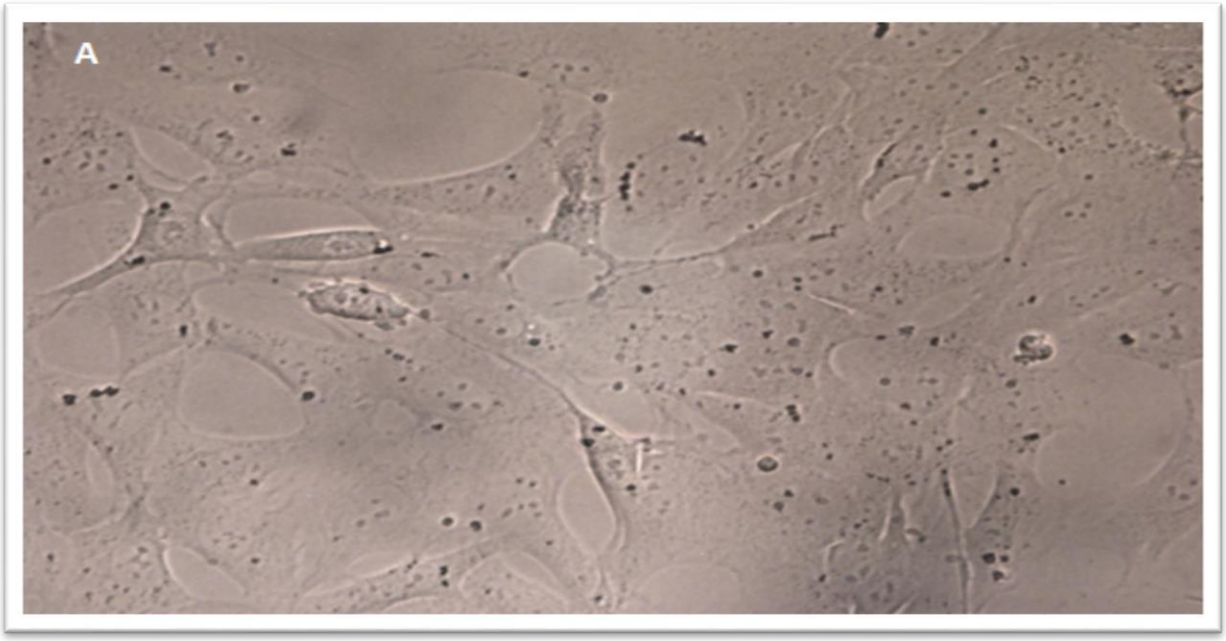

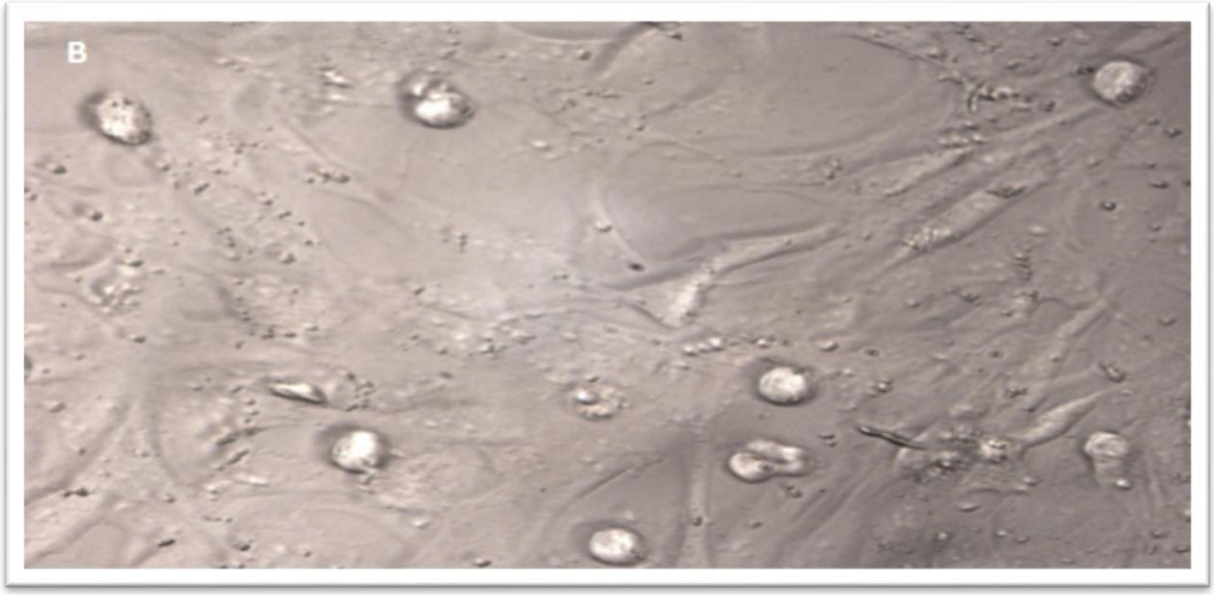

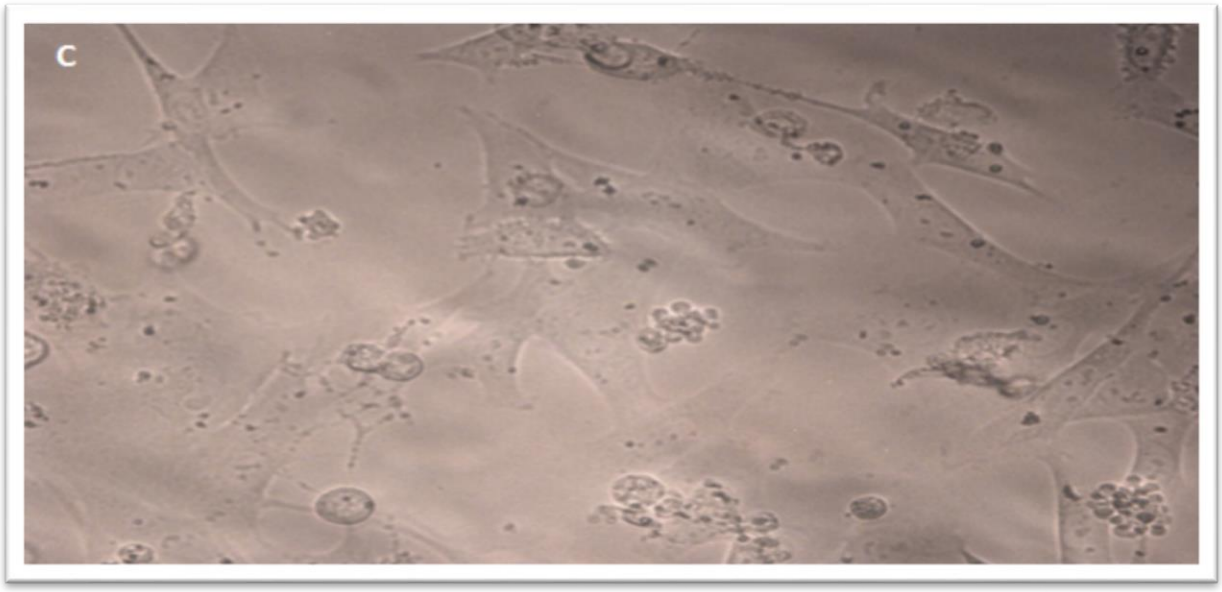

Figure 3.1 Effect of conditioned media containing $MnCl_2$ on DRG neurons. Photomicrographs of DRG neurons treated with COC for 24 hours were shown in the above photomicrographs. A, B and C correspond to DRG neurons treated with 0, 100 or 200 µM $MnCl_2$ containing conditioned medium respectively.

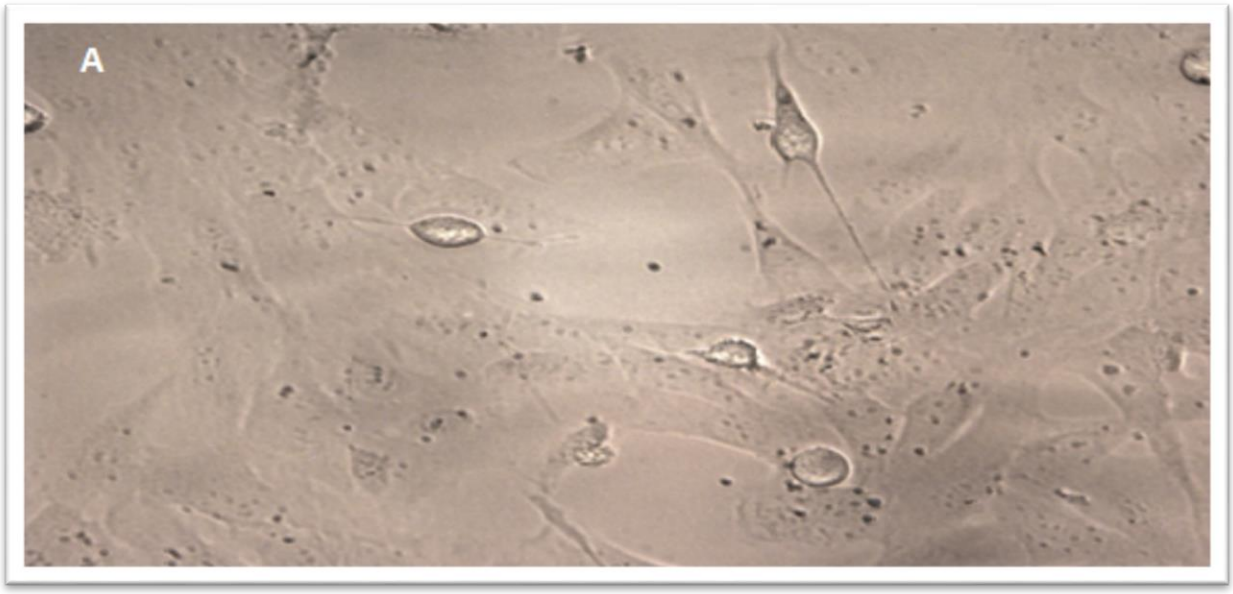
A

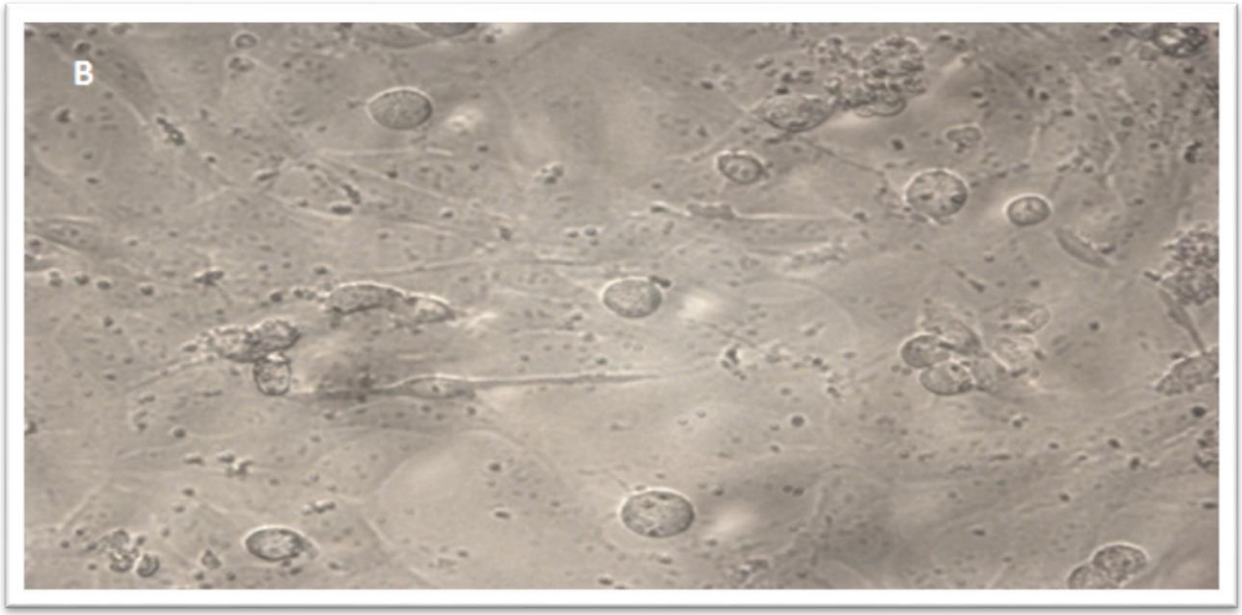
B

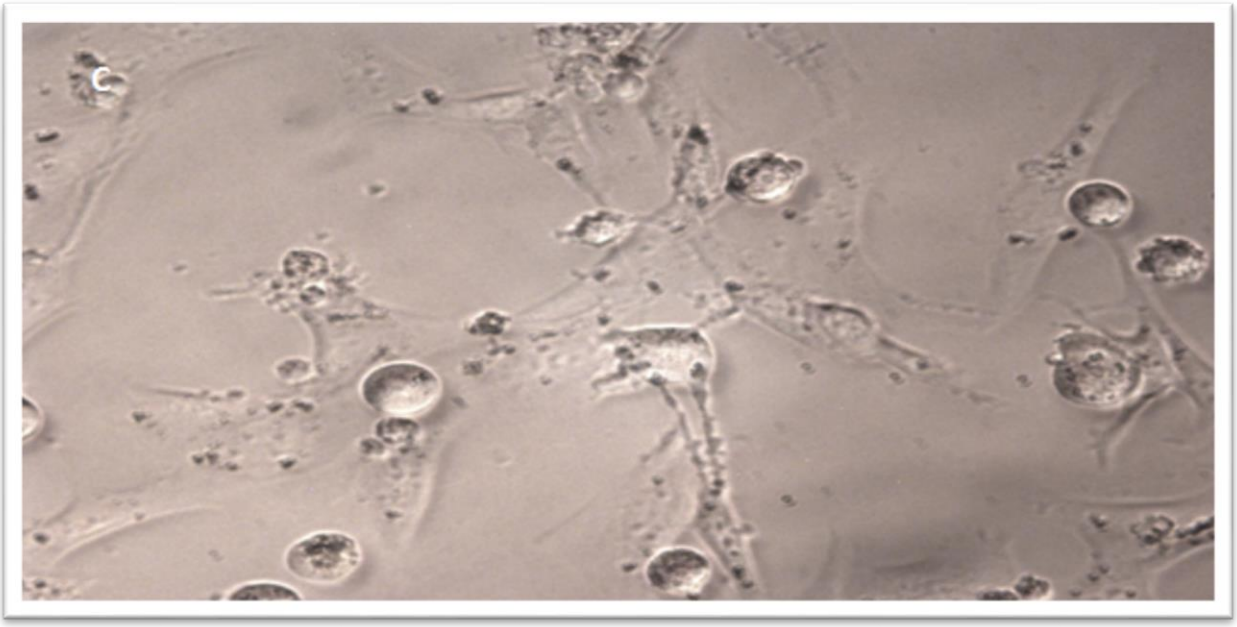

Figure 3.2 Effect of conditioned media containing $MnCl_2$ from monotypic cultures on DRG neurons.

Photomicrographs of DRG neurons treated with MOC for 24 hours were shown in the above photomicrographs. A, B and C correspond to DRG neurons treated with 0, 100 or 200 µM $MnCl_2$ containing conditioned medium respectively.

Note: MOC- CTRL, mono culture control (0 µM of manganese); MOC-100, monoculture, 100 µM of manganese; MOC−200, monoculture, 200 µM of manganese; COC- CTRL, co-culture control (0 µM of manganese); COC-100, co-culture, 100µM of manganese; COC-200, co-culture, 200µM of manganese.

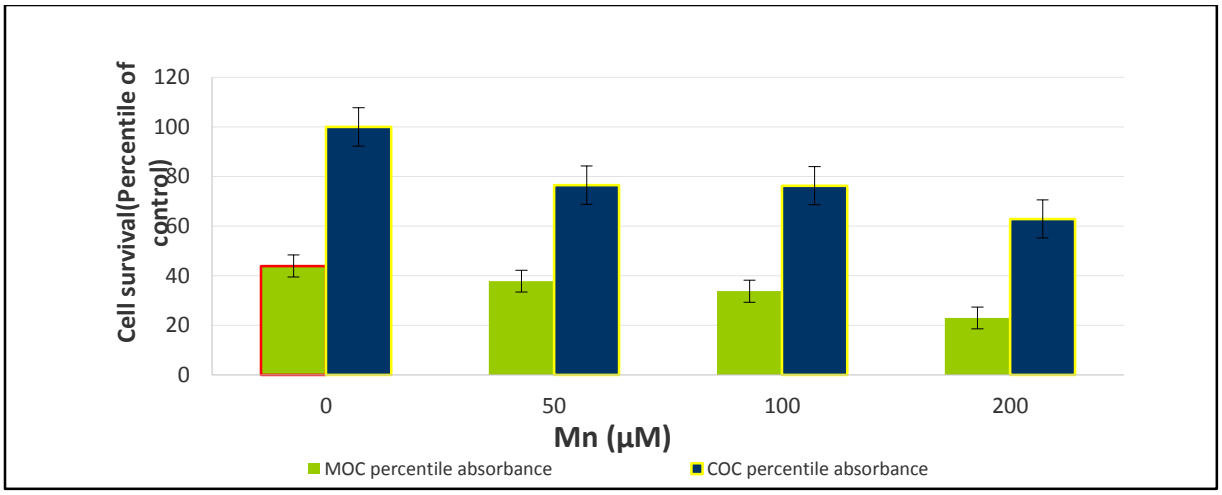

Figure 3.3 Effect of MOC or COC on the survival of DRG neurons.

DRG neurons were treated with MOC or COC for 24 hours and their survival was measured employing MTT assay (Values are mean ± SEM of 3 replicates; *p<0.05 vs MOC control).

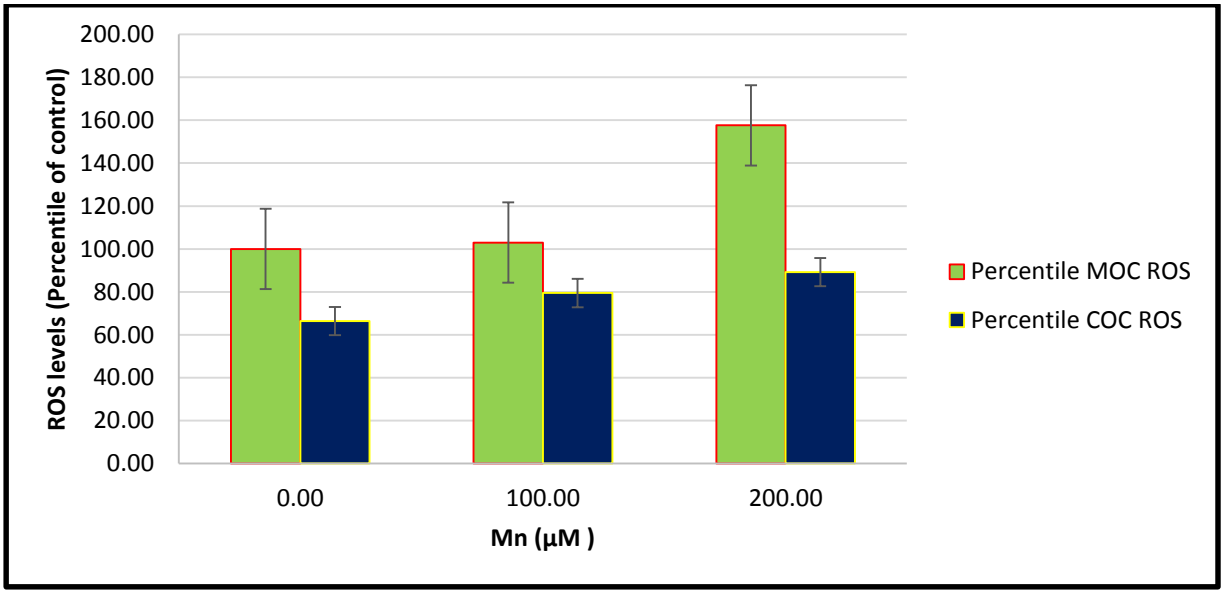

Figure 3.4 Effect of MOC or COC on ROS levels in DRG neurons.

DRG neurons were treated with MOC or COC and their intracellular ROS levels were measured employing ROS assay. (Values are mean ± SEM of 3 replicates; *p<0.05vsMOCcontrol).

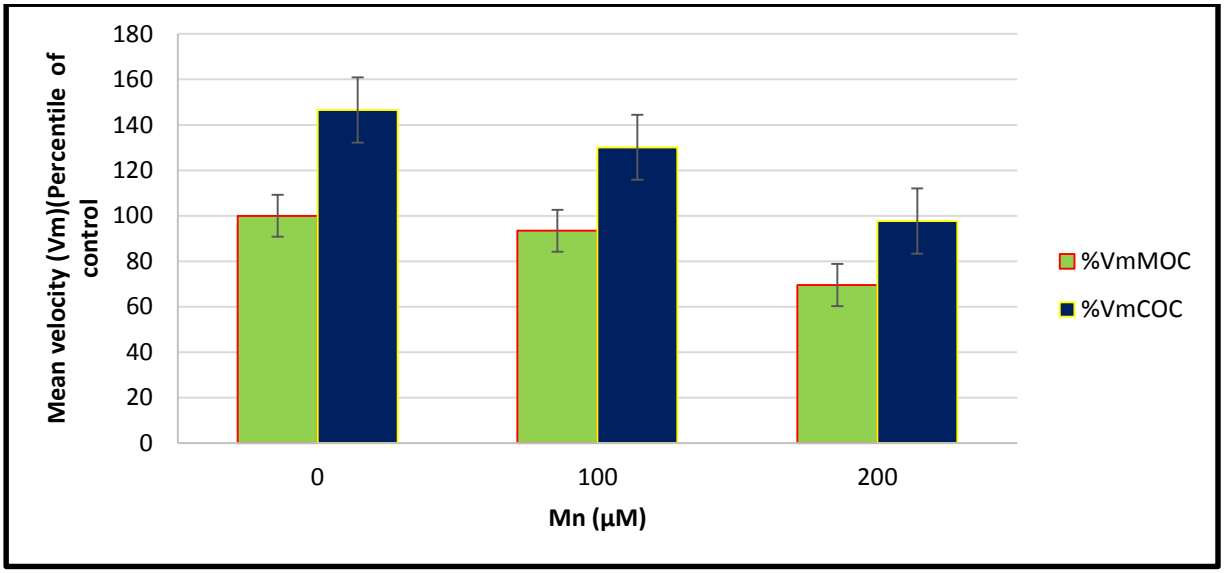

Figure 3.5 Effect of MOC or COC on GSH levels in DRG neurons.

DRG neurons were treated with MOC or COC and their intracellular GSH levels measured by employing GSH assay. The mean velocity is proportional to GSH levels and reflects GSH levels in the cells (Values are mean ± SEM of 3 replicates; *p<0.05vsMOCcontrol).

Figure 3.6 Effect of MOC or COC on the level of caspase-3 in DRG neurons.

DRG neurons were treated with MOC or COC for 24 hours and the cells were harvested and homogenized. The cell homogenate was probed for Caspase-3 employing western blot.

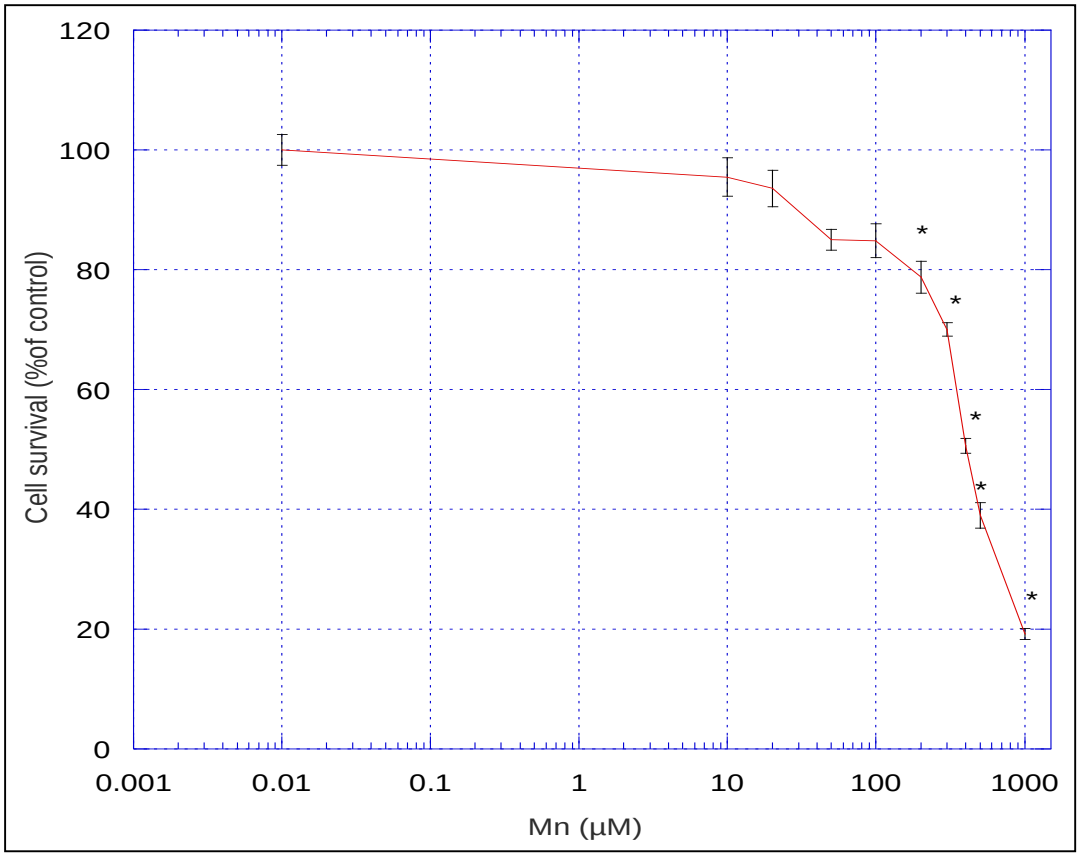

Figure 3.7 Effect of $MnCl_2$ on the survival of DRG neurons which were pre-treated with forskolin.

DRG neurons were pre-treated with DMEM medium containing forskolin for 24 hours. Later, medium was replaced with Mn containing medium and incubated for 24 hours. The survival of the DRG neurons was measured employing MTT assay (Values are mean ± SEM of 9 replicates *$p<0.05$ vs control or 0µM).

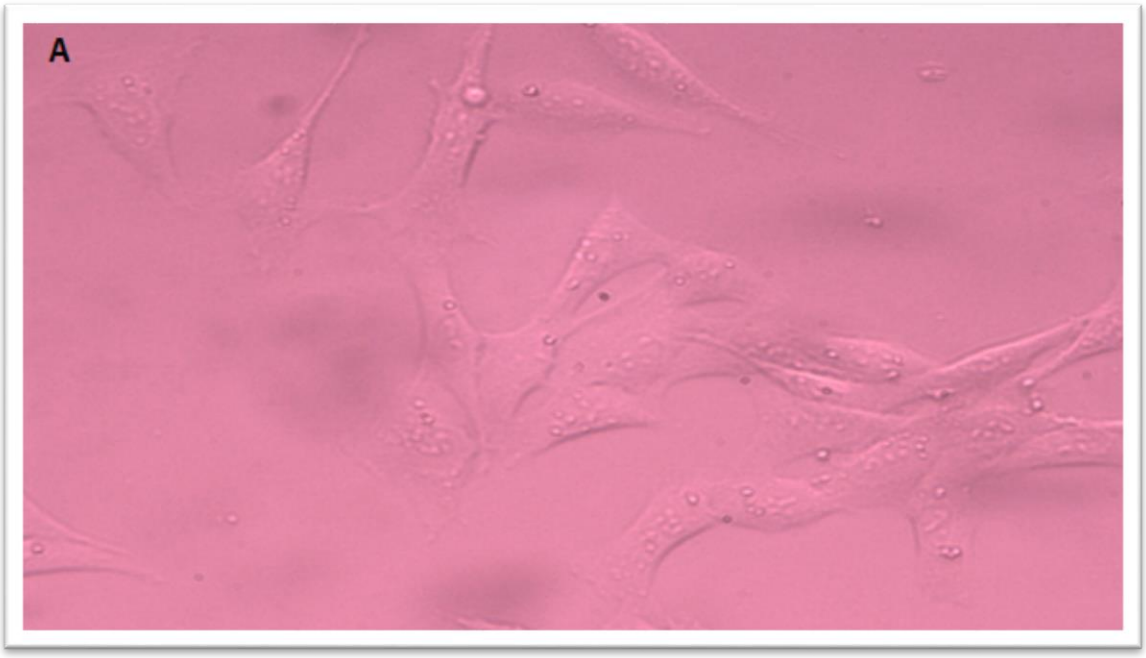
A

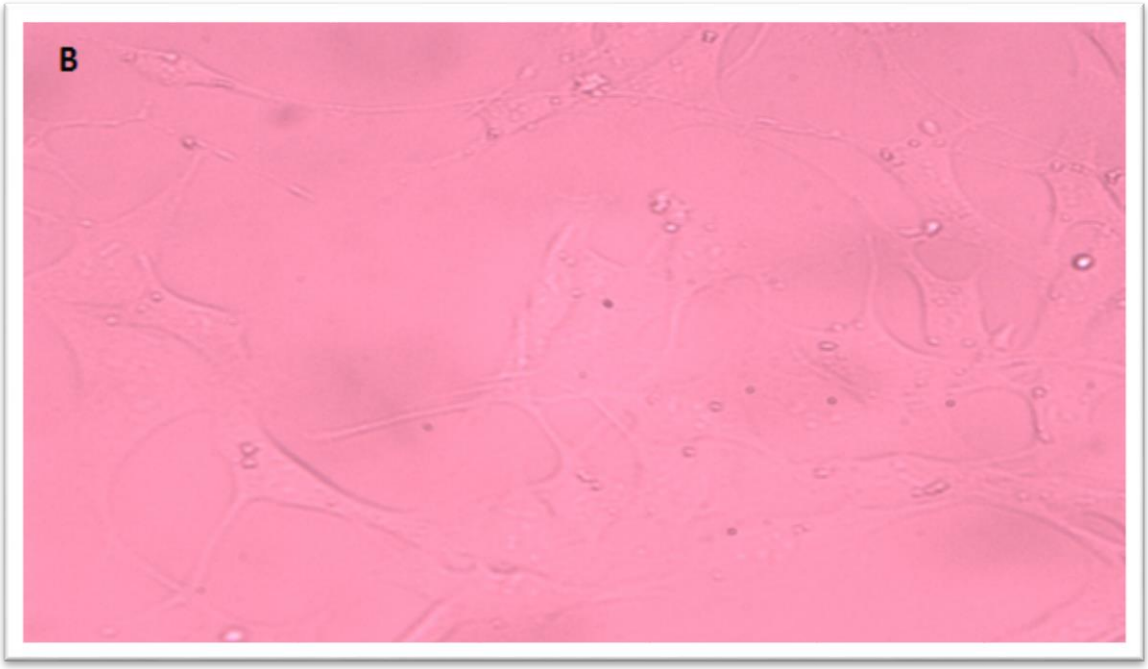
B

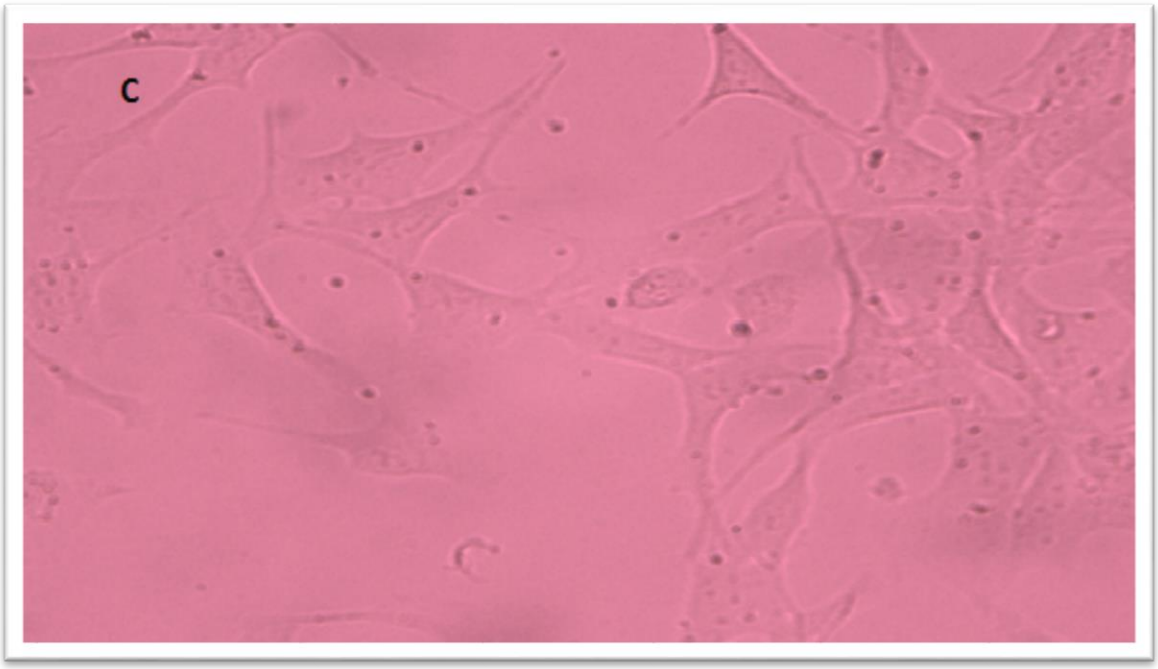
C

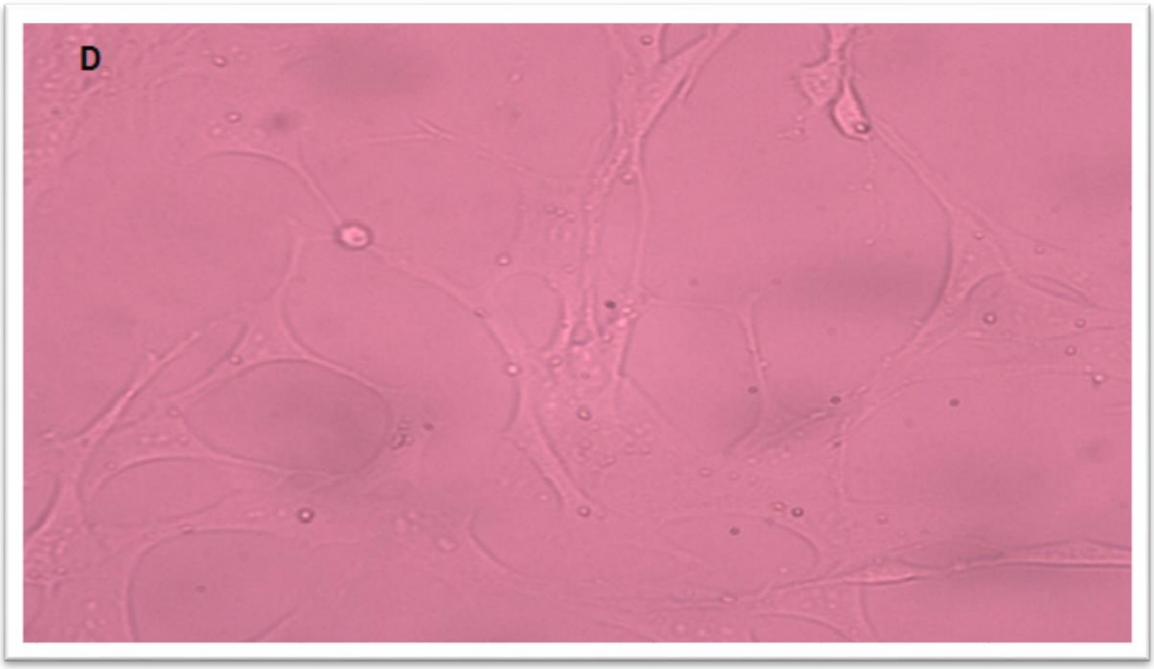
D

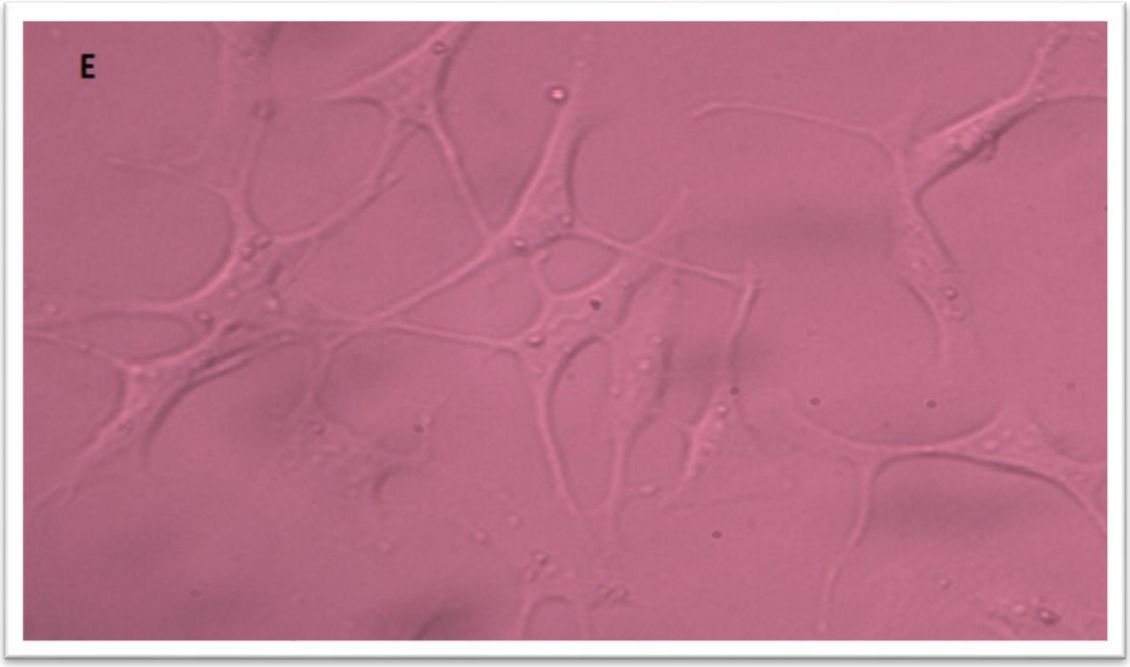
E

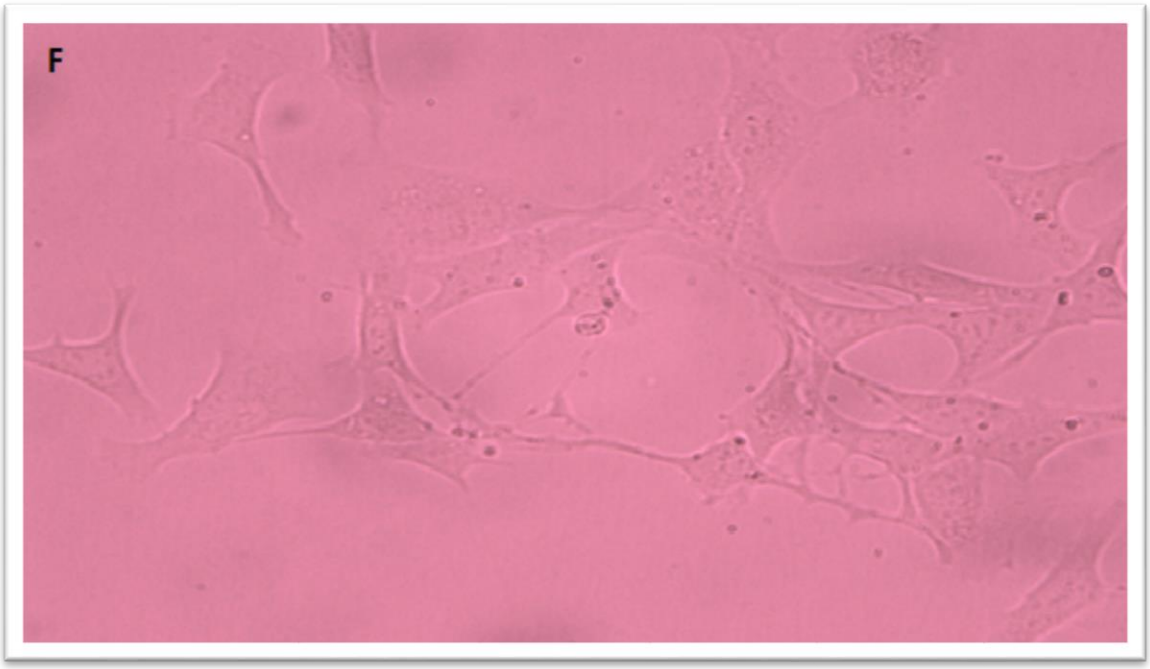
F

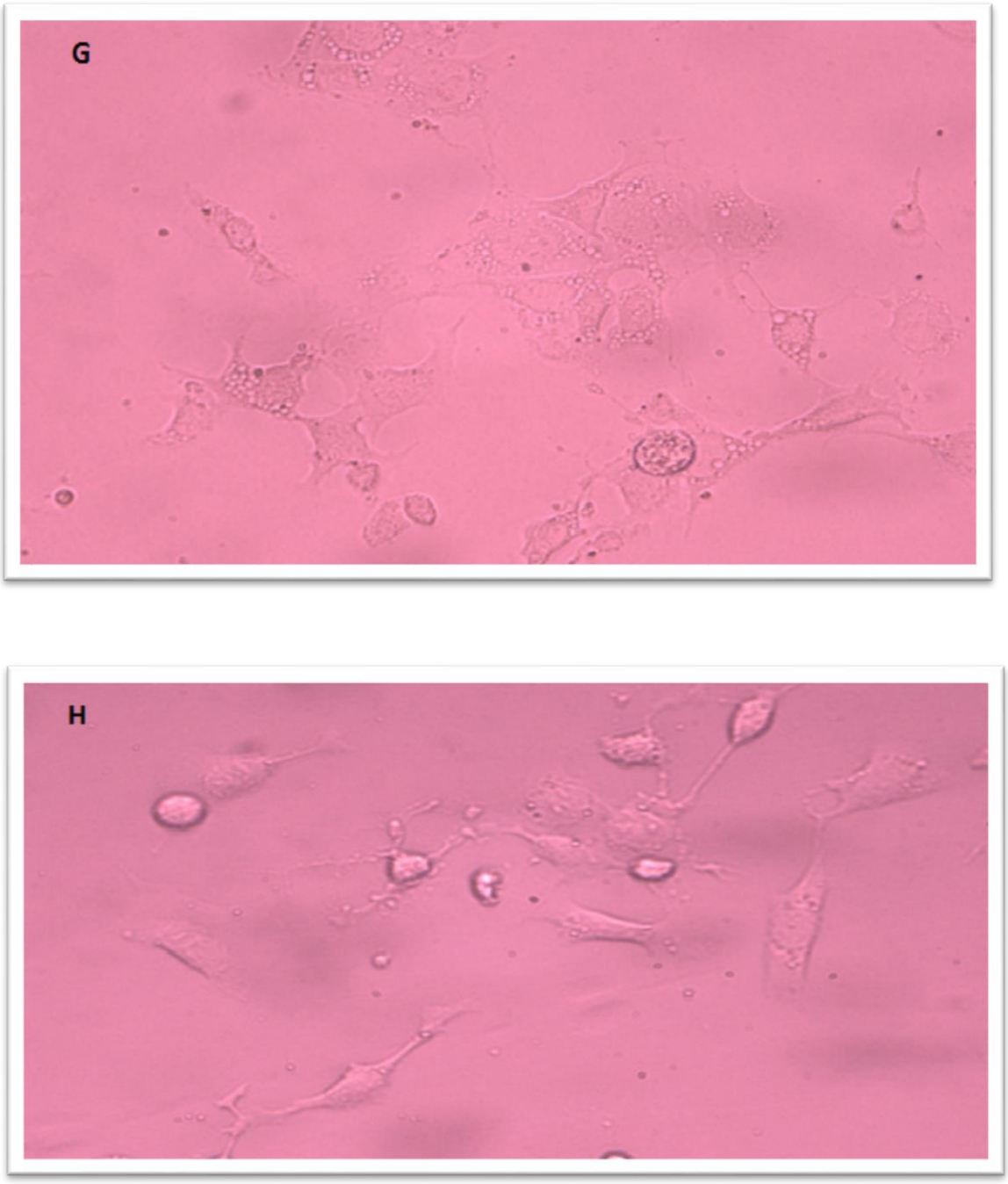

Figure 3.8 Effect of different concentrations of forskolin on DRG neurons.

DRG neurons were treated with 0, 10, 20, 40, 50, 60, 80 and 100 µM of forskolin for 24 hours and photomicrographs of DRG neurons were taken using Leica microscope. Magnification = 400 X

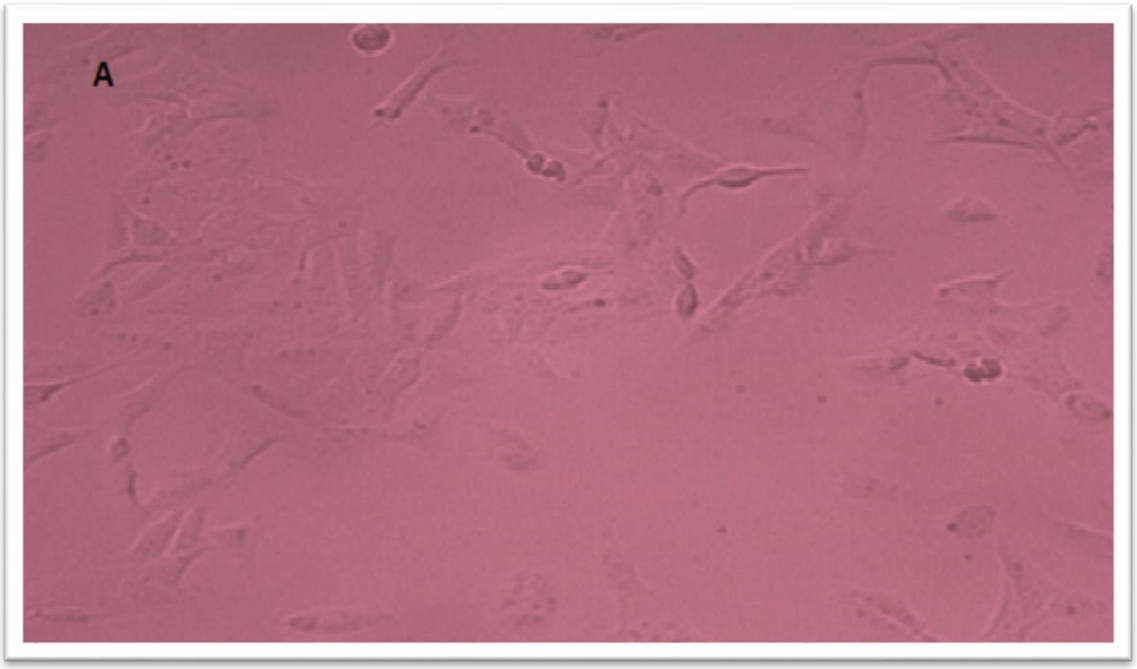
A

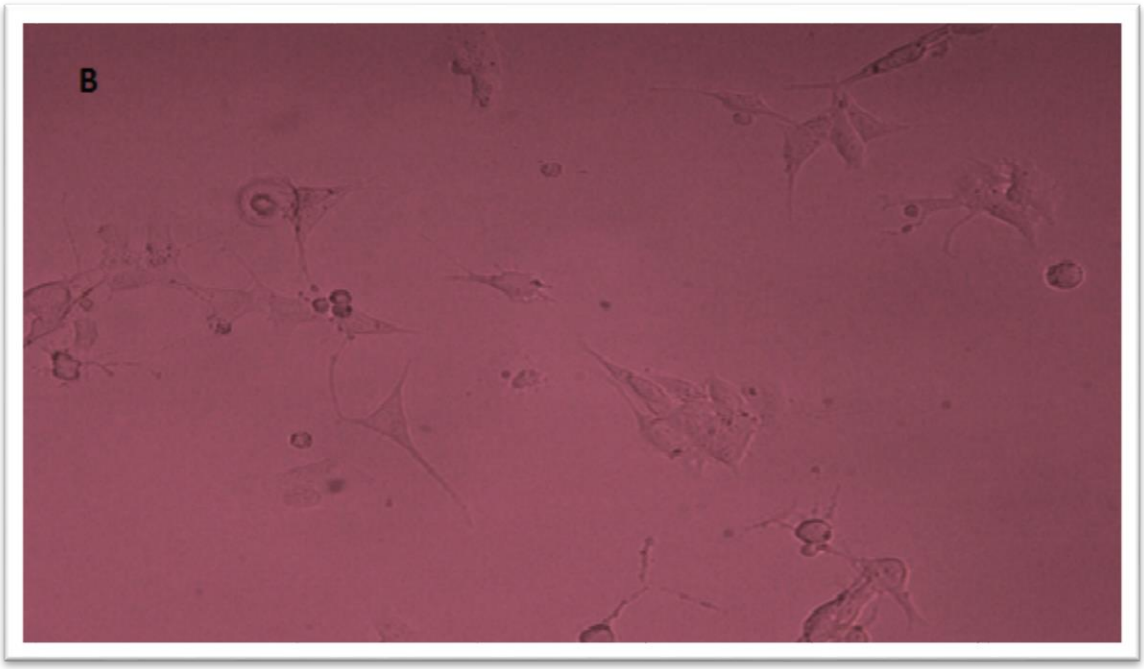
B

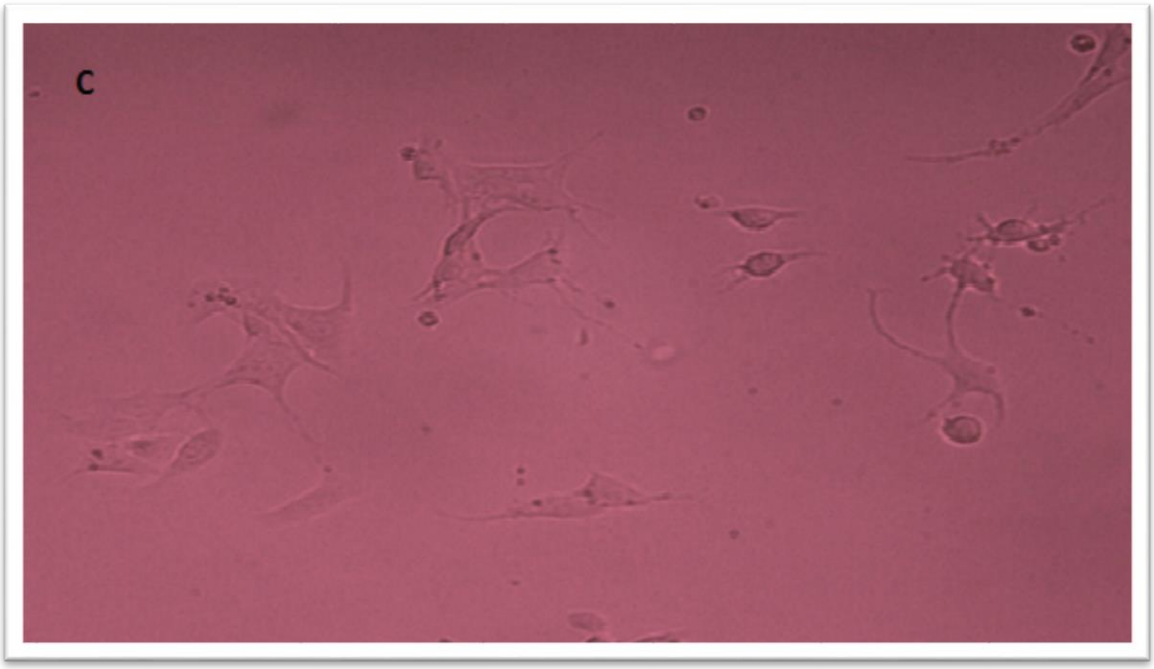

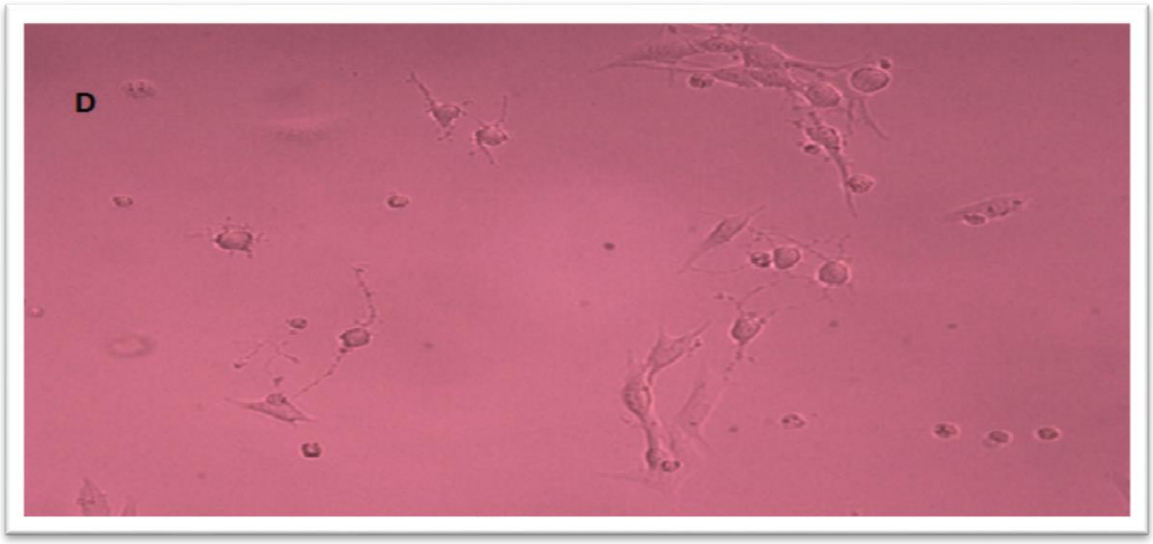

Figure 3.9 Changes in the morphology of DRG neurons treated with forskolin at different time points.

DRG neurons were treated with 50 µM forskolin for 8, 18, 20 and 24 hours and pictures were taken at above mentioned time periods. Photomicrographs from A to D represent

changes in DRG neurons treated with 50 µM of forskolin for 8, 18, 20 and 24 hours respectively. Magnification = 200 X

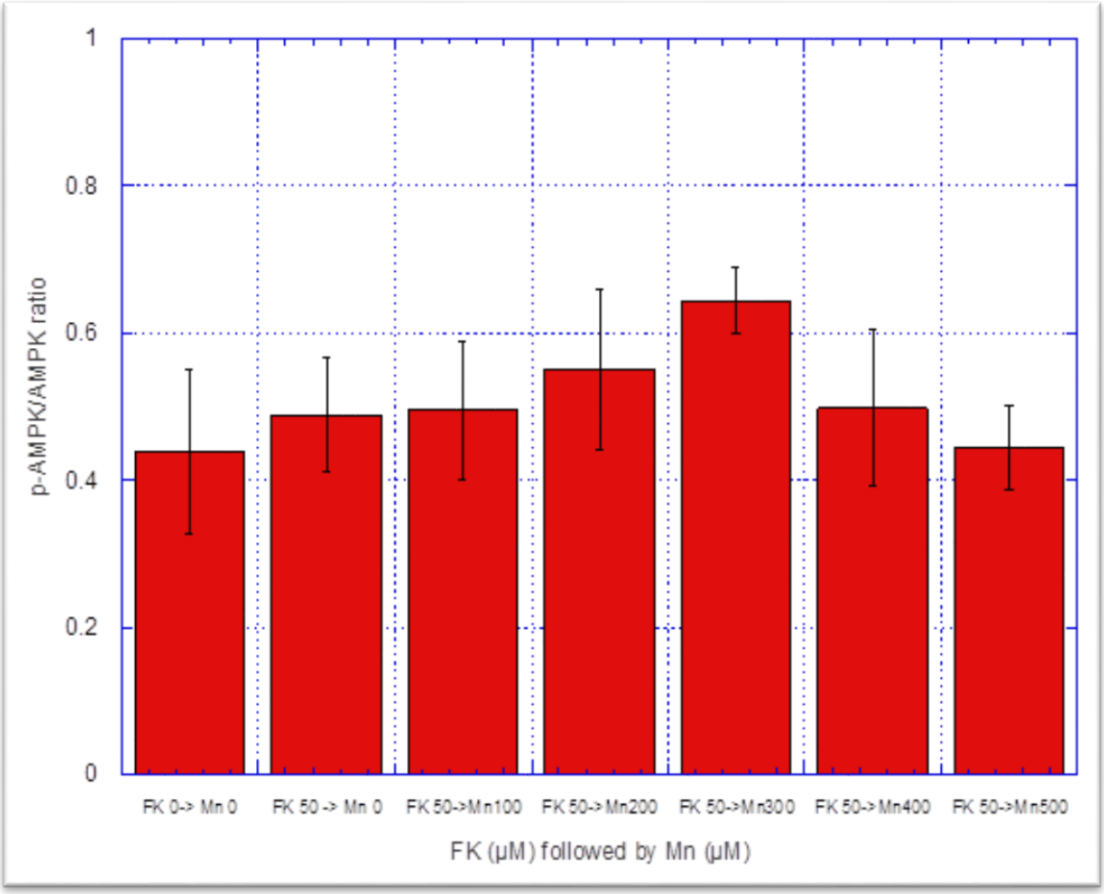

Figure 3.10 Effect of $MnCl_2$ on AMPK and p-AMPK ratio in DRG neurons pretreated with forskolin.

DRG neurons were treated with 50 µM forskolin for 24 hours. Later, the medium was replaced with medium containing 100, 200, 300, 400 or 500 µM of $MnCl_2$ and incubated for 24 hours. The treated or the control neurons were harvested and immunocytochemical analysis for AMPK and p-AMPK was performed as described earlier. The ratio of the

median fluorescent intensity of p-AMPK and AMPK were calculated (Values are mean ± SEM of 3 replicates).

CHAPTER 4. GENERAL DISCUSSION, CONCLUSIONS, AND PROSPECTS FOR FUTURE STUDIES

4.1 GENERAL DISCUSSION AND CONCLUSIONS

Cancerous cells differ from the corresponding normal cells due to a plethora of biochemical changes driven by various oncogenes. A classic example of such tumor-specific biochemical alterations is the Warburg effect. Furthermore, functional changes in oxidative enzymes such as succinic dehydrogenase (SDH), fumarate hydratase (FH) and isocitrate dehydrogenase (IDH) lead to changes in redox status in a cell (Simone and Maria , 2012). Thus, tumor cell models exhibit cellular energetics and mitochondrial functions that are dissimilar to those in their corresponding normal counterparts. Consequently, in vitro toxicity studies employing neurotumor cell models may not constitute the most ideal approach in elucidating the mechanisms underlying neurotoxicity of manganese (Mn) in neurons or glial cells. The recent availability of dorsal root ganglion (DRG) neurons not derived from tumor cells (Chen et al., 2007) have allowed us to employ them to develop neural cell models in vitro for investigating cellular and molecular mechanisms of peripheral neuropathy and those underlying toxin-induced neurodegeneration (Jaiswal et al., 2010; Jaiswal et al., 2011).

Employing the neural cell models in vitro derived from the peripheral nervous system consisting of DRG neurons and Schwann cells (Jaiswal et al., 2010; Jaiswal et al., 2011), this study has demonstrated that treatment with $MnCl_2$ induced concentration-related decreases in survival of DRG neurons and Schwann cells; however, this Mn-induced effect was more pronounced in DRG neurons than in Schwann cells indicating

that DRG neurons are more susceptible than Schwann cells to the cytotoxic effects of Mn (Chapter 2). Thus, the findings of this study (Chapter 2) are similar to those of the earlier study of Lai et al. (1985) who showed that cerebrocortical neurons in primary culture are more susceptible than glial cells to neurotoxic effects of manganese and to those of Hernandez et al. (2011) who studied the effects of $MnCl_2$ on the survival of cerebrocortical neurons in primary culture. Moreover, the present findings (Chapter 2) are also compatible with our previous observation that human neuroblastoma SK-N-SH (neurons-like) cells are also more susceptible than human astrocytoma U87 (astrocytes-like) cells to the neurotoxicity of Mn (Malthankar et al., 2004); however, the IC_{50} values for $MnCl_2$ in lowering the survival of SK-N-SH and U87 cells (>500 µM; Malthankar et al., 2004) are much higher than the corresponding values in DRG neurons and Schwann cells. This study also noted that both apoptosis and necrosis constitute the cell death mechanisms underlying the Mn-induced lowering of survival of DRG neurons (Chapter 2), a finding similar to those obtained in human neuroblastoma SK-N-SH (neurons-like) cells (Malthankar et al., 2004; Dukhande et al., 2006).

AMPK is an important sensor of energy status of a cell and controls cell metabolism. This study has reported the p-AMPK to AMPK ratios showed a trend of increase in DRG neurons treated with 400 µM $MnCl_2$ but this ratio was decreased in DRG neurons treated with 500 µM $MnCl_2$ (Chapter 2) suggesting that Mn induced disturbances in energy homeostasis in DRG neurons. These findings are compatible with our observation that Mn induced decreases in LDH and MDH in DRG neurons (Chapter 2).

In many neurodegenerative diseases, the underlying cell death mechanisms have not been fully elucidated; however, morphological, biochemical and genetic studies have suggested a potential role of mitochondria (Martin, 2010). In studies related to neurodegenerative conditions induced by manganese exposure, mitochondrial dysfunction was commonly observed (Martin, 2010). Manganese primarily targets mitochondria and disturbs calcium homeostasis, thereby, causes mitochondrial dysfunction (Lai et al., 1985; Lai and Leung, 2013). Consequently, many physiological processes such as oxidative metabolism and cellular respiration located in mitochondria are expected to be disturbed in neurodegeneration. Here we found treatment with 100 μM and 200 μM $MnCl_2$ induced substantial decreases in activities of LDH and MDH in DRG neurons (Chapter 2), suggesting that Mn treatment induced energy failure. This conclusion is in accord with our previous observation that Mn treatment induced dose-related decreases in many glycolytic, tricarboxylic acid cycle and related enzymes in human neuroblastoma SK-N-SH (neurons-like) cells (Malthankar et al., 2004).

This study is the first to report that Mn treatment of DRG neurons induces a shift in their mitochondrial dynamic balance between fusion and fission in favor of fission (Chapter 2). This observation is important and pathophysiological relevant because a balance between mitochondrial fusion and fission is critical in maintaining normal functioning of mitochondria (Galloway et al., 2012).

The role of glial cells is critical for maintaining the structural and functional integrity of neurons (Siegel et al., 2006). For example, peripheral neurons are dependent on Schwann cells for their supply of many metabolic intermediates. This study therefore

also investigated the hypothesis that Schwann cells exert protective effect on DRG neurons against Mn-induced cytotoxicity and neurotoxicity (Chapter 3).

This is the first study that demonstrates that the conditioned medium derived from co-cultures of DRG neurons and Schwann cells containing 100 or 200 μM $MnCl_2$ conferred on DRG neurons some protection against the neurotoxic effect of Mn (Chapter 3). The same condition medium also induced a lowering of the Mn-induced oxidative stress in DRG neurons by lowering their ROS production but enhancing their GSH levels (Chapter 3). Thus, results of this study are consistent with the hypothesis that Schwann cells can protect DRG neurons from Mn-induced neurotoxicity.

All in all, the results of this study strongly suggest that DRG neurons constitute an excellent cell model in vitro for elucidating the cellular and molecular mechanisms underlying Mn-induced neurotoxicity in neurons. They demonstrate $MnCl_2$ induced both apoptosis and necrosis in DRG neurons depending on its concentrations by exerting oxidative stress, disrupting their cellular energetics and shifting the balance of their mitochondrial dynamics between fusion and fission in favor of fission. Furthermore, our results also showed the conditioned medium derived from co-cultures of DRG neurons and Schwann cells containing 100 or 200 μM $MnCl_2$ conferred on DRG neurons some protection against the neurotoxic effect of Mn. The same condition medium also induced a lowering of the Mn-induced oxidative stress in DRG neurons by lowering their ROS production but enhancing their GSH levels. Consequently, as such, our results may assume pathophysiological importance in peripheral neuropathy in particular and neurodegeneration in general.

4.2 PROSPECTS FOR FUTURE STUDIES

Our project has yielded new, important and relevant data that can readily attest to the validity and usefulness of employing DRG neurons as a cell model in vitro to further elucidate the roles of mitochondria and cell signaling pathways in Mn-induced neurotoxic conditions. There is a need to further characterize the changes in mitochondria in DRG neurons upon exposure to Mn. Studies should also focus on mitochondrial and cytoplasmic enzyme systems other than those investigated in this study to more accurately characterize the consequences of mitochondrial dysfunction in neurons when exposed to toxic levels of Mn. In addition, further studies on the regulation of mitochondrial dynamics in Mn- induced neurotoxicity would help us critically and better understand the role of mitochondria in neurodegeneration.

4.3 REFERENCES

Chen, W., Ruifa, M., Haughey, N., Oz, M., Höke, A. Immortalization and characterization of a nociceptive dorsal root ganglion sensory neuronal line. J Peripher Nerv Syst. 2007; 12(2): 121–130.

Dukhande, V.V., Malthankar-Phatak, G. H., Hugus, J. J., Daniels, C. K., Lai, J. C. K. Manganese-induced neurotoxicity is differentially enhanced by glutathione depletion in astrocytoma and neuroblastoma cells. Neurochem. 2006; 31(11): 1349-1357.

Galloway, C. A., Yoon, Y. Perspectives on: SGP Symposium on Mitochondrial Physiology and Medicine. What comes first, misshape or dysfunction? The view from metabolic excess. J Gen Physiol.2012; 139(6): 455–463.

Hernandez, R. B., Farina, M., Esposito, B. P., Souza-Pinto, N. C., Barbosa, Jr, F., Sunol, C. Mechanisms of manganese-induced neurotoxicity in primary neuronal cultures: The role of manganese speciation and cell type. Toxicol Sci. 2011; 124(2): 414–423.

Jaiswal, A. R., Wong, Y. Y. W., Bhushan, A., Daniels, C. K., Lai, J. C. K. A noncontact co-culture model of peripheral neural cells for nanotoxicity, tissue engineering and pathophysiological studies. In chapter 8: Environment, Health and Safety, in Technical Proceedings of the 2010 NSTI Nanotechnology Conference and Expo-Nanotech 2010. 2010; 3: 527–531.

Jaiswal, A. R., Lu, S. Y., Pfau, J., Wong, Y. Y. W., Bhushan, A., Leung, S. W., Daniels, C. K., Lai, J. C. K. Effects of silicon dioxide nanoparticles on peripheral nervous system neural cell models. In chapter 7: Environment, Health and Safety, Technical Proceedings of the 2011 NSTI Nanotechnology Conference and Expo-Nanotech 2011. 2011; 3: 541–544.

Lai, J. C. K., Leung, S. W. Manganese, interrelation with other metal ions in health and disease. Encyclopedia of Metalloproteins. 2013; pp. 1308-1314.

Lai, J. C. K., Leung, T. K. C., Lim, L. Effects of metal ions on neurotransmitter function and metabolism. In metal ions in neurology and psychiatry (Neurology and Neurobiology, Vol. 15) (Gabay S, Harris J & Ho BT, eds.). 1985; 15: 177-197, Alan Liss, New York.

Malthankar, G. V., White, B. K., Bhushan, A., Daniels, C. K, Rodnick, K. J. Lai J. C. K. Differential lowering by manganese treatment of activities of glycolytic and tricarboxylic

acid (TCA) cycle enzymes investigated in neuroblastoma and astrocytoma cells is associated with manganese-induced cell death. Neurochem Res. 2004; 29(4): 709-717.

Martin, L. J. Mitochondrial and cell death mechanisms in neurodegenerative diseases. Pharmaceuticals. 2010; 3: 839-915.

Siegel, G. J., Wayne, R. A., Scott, T. B., Donald, L. P. Basic neurochemistry: Molecular, cellular and medical aspects. Elsevier. 2006, seventh edition.

Cardaci, S., Ciriolo, M. R. TCA cycle defects and cancer: When metabolism tunes redox state. Int J Cell Biol. 2012; 2012: 1-9.